JPRS L/9650

7 April 1981

# USSR Report

## METEOROLOGY AND HYDROLOGY

No. 11, November 1980

FBIS FOREIGN BROADCAST INFORMATION SERVICE

NOTE

JPRS publications contain information primarily from foreign newspapers, periodicals and books, but also from news agency transmissions and broadcasts. Materials from foreign-language sources are translated; those from English-language sources are transcribed or reprinted, with the original phrasing and other characteristics retained.

Headlines, editorial reports, and material enclosed in brackets [] are supplied by JPRS. Processing indicators such as [Text] or [Excerpt] in the first line of each item, or following the last line of a brief, indicate how the original information was processed. Where no processing indicator is given, the information was summarized or extracted.

Unfamiliar names rendered phonetically or transliterated are enclosed in parentheses. Words or names preceded by a question mark and enclosed in parentheses were not clear in the original but have been supplied as appropriate in context. Other unattributed parenthetical notes within the body of an item originate with the source. Times within items are as given by source.

The contents of this publication in no way represent the policies, views or attitudes of the U.S. Government.



APPROVED FOR RELEASE: 2007/02/08: CIA-RDP82-00850R000300100013-3

JPRS L/9650

7 April 1981

# USSR REPORT

## METEOROLOGY AND HYDROLOGY

No. 11, November 1980

Translation of the Russian-language monthly journal METEOROLOGIYA I GIDROLOGIYA published in Moscow by Gidrometeoizdat.

## CONTENTS

UDC 551.511.32(-062.4)

# WAVE TRIPLETS IN THE ATMOSPHERIC EQUATORIAL ZONE

Moscow METEOROLOGIYA I GIDROLOGIYA in Russian No 11, Nov 80 pp 5-15

[Article by Ye. M. Dobryshman, professor, Institute of Atmospheric Physics, manuscript submitted 22 May 80]

[Text]

Abstract: The existence of a triplet of waves, which are in resonance interaction, is established for a system of two nonlinear equations relating the stream function and temperature in a very simple model of circulation in a narrow equatorial zone. The article gives an analysis of interacting wave vectors and graphs of the geometrical locus of points representing the ends of pairs of vectors interacting with a third. The solution for the amplitudes of interacting vectors in the wind and temperature fields is expressed through elliptical Jacobi functions. A comparison is given with a simpler case -- Rossby waves, being a solution of one nonlinear equation.

More and more attention is being devoted to an investigation of nonlinear processes in the atmosphere. This is entirely understandable since it is primarily nonlinear processes which are responsible for the restructuring of circulation mechanisms of the most different scales. The general difficulties in study of nonlinear processes are well known and therefore it need only be mentioned that virtually every nonlinear problem requires its own approach and the formulation of its own solution method. True, the general nature of the nonlinearity of the equations of hydrodynamics also makes it possible to employ some general procedures for solving individual classes of problems. Among such classes is the problem of wave triplets, that is, three waves with different components of the wave vectors which are in resonance interaction -- there is an exchange of energies (the total energy of the triplet is conserved). It can be noted at once that the solutions found are usually not absolutely precise; they are obtained using different approximations. The most used variant is the weak interaction approximation, which will be discussed below.

Within the framework of linear theory, or better said, linear approximation theory, the amplitude and phase of each wave are independent characteristics of the process and thus the waves do not interact with one another. Rossby waves are the most important macroscale waves in the atmosphere. A single Rossby wave is a precise solution of the nonlinear vorticity equation (to be more precise, the projection of the vorticity vector onto the vertical axis z) within the framework of quasi-horizontality of motion, characteristic for processes of a synoptic scale everywhere except for a narrow equatorial zone [5]. Source [2] gave a general procedure for seeking solutions of the nonlinear vorticity equation in the form of the sum of noninteracting waves. This method was developed further in different aspects (see [3, 7]). The nonlinearity of the corresponding operator indicates the existence of interaction between waves and in the 1960's studies appeared with individual special solutions in the form of sums of specially "selected" Rossby waves in one way or another interacting with one another. An important step in its theoretical aspects was [6], which gave a method for analysis of a resonance triplet; the nonlinear part of the triplet is described by an operator $(\psi, \Delta\psi)$ which is natural for hydrodynamics -- vorticity advection. In numerous subsequent studies the method was refined and developed in the most different directions, the most important of which, indeed, is a study of the interaction of two waves with the zonal flow -- the "third wave."

The objective of the article is to demonstrate that in a more complex case, specifically for a system of two nonlinear equations describing the simplest models of circulation in a narrow equatorial zone, resonance triplets can exist.

1. Formulation of problem. The simplest zonal models of small-scale processes, that is, not dependent on the x-coordinate along the equator, are described by a system of equations correct for a narrow equatorial zone [4];

$$\left.\begin{aligned} &\frac{\partial U}{\partial t} + (\psi, U) = 0 \\ &\frac{\partial \Delta\psi}{\partial t} + (\psi, \Delta\psi) = \alpha \frac{\partial T}{\partial y} \\ &\frac{\partial T}{\partial t} + (\psi, T) = -\Gamma \frac{\partial \psi}{\partial y} \end{aligned}\right\}. \tag{1}$$

Here t is time, y is the horizontal coordinate, reckoned from the equator to the north, z is the vertical coordinate, $\alpha \approx 1/30$ m·sec$^{-2}$·°C$^{-1}$ is the buoyancy parameter, $\Gamma \approx 3\cdot10^{-3}$ °C·m$^{-1}$ is the parameter of vertical atmospheric stability, $U = u - \omega y^2/r_0 + 2\omega z$ is zonal angular moment, u is the zonal velocity component, $\omega = 7.29\cdot10^{-5}$ is the angular velocity of the earth's rotation, $r_0 = 6.37\cdot10^6$ m is the earth's mean radius, $\psi$ is the stream function in the meridional plane, so that $v = -\partial\psi/\partial z$; $w = \partial\psi/\partial y$ are the velocity components along the y and z axes respectively, T is the deviation of temperature from a linear profile along z;

$$(A, B) \equiv \frac{\partial A}{\partial y}\frac{\partial B}{\partial z} - \frac{\partial A}{\partial z}\frac{\partial B}{\partial y} \text{ is a Jacobian,}$$

$$\Delta \equiv \frac{\partial^2}{\partial y^2} + \frac{\partial^2}{\partial z^2},$$

It can be seen from system (1) that first of all, the movement is three-dimensional -- all three velocity components are different from zero, and second, U, and this means, u as well, are determined after finding the $\psi$ and T functions.

System (1), even in more general form, has a number of solutions of the type of waves superposed on some basic state characterized by constant values of the meridional and vertical wind velocity components [5].

We will attempt to find a solution of the system of equations

$$\frac{\partial \Delta\psi}{\partial t} + (\psi, \Delta\psi) = \alpha \frac{\partial T}{\partial y}; \quad \frac{\partial T}{\partial t} + (\psi, T) = -\Gamma \frac{\partial \psi}{\partial y} \tag{1'}$$

in the form

$$\left.\begin{aligned} \psi &= \psi_0 - Vz + \sum_{k=1}^{N} \psi_k e^{i(m_k y + n_k z - \sigma_k t)} \\ T &= \Sigma T_k e^{i(m_k y + n_k z - \sigma_k t)} \end{aligned}\right\} \tag{2}$$

(all the parameters are constants).

After the substitution of (2) into the first equation of system (1') and shortening by the factor i we obtain

$$\left.\begin{aligned} &\sum_{k=1}^{N} \sigma_k \rho_k^2 \psi_k e^{i(\ )_k} + i \sum_{k=1}^{N} m_k \psi_k e^{i(\ )_k} \cdot \sum_{j=1}^{N} (-n_j \rho_j^2 \psi_j e^{i(\ )_j}) - \\ &- \left[ -V + i \sum_{k=1}^{N} n_k \psi_k e^{i(\ )_k} \right] \cdot \sum_{j=1}^{N} (-m_j \rho_j^2 \psi_j e^{i(\ )_j}) = \\ &= \alpha \sum_{k=1}^{N} m_k T_k e^{i(\ )_k} \end{aligned}\right| , \tag{3}$$

where $\rho_k^2 = m_k^2 + n_k^2$ is the square of the wave vector modulus,

$$(\ )_k = (m_k y + n_k z - \sigma_k t).$$

Equating the coefficients on $e^{i(\ )k}$, we obtain N expressions

$$(\sigma_k - m_k V)\, \rho_k^2 \psi_k = \alpha m_k T_k \qquad (k = \overline{1, N}). \tag{4}$$

When multiplying the nonlinear terms it is necessary to examine two cases: when j = k and j $\neq$ k. In the first case the coefficients on the doubled frequencies become equal to zero. For j $\neq$ k it is possible to avoid combination frequencies by requiring that the coefficients on $\varphi_k$, $\varphi_j$ become equal to zero. These, it is easy to see, will be as follows:

$$(\rho_k^2 - \rho_j^2)(m_k n_j - m_j n_k). \tag{5}$$

The first possibility

$$\rho_k^2 - \rho_j^2 = 0 \Longrightarrow \rho_k = \text{const} = \rho$$

is of no interest (the same as with Rossby waves [3]). It leads to the trivial result

$$\frac{\sigma_k}{m_k} = V \pm \sqrt{\frac{\alpha \Gamma}{\rho^2}}, \tag{6}$$

and thus the linear velocity of all the waves $\sigma_k/m_k$ is one and the same.

The second possibility is:

$$m_k n_j - m_j n_k = 0. \tag{7}$$

The number of expressions (7) will be $C_N^2 = N(N + 1)/2$; however, only N - 1 will be independent. With N = 3 the number of independent expressions will be equal to 2; this circumstance will be used in the future.

Substituting (2) into the second equation of system (1'), after similar calculations, we first obtain N expressions

$$(\sigma_k - m_k V)\ T_k = \Gamma m_k \psi_k \tag{8}$$

and second, N(N - 1)/2 expressions $\psi_k T_j (m_k n_j - m_j n_k) = 0$, that is, the same expressions (7), which can be represented in the form

$$m_k/n_k = q \Longrightarrow \rho_k^2 = m_k^2(1 + q^2).$$

Solving (7) and (8) jointly, we find

$$(\sigma_k - m_k V)^2 = \frac{\alpha \Gamma m_k^2}{\rho_k^2} = \frac{\alpha \Gamma}{1 + q^2} \Longrightarrow \sigma_k = m_k V \pm \sqrt{\frac{\alpha \Gamma}{1 + q^2}} \tag{9}$$

and

$$\psi_k = \pm \sqrt{\frac{\alpha}{\Gamma}} \frac{T_k}{m_k \sqrt{1 + q^2}}. \tag{10}$$

Thus, there are waves moving along and against the flow; their linear velocity relative to the flow $\sigma_k/m_k - V = \pm\sqrt{\alpha \Gamma (1 + q^2)}/m_k$, all other conditions being equal, is the greater the greater the dimension of the wave along the meridian (that is, the lesser the $m_k$ value). The amplitude of the wave in the $\psi$ field, first of all, is proportional to the amplitude of the wave in the temperature field, and second, is the greater the lesser the q value, that is, the lesser the ratio of the wave length vertically to the wave length along the meridian. The superposing of such waves can give a rather mottled pattern.

We emphasize that these wave solutions are precise solutions of a nonlinear system of equations. However, the described waves do not interact with one another (there is no energy exchange) and this means that one of the important characteristics of virtually any nonlinear process has not found its reflection in solutions determined by formulas (2)-(10).

It is possible to find the interacting waves if it is noted that with N = 3 it is not mandatory to require annulment of a fluctuation with the combination frequency $(\ )_k + (\ )_j$. In this case there should be terms compensating the combination frequencies. We introduce the hypothesis of weak interaction, namely that the amplitudes of the triplet $\psi_k$, $T_k$; k = 1, 2, 3 are not great and slowly change with time so that the order of magnitude of the parameters $d\psi_k/dt$, $dT_k/dt$ and the quadratic terms $\psi_k\,\psi_j$, $\psi_k T_j$ is identical.

We will seek the solution of (1') in the form

$$\left.\begin{aligned}\psi &= \psi_0 - Vz + \sum_{k=1}^{3} \psi_k(t)\, e^{i(\ )_k} \\ T &= \sum_{k=1}^{3} T_k(t)\; e^{i(\ )_k}\end{aligned}\right\} . \qquad (11)$$

Substituting (11) into (1'), we obtain (summation occurs everywhere from 1 to 3; therefore, in the future the summation limits will not be indicated)

$$\left.\begin{aligned}&\Sigma\left(-\rho_k^2 \frac{d\psi_k}{dt}\, e^{i(\ )_k}\right) + i\,\Sigma\sigma_k \rho_k^2 \psi_k\, e^{i(\ )_k} + [\Sigma(-im_k \rho_k^2 \psi_k)\times \\ &\times \Sigma\, in_j \psi_j\, e^{i(\ )_j} - (V - \Sigma\, in_k \psi_k\, e^{i(\ )_k})\cdot\Sigma(-im_j \rho_j^2 \psi_j e^{i(\ )_j})] = \\ &= i\alpha\Sigma\, T_k m_k\, e^{i(\ )_k}\end{aligned}\right\} , \qquad (12)$$

$$\left.\begin{aligned}&\Sigma\, \frac{dT_k}{dt}\, e^{i(\ )_k} - i\,\Sigma\sigma_k T_k e^{i(\ )_k} + [\Sigma\, m_k \psi_k e^{i(\ )_k}\cdot \Sigma\, n_j T_j e^{i(\ )_j} - \\ &- (-V + i\,\Sigma\, n_k \psi_k e^{i(\ )_k})\cdot \Sigma\, im_j T_j e^{i(\ )_j} = -\Gamma\,\Sigma\, im_k \psi_k e^{i(\ )_k}\end{aligned}\right\} . \qquad (13)$$

The linear (final) terms give the expressions (4) and (8); we will not repeat them. They determine the phase velocities of the triplet

$$\sigma_k = m_k V \pm m\sqrt{\alpha\Gamma}/\rho_k \qquad (14)$$

and the relationship between the amplitudes of the waves

$$\psi_k = \pm\sqrt{\alpha/\Gamma}\, T_k/\rho_k. \qquad (15)$$

In order to compensate the small terms it is necessary to require that each combination frequency, that is, the sum of two interacting frequencies $(\ )_k + (\ )_j$, be equal to the third, for example,

$$(m_1 y + n_1 z - \sigma_1 t) + (m_2 y + n_2 z - \sigma_2 t) = (m_3 y + n_3 z - \sigma_3 t) \qquad (16)$$

and similarly $(\ )_2 + (\ )_3 = (\ )_1$; $(\ )_3 + (\ )_1 = (\ )_2$. Since the components of the wave vectors $m_k$, $n_k$ can be of different signs, the same as $\sigma_k - m_k V$, without loss of universality it is possible to write expression (16) and two expressions similar to it in the simple form

$$[(m_1 + m_2 + m_3)\, y + (n_1 + n_2 + n_3) z - (\sigma_1 + \sigma_2 + \sigma_3)\, t] = 0.$$

Since this should be satisfied for any y, z and t, we obtain two expressions for the components of the wave vectors

$$\left.\begin{array}{l} m_1 + m_2 + m_3 = 0 \\ n_1 + n_2 + n_3 = 0 \end{array}\right\} \quad (17)$$

and one expression for the phase velocities of waves

$$\sigma_1 + \sigma_2 + \sigma_3 = 0. \quad (17')$$

This synchronism condition, after the substitution (14) and allowance for the first expression from (17), assumes the form

$$m_1 \rho_1 + m_2 \rho_2 + m_3 \rho_3 = 0. \quad (18)$$

Thus, the triplet can be in resonance interaction only under the condition that their wave vectors and phase velocities satisfy expressions (17)-(18).

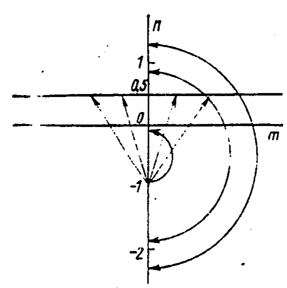


Fig. 1. Locus of points of ends of pairs of vectors which can interact with the vector (0, -1) (limiting case).

II. Analysis of interacting wave vectors. On the plane of wave vectors (m, n) it is necessary to find a trio of points which are related by formulas (17)-(18). We note, first of all, that formulas (17)-(18) are symmetric relative to the subscripts and since $m_k$ and $n_k$ can have arbitrary signs it is sufficient to limit ourselves to an examination of one quadrant, for example IV: $m \geqslant 0$; $n \leqslant 0$ (see Fig. 1). For $m \leqslant 0$ the picture will be a mirror reflection relative to the n-axis, for $n \geqslant 0$ -- relative to the m-axis.

One of the vectors, for example ($m_3$, $n_3$), should be stipulated and it is necessary to find the locus of pairs of points ($m_1$, $n_1$); ($m_2$, $n_2$), which can interact with the stipulated vector. The answer is ambiguous since there is not only one pair of numbers, but a locus, and therefore with stipulated ($m_3$, $n_3$) for the remaining four numbers there are only three correlations. First we will examine a limiting case when $m_3 = 0$ and $n_3$ is arbitrary, that is, one wave is "infinite" in length along y. [Except for the case $n_3 = 0$. With $m_3 = n_3 = 0$ in actuality there are two waves in the solution (11), which, as is easy to see, do not interact with one another.] It follows from (17)-(18) that $m_1 = m_2 = 0$ and the locus of the pairs of points is situated on the vertical axis (n); the pairs of points satisfy the expression $n_1 + n_2 = -n_3$; or -- $m_1 = -m_2 \neq 0$, and then

$$\sqrt{m_1^2 + (-n_3 - n_1)^2} - \sqrt{m_1^2 + n_1^2} = 0 \Rightarrow n_1 = -1/2n_3,$$

that is, the pair of vectors interacting with the (0, -n) vector is situated symmetrically relative to the n-axis. Thus, the locus of the points in this case involves two mutually perpendicular straight lines: one is the n-axis and the other is a straight line parallel to the m-axis and separated from it by the distance $n = -1/2\ n_3$. Figure 1 shows these straight lines and examples of pairs of vectors interacting with the vector $(0, n_3)$ and with $n_3 = -1$. (If $n_3 \neq -1$, it is necessary simply to change the scale by a factor of $|n_3|$).

In a general case it is convenient to make an analysis of the system of equations (17)-(18) in polar coordinates $m = \rho \cos \varphi$, $n = \rho \sin \varphi$.

Now (17)-(18) are rewritten in the form

$$\left.\begin{array}{c}\rho_1 \cos \varphi_1 + \rho_2 \cos \varphi_2 = -\rho_3 \cos \varphi_3; \quad \rho_1 \sin \varphi_1 + \rho_2 \sin \varphi_2 = -\rho_3 \sin \varphi_3 \\ \cos \varphi_1 + \cos \varphi_2 = -\cos \varphi_3\end{array}\right\}. \quad (19)$$

The system (19) can be simplified by introducing the ratios $\rho_1/\rho_3 = \varkappa_1$; $\rho_1/\rho_3 = \varkappa_2$. (In the sense $\varkappa_1, \varkappa_2 > 0$). We obtain

$$\left.\begin{array}{l}\varkappa_1 \cos \varphi_1 + \varkappa_2 \cos \varphi_2 = -\cos \varphi_3 \\ \varkappa_1 \sin \varphi_1 + \varkappa_2 \sin \varphi_2 = -\sin \varphi_3 \\ \cos \varphi_1 + \cos \varphi_2 = -\cos \varphi_3\end{array}\right\}. \quad (20)$$

The problem is reduced to the following: with a stipulated wave vector, lying on a single circle, find the possible pairs of vectors $\varkappa_1, \varphi_1; \varkappa_2, \varphi_2$, forming a resonance triplet.

We will note some corollaries which follow easily from system (20); $\varkappa_1$ and $\varkappa_2$ cannot be of different orders of magnitude. Assuming the opposite $(1 \ll \varkappa \ll \varkappa_2)$, we see that $\varkappa_2 \cos \varphi_2 \approx 0 \Rightarrow \varphi_2 \approx \pm \pi/2$ and $\varkappa_2 \sin \varphi_2 \approx 0 \Rightarrow \varphi_2 \approx 0; \pi$, that is, we obtain a contradiction. If $\varkappa_1 \ll 1$, then $\varkappa_2 \cos \varphi_2 = -\cos \varphi_3$ and $\varkappa_2 \sin \varphi_2 \approx -\sin \varphi_2 \Rightarrow \varkappa_2^2 \approx 1$. This means that if one of the triplet vectors is small the other two in absolute value will be close to unity. Then we will examine a case when $\varkappa_1, \varkappa_2 \gg 1$. It is evident that this is possible only when $\cos \varphi_1 \approx -\cos \varphi_2$ and $\sin \varphi_1 \approx -\sin \varphi_2$. It therefore follows that $\varphi_2 \approx \pi + \varphi_1$ and that $\cos \varphi_3 \approx 0 \Rightarrow \varphi_3 \approx \pm \pi/2$, that is, a pair of "large" wave vectors can interact only with a vector for which $|m_3| \ll |n_3|$, Then, by virtue of symmetry of the system relative to the subscripts 1 and 2 the locus of the points will be a curve with two axes of symmetry. The curve has four points in common with the circle $\rho = 1$. These points are arranged in the following way: $\varphi_3 \pm 2\pi/3$ and $\pm \varphi_3 + \pi$. With $\varphi_3 = 0$ $(m_3 = 1;\ n_3 = 0)$ the second pair of points merges into one -- the curve touches the circle on the outside. With $\varphi_3 = -\pi/6$ the points $\varphi_3 - 2\pi/3$ and $\pi + \varphi_3$ merge -- the curve touches the circle from the inside. Thus, with different $\varphi_3$ angles the curves can pass through one and the same points of the circle (two points), for example, for $\varphi_3 = -\pi/18$ and $\varphi_3 = -8/9\pi$ such points will be $\varphi = 10/9\pi$ and $\varphi = 17/18\pi$.

The first two equations of system (20) are a system of linear equations relative to $\varkappa_1$ and $\varkappa_2$. Accordingly, the procedure for computing the locus of the points of the ends of the pairs of vectors, interacting with given $(\varphi_3)$, is carried out most simply in the following way. Stipulating $\varphi_3$ and $\varphi_2$, we will determine $\varphi_1$ from the third equation (there may be either two solutions or none). This means that the coefficients on $\varkappa_1$ and $\varkappa_2$ become known after $\varkappa_1$ and $\varkappa_2$ (only positive solutions are suitable) are found using the formulas

$$\varkappa_1 = \frac{\sin(\varphi_3 - \varphi_2)}{\sin(\varphi_2 - \varphi_1)}, \quad \varkappa_2 = -\frac{\sin(\varphi_3 - \varphi_1)}{\sin(\varphi_2 - \varphi_1)}.$$

As we saw above, the denominator can be close to zero only for $\varphi_3 \approx \pm\pi/2$, and then $\varphi_2 \approx \varphi_1 \approx 0$ or $\varphi_2 \approx \varphi_1 + \pi$ ; this is the case which is close to the limiting case represented in Fig. 1.

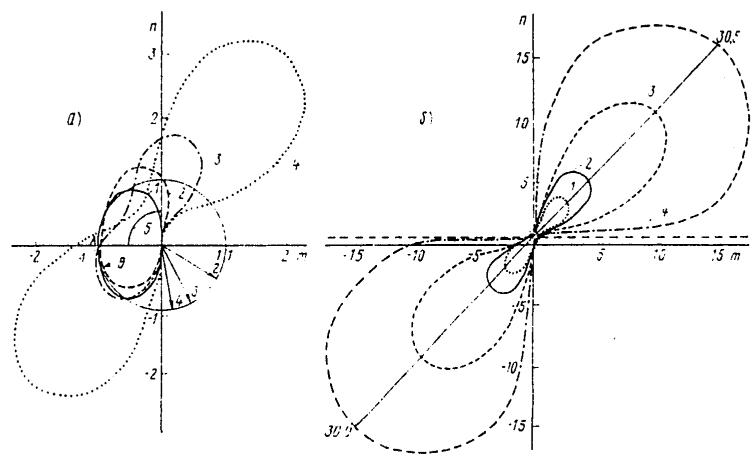

Fig. 2. Locus of pairs of ends of vectors which can interact with a stipulated vector. The numbers of the four curves correspond to the numbers of the stipulated vectors. a) 1) $\varphi_3 = 0°$; 2) $\varphi_3 = -30°$; 3) $\varphi_3 = -60°$; 4) $\varphi_3 = -80°$; 5) circle of the radius r = 0.5 -- locus of centers of curves. The point A ($\varphi = \pi$) is double, where curve 1, corresponding to $\varphi_3 = 0$, touches circles of a unit radius from the outside. The point B($\varphi = 7/6\,\pi$) is double, corresponding to $\varphi_3 = -\pi/6$, touching circles of a unit radius from within. b) 1) $\varphi_3 = -80°$ (that is, curve 4 in Fig. 2a); 2) $\varphi_3 = -85.0°$; 3) $\varphi_3 = -87.5°$; 4) $\varphi_3 = -89.0°$. For curve 4 the scales are not adhered to for the length of the "lobes": the numbers at the ends of the maximum diameter indicate the approximate $\varkappa_1$ and $\varkappa_2$ values. The dashed line represents the limiting straight line n = 0.5.

It is easy to establish that as in the case of Rossby waves [6], with $\varphi_3 = 0$ the locus of the points is an oval curve; its minimum diameter lies on the m-axis and is equal to 1; the maximum diameter is parallel to the n-axis and is equal to $\sqrt{3}$. Figure 2a shows the curves corresponding to four $\varphi_3$ values. As indicated by computations, the locus of the centers of the curves is a circle of the radius 0.5.

With approach of $\varphi_3$ to $-\pi/2$ the "lobes" are broadened and elongated, the "waist" is narrowed, and at the limit with $\varphi_3 \to -\pi/2$ the contours of the "lobes" tend to occupy the values -- n-axis and the line n = 1/2, shown in Fig. 1, whereas the "waist" is drawn to the point (0, 1/2). The tendency to a limiting value is slow, as is illustrated in Fig. 2b, which, at a scale reduced by a factor of 5 in comparison with Fig. 2a, shows curves corresponding to $\varphi_3$ values close to $-\pi/2$. With movement of the end of the stipulated vector for the unit circle from 0 to $-\pi/2$ the maximum diameter of the curve (the same as the minimum diameter) rotates by a half-angle and when $\varphi_3 = -\pi/2$ attains values $\pi/4$. Thus, for the stipulated vector ($m_3$, $n_3$) (length of 1) the pair of vectors is situated at the ends of the diameter of the corresponding curve. If the length of the stipulated vector ($m_3$, $n_3$) is changed by a factor of $\rho_3$, all the scales also change by a factor of $\rho_3$. (In this sense and also for Rossby waves the first three figures cited in [6] in actuality should duplicate one another; there is only a change in scales along both axes. The fourth figure and its interpretation are not entirely precise, which is associated primarily with the simplifications adopted in order to facilitate analysis of "very long" waves).

III. Analysis of amplitude functions. The "small" terms have remained in expressions (12) and (13). Equating of these terms gives a system of nonlinear equations for amplitude functions. From equation (12) we obtain

$$\left.\begin{aligned} \rho_1^2 \frac{d\psi_1}{dt} &= [m_2 n_3 - m_3 n_2](\rho_2^2 - \rho_3^2)\, \psi_2 \psi_3 \\ \rho_2^2 \frac{d\psi_2}{dt} &= [m_3 n_1 - m_1 n_3](\rho_3^2 - \rho_1^2)\, \psi_3 \psi_1 \\ \rho_3^2 \frac{d\psi_3}{dt} &= [m_1 n_2 - m_2 n_1](\rho_1^2 - \rho_2^2)\, \psi_1 \psi_2 \end{aligned}\right\} . \quad (21)$$

The expressions in brackets are equal to one another, as can be confirmed easily by using expressions (17). (This is easily understood from "vector" considerations: the triplet of vectors forms a triangle and each bracket is a result of the vector product of two sides of the triangle, that is, is equal to double the area of the triangle). Therefore, we will denote [ ] as a.

System (21) has two integrals which can contain arbitrary parameters. In order to obtain one integral we will multiply the first equation by $(A/\rho_3^2\rho_2^2 + B + C\rho_1^2)$, the second by $(A/\rho_1^2\rho_3^2 + B + C\rho_2^2)$, the third by $(A/\rho_1^2\rho_2^2 + B + C\rho_3^2)$ and add. On the right-hand side we obtain zero and after integration we find the "conservation law" in the general form

$$\Sigma \left( \frac{A}{\rho_{k-1}^2 \rho_{k+1}^2} + B + C\rho_k^2 \right) \psi_k^2 = \text{const} = M \quad (\rho_0 = \rho_3;\ \rho_4 = \rho_1), \quad (22)$$

where A, B, C, M are constants. The latter is determined from initial data, that is, with t = 0 $\psi_{k0}$ should be known, and thus M is equal to the value of the sum in (22) with the replacement of $\psi_k^2$ by $\psi_{k0}^2$. With A = C = 0 expression (22) can be interpreted as conservation of the "density" energy of the triplet, that is, the sum of the energy of the waves, multiplied by the "area" of the wave vector ($\rho_k^2$), and with A = B = 0 (by analogy with Rossby waves) as conservation of "vorticity." With $A \neq 0$ an interpretation is difficult. Such a great arbitrariness (three free parameters: A, B, C) evidently is attributable entirely to the simplification of the weak interaction, since for the initial system of equations (1') it is not possible to find the conservation law in such general form. In order to obtain another integral we multiply the first equation by $\psi_1/(\rho_2^2 - \rho_3^2)$, the second by $\psi_2(\rho_3^2 - \rho_1^2)$ and subtract. After integration we obtain

$$\rho_1 \psi_1^2/(\rho_2^2 - \rho_3^2) - \rho_2^2 \psi_2^2/(\rho_3^2 - \rho_1^2) = N_1 = \text{const.} \qquad (23)$$

Combining in completely the same way, for example, the second and third equations, it is possible to obtain the expression

$$-\rho_2^2 \psi_2^2/(\rho_3^2 - \rho_1^2) + \rho_3^2 \psi_3^2 (\rho_1^2 - \rho_2^2) = N_2 = \text{const.} \qquad (23')$$

However, the integrals (22) and (23), (23') are linearly dependent, as is easily confirmed, computing the rank of the matrix from the coefficients on $\psi_k^2$. It is equal to 2.

Since with equal moduli of the wave vectors no energy exchange occurs, without limiting universality it can be assumed that $\rho_1 > \rho_2 > \rho_3$. (This means that $N_1 > 0$, $N_2 > 0$). It follows from (21) that

$$\frac{\rho_1^2}{\rho_2^2 - \rho_3^2} \frac{d\psi_1^2}{dt} = \frac{\rho_2^2}{\rho_3^2 - \rho_1^2} \frac{d\psi_2^2}{dt} = \frac{\rho_3^2}{\rho_1^2 - \rho_2^2} \frac{d\psi_3^2}{dt} = 2a\psi_1\psi_2\psi_3.$$

It is clear that if the sign on $a\psi_1\psi_2\psi_3$ is positive, then $\psi_1^2$ and $\psi_3^2$ increase -- there is "suction" of energy from the middle to the outer waves; if $a\psi_1\psi_2\psi_3 < 0$, the picture is the opposite -- there is an increase in the modulus of the amplitude of the middle wave at the expense of the outer waves. There can be no other situations.

After this brief analysis it is possible to rewrite system (21) in one of two equivalent forms (the parameters are dimensionless):

$$\psi_1' = \psi_2\psi_3; \quad \psi_2' = -\psi_1\psi_3; \quad \psi_3' = \psi_1\psi_2, \qquad (21')$$

or

$$\psi_1' = -\psi_2\psi_3; \quad \psi_2' = +\psi_1\psi_3; \quad \psi_3' = -\psi_1\psi_2. \qquad (21'')$$

Excluding $\psi_1$ and $\psi_3$ in any of these systems using expressions of the type (23), which in dimensionless form are written $\psi_1^2 + \psi_2^2 = P_1^2$; $\psi_3^2 + \psi_2^2$; $P_1$, $P_2$ are constants, we obtain an equation for $\psi_2$, leading to an elliptical integral of the first kind [1] $F(\varphi\backslash\alpha)$. [$P_1 \neq P_2$; in the opposite case a divergent interval is obtained.]

$$t - t_0 = \int_{\psi_{20}}^{\psi_2} \frac{d\psi_2}{\sqrt{(P_1^2 - \psi_2^2)(P_2^2 - \psi_2^2)}} = F(\varphi\backslash\alpha) - F(\varphi_0\backslash\alpha),$$

where

$$\varphi = \arcsin \psi_2/P_2; \quad \varphi_0 = \arcsin \psi_{20}/P_2; \quad (P_1 > P_2); \quad \sin\alpha = P_2/P_1.$$

The subscript 0 denotes the value at the initial moment.

Now it is easy to compute $\psi_1$ and $\psi_3$ using the formulas for $P_1^2$ and $P_2^2$. In order to simplify the computations and for greater clarity we assume for the initial moment $t_0 = 0$ and $\psi_{20} = 0$. Then the solution for $\psi_1$, $\psi_2$ and $\psi_3$ acquires an especially simple form when using elliptical Jacobi functions. Specifically

$$\psi_1 = P_1 \,\mathrm{dn}\,(t|\alpha); \quad \psi_2 = P_2 \,\mathrm{sn}\,(t|\alpha); \quad \psi_3 = P_2 \,\mathrm{cn}\,(t|\alpha).$$

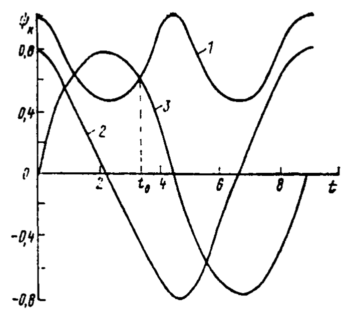


Fig. 3. Curves of change of amplitude functions with time (the parameters are dimensionless). 1) $\psi_1$; 2) $\psi_3$; 3) $\psi_2$.

Figure 3 shows $\psi_k$ curves for $P_2/P_1 = 0.8$. If at the initial moment $t_0$ $\psi_{20} \neq 0$, in Fig. 3 the t-axis must be displaced to the right by the $t_0$ value, and beginning the reading from the moment $t_0$, the curves are continued to a complete doubled period of the elliptical functions (with selected values of the parameters to 9.0 + $t_0$). The vertical dashed line shows an example when with $t = t_0$ $\psi_{20} \approx 0.6$ and $d\psi_2/dt < 0$.

It remained to analyze the behavior of the amplitude functions for temperature waves. Using (13) we obtain a system of three linear differential equations for three functions

$$\frac{dT_1}{dt} = m_2 n_3 \psi_2 T_3 - m_3 n_2 \psi_3 T_2$$

and two similar equations with a cyclic replacement of the subscripts. Although the system is linear, the coefficients on the right-hand sides are elliptical functions and therefore it is difficult to integrate it as a linear system. It is simpler to use the correlation between $\psi_k$ and $T_k$ (15) and obtain a system of nonlinear equations which now will be easy to integrate:

$$\frac{dT_1}{dt} = \sqrt{\alpha/\Gamma}\left[\frac{m_2 n_3}{\rho_2} - \frac{m_3 n_2}{\rho_3}\right] T_3 T_2 \qquad (24)$$

(and two similar systems). Since $m_k/\rho_k = \sigma_k$, and $\sigma_k$ conform to the synchronism condition (17'), it is easy to establish that one and the same number will stand in the brackets for all three functions. Thus, with an accuracy to one and the same factor for all three functions $T_k$ the system of nonlinear equations for T is the same as for $\psi_k$. The system (24) has an integral dependent on the parameters A and B. Multiplying each of the equations (24) by $AT_k + B\psi_k$ and adding, we obtain

$$\Sigma (AT_k^2 + BT_k \psi_k) = \text{const} = \Sigma (AT_{k0}^2 + BT_{k0} \psi_{k0}),$$

where the subscript 0 denotes the values at the initial moment.

After introducing the dimensionless parameters, system (24) assumes precisely the same form as (21') or (21") with the replacement of $\psi_k$ by $T_k$, and this means that its solution can be obtained simply from the solution for $\psi_k$.

***

Since wave triplets have been theoretically substantiated for waves of different nature, it is desirable to develop a common method for processing the observational data on the wind and temperature fields so that, on the one hand, the theory is reinforced, and on the other hand, so that the physical picture of nonlinear interaction of atmospheric processes will be refined. American meteorologists propose that correlation coefficients between the wave parameters be used for finding the interacting triplet of Rossby waves. Along these lines the finding of a triplet in the equatorial atmosphere requires greater care and involves more complexities than in the case of Rossby waves in accordance with the model in [6]. It can be shown that the triplet of Rossby waves can exist against a background of a zonal constant flow.

Note. Equations (17) are universal for any model of weak interaction in hydrodynamics since they are generated by the operator $(\psi, \Delta\psi)$. This determines the topological nature of the locus of points -- the triplet of vectors forms a triangle; two vectors (in absolute value) are close, because it follows from (20) that $|\varkappa_2 - \varkappa_1| \leqslant 1$. The specific form of the curve is determined by the phase velocities, that is, by the specific formulation of the problem.

BIBLIOGRAPHY

1. Abramovits, M., Stigan, I., SPRAVOCHNIK PO SPETSIAL'NYM FUNKTSIYAM (Manual on Special Functions), Moscow, Nauka, 1979.

2. Blinova, Ye. N., "Determination of the Velocity of Troughs and Ridges from a Nonlinear Vorticity Equation," PRIKLADNAYA MATEMATIKA I MEKHANIKA (Applied Mathematics and Mechanics), No 5-6, 1946.

3. Dobryshman, Ye. M., "Examples of Precise Solutions of Nonlinear Prognostic Equations," IZV. AN SSSR, SERIYA GEOFIZICH. (News of the USSR Academy of Sciences: Geophysical Series), No 2, 1961.

4. Dobryshman, Ye. M., "Wave Movements in the Equatorial Zone," METEOROLOGIYA I GIDROLOGIYA (Meteorology and Hydrology), No 1, 1977.

5. Dobryshman, Ye. M., DINAMIKA EKVATORIAL'NOY ATMOSFERY (Dynamics of the Equatorial Atmosphere), Leningrad, Gidrometeoizdat, 1980.

6. Longuet-Higgins, M. S., Gill, A. E., "Resonance Interaction of Planetary Waves," NELINEYNAYA TEORIYA RASPROSTRANENIYA VOLN (Nonlinear Theory of Wave Propagation), Moscow, Mir, 1970.

7. Sharinova, S. M., "Computation and Use of Examples of Precise Solutions of Nonlinear Prognostic Equations," TRUDY MMTs (Transactions of the Moscow Meteorological Center), No 4, 1964.

UDC 551.(513:509.313)

MODEL OF GENERAL CIRCULATION OF THE ATMOSPHERE USED AT THE USSR HYDROMETEOROLOGICAL CENTER

Moscow METEOROLOGIYA I GIDROLOGIYA in Russian No 11, Nov 80 pp 16-26

[Article by I. V. Trosnikov, candidate of physical and mathematical sciences, USSR Hydrometeorological Scientific Research Center, manuscript submitted 28 May 80]

[Text]

Abstract: The article describes a finite-difference model of general circulation of the atmosphere developed at the USSR Hydrometeorological Center. Basic information is given concerning the model: system of equations, spatial and temporal discretization, interpolation method. The model takes into account the principal physical processes forming the circulation: radiation, interaction with the underlying surface, turbulent mixing. The hydrological cycle, including the accumulation of water in the soil and the formation of the snow cover, is taken into account quite fully. The results of a numerical experiment for the modeling of January circulation are given.

1. Introduction. At the present time the numerical modeling of macroscale atmospheric processes is one of the principal methods for investigating general circulation of the atmosphere and also its evolution in the past and future. Using models of general circulation of the atmosphere it is possible to study the interaction of processes at different scales, synthesize into a unified picture the diverse and far from complete observations and using these data predict the future state of the atmosphere. Such a broad circle of problems, solvable by means of numerical models, determines their great diversity because a new problem can require modification of the entire model. At the same time, models of general circulation of the atmosphere have common structural and organizational characteristics. This makes it possible to have a common program "core" on the basis of which different variants of the model can be formulated. At the USSR Hydrometeorological Center specialists have developed such a program "core," including packets of control and servicing programs. It has served as a basis for creating several variants of a model of general circulation of the atmosphere. The following sections give a description of one of them, applied using the CDC-172 computer, and the results obtained in the reproduction of January circulation in the northern hemisphere.

# 2. Description of Model

## 2.1. Notations and System of Model Equations

### 2.1.1. List of notations

p is pressure, t is time, $\lambda$ is longitude, $\varphi$ is latitude; $\dot{C}$ is the rate of condensation. The quantity of condensing moisture per unit mass of dry air per unit time; $c_D$ is the drag coefficient; $D_x^y$ are the influxes of momentum (x = V), heat (x = T) and moisture (x = q) to a unit air mass per unit time caused by horizontal turbulence (y = H) and vertical turbulence (y = V); $\dot{E}$ is the evaporation rate. The quantity of water evaporating from a unit surface in a unit time; $f = 2\Omega \sin\varphi$ is the Coriolis parameter; $F_{\downarrow}$ is the flux of outgoing long-wave radiation at the upper boundary of the atmosphere; $F_s$ is the flux of short-wave solar radiation at the upper boundary of the atmosphere; $F_I^{\downarrow}$ is the effective long-wave radiation of the earth's surface; $F_s^S$ is the total short-wave radiation at the earth's surface; $\dot{H}$ is the turbulent heat flux at the earth's surface; k is a unit vector normal to the earth's surface; $k_M$, $k'_M$, $k''_M$ are horizontal turbulence coefficients; $k_V$ is the coefficient of vertical turbulence; $\dot{m}$ is the moisture content of the soil. The quantity of water in the meter layer of soil of a unit area; m is the rate of snow thawing. The quantity of thawing snow in a unit area in a unit time; n is the tenths of cloud cover; q is the mixing ratio; $q_a$ is the mixing ratio for surface air; $\dot{Q}_{RC}$ is the energy influx to a unit air mass, governed by radiation and convective processes; $\dot{P}$ is precipitation. The quantity of water falling on the earth's surface per unit area and unit time; $p_s$ is pressure at the earth's surface; $\dot{R} = F_s^S (1 - \alpha_s) = F_I^{\downarrow}$ is the radiation balance at the earth's surface; S is the depth of the snow cover. The quantity of snow per unit surface, determined as the equivalent quantity of water, multiplied by 10; $\dot{S}$ is the intensity of falling of the snow. The quantity of snow falling on a unit area in a unit time; T is air temperature; $T_a$ is temperature of the surface air; $T_s$ is temperature of the ground surface; $t_r$ is the relaxation time of radiation processes; V is horizontal wind velocity; u is the V component directed along $\lambda$; v is the V component directed along $\varphi$; $V_s$ is the velocity of surface air;

$$\tilde{\mathbf{V}}(p) = \frac{1}{p_s}\int_0^p V\,dp$$

is integral velocity; z is the altitude of the isobaric surface; $z_T$ is altitude of the tropopause; $\alpha$ is planetary albedo; $\alpha_s$ is the albedo of the underlying surface; $\delta\lambda$, $\delta\varphi$, $\delta p$, $\delta t$ are the discretization intervals in space and time; $\nu(x)$ is a step function equal to zero when $x \leqslant 0$, equal to unity when $x > 0$; $\tau$ is the vector of frictional stress; $\tau_\lambda$, $\tau_\varphi$ are the components of the $\tau$ vector directed along $\lambda$ and $\varphi$; $\theta = T(p_0/p)^{\varkappa}$ is potential temperature; $\omega = dp/dt$ is vertical velocity in a p-coordinate system; $a = 6.37 \cdot 10^6$ m is the earth's radius; $c_p = 1005$ J/(kg·K) is the specific heat capacity of dry air at a constant pressure; $c_v = 718$ J/(kg·K) is the specific heat capacity of dry air at a constant volume; $g = 9.81$ m/sec$^2$ is the acceleration of free falling; $L = 2.501 \cdot 10^6$ J/kg is the latent heat of condensation of water vapor; $p_0 = 1000$ mb is standard pressure; R = 287 J/(kg·K) is the gas constant of dry air; $R_v = 461.5$ J/(kg·K) is the gas constant of water vapor; $\gamma_m = 6.5$°C/km is the standard vertical temperature gradient; $\varkappa = R/c_p = 0.288$; $\sigma = 5.67 \cdot 10^{-8}$ W/(m$^2$·K$^4$) is the Stefan-Boltzmann constant; $\Omega = 7.29 \cdot 10^{-5}$ sec$^{-1}$ is the angular velocity of the earth's rotation.

### 2.1.2. System of Equations

$$\frac{\partial X}{\partial t} = F_1(X, Y) + F_2(X, Y) + Q,$$

$$\frac{\partial Y}{\partial p} = GX,$$

$$F_1 = \begin{Vmatrix} -\nabla \cdot VV - \frac{\partial \omega V}{\partial p} \\ -\nabla \cdot VT - \frac{\partial \omega T}{\partial p} \\ -\nabla \cdot Vq - \frac{\partial \omega q}{\partial p} \\ 0 \\ 0 \\ 0 \end{Vmatrix}, \quad F_2 = \begin{Vmatrix} -fk \times V - g\nabla z \\ \frac{RT\omega}{pc_p} \\ 0 \\ 0 \\ 0 \\ -\nabla \cdot p_s \tilde{V}(p_s) \end{Vmatrix},$$

$$Q = \begin{Vmatrix} D_V^H + D_V^V \\ D_T^H + D_T^V + (\dot{Q}_{RC} + L\dot{C})/c_p \\ D_q^H + D_q^V - \dot{C} \\ (1 - \nu(s))(\dot{P} - \dot{E}) - 0{,}1\,\dot{m} \\ \dot{S} - 10\,\dot{E} - \dot{m} \\ 0 \end{Vmatrix}, \quad G = \begin{Vmatrix} -\nabla & 0 & 0 & 0 & 0 & 0 \\ 0 & -R/gp & 0 & 0 & 0 & 0 \\ 1 & 0 & 0 & 0 & 0 & 0 \end{Vmatrix},$$

$$X = \begin{Vmatrix} V \\ T \\ q \\ m \\ S \\ p_s \end{Vmatrix}, \quad Y = \begin{Vmatrix} \omega \\ z \\ \tilde{V} \end{Vmatrix}, \quad D_V^{H,V} = \begin{Vmatrix} D_u^{H,V} \\ D_v^{H,V} \end{Vmatrix},$$

$$\nabla \cdot VX = \frac{1}{a\cos\varphi}\left(\frac{\partial uX}{\partial \lambda} + \frac{\partial vX\cos\varphi}{\partial \varphi}\right),$$

$$\nabla X = \left(\frac{1}{a\cos\varphi}\frac{\partial X}{\partial \lambda}, \quad \frac{1}{a}\frac{\partial X}{\partial \varphi}\right),$$

$$\Delta X = \frac{1}{a^2\cos\varphi}\left(\frac{1}{\cos\varphi}\frac{\partial^2 X}{\partial \lambda^2} + \frac{\partial}{\partial \varphi}\cos\varphi\frac{\partial X}{\partial \varphi}\right).$$

### 2.2. Vertical Structure of Model

Figure 1a shows the vertical structure of the model and the method for stipulating the sought-for variables. In those cases when it is necessary to predetermine the function at the level where it has not been determined this is done by linear interpolation.

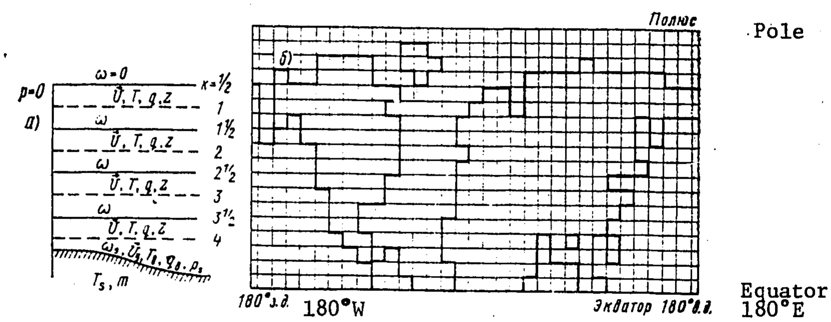


Fig. 1. Grid region. a) vertical structure of model; b) latitude-longitude grid of model.

2.3. Integration Region

The integration of the model equations is carried out in a latitude-longitude grid determined by the parameters: NF = 18 is the number of latitudes, ML = 32 is the number of longitudes (Fig. 1b). The grid points whose indexing is determined by the number of the latitude i and the number of the longitude j, have the coordinates:

$$\varphi = 90° + (1/2 - i)\,\delta\varphi, \quad i = 1, \ldots, NF;$$

$$\lambda = -180° + (j - 1)\,\delta\lambda, \quad j = 1, \ldots, ML.$$

where $\delta\varphi = 5°$, $\delta\lambda = 11.5°$.

2.4. Boundary Conditions

At the upper boundary of the atmosphere with p = 0 it is assumed that vertical velocity $\omega$, integral velocity $\tilde{V}$ and the fluxes of momentum, heat and moisture become equal to zero. The fluxes of momentum, heat and moisture are stipulated at the underlying surface with $p = p_s$.

At the lateral boundaries along $\lambda$ natural periodicity conditions are assumed and along $\varphi$ are assumed in the zone $\partial z/\partial\varphi = 0$, together with limitation of wind velocity; at the equator $\partial z/\partial\varphi = 0$ and v = 0.

2.5. Spatial Approximation

In approximating the model system of equations use is made of finite-difference formulas making it possible, in the case of absence of fluxes and internal sources at the lateral boundaries, to "conserve" the quadratic integrals [9, 11]. In the notations generally employed in the meteorological literature

$$\bar{a}^x = \frac{1}{2}(a_{i+1/2} + a_{i-1/2}), \quad \delta_x a = a_{i+1/2} - a_{i-1/2},$$

these expressions can be written as follows:

$$\frac{\partial X}{\partial \lambda} = \frac{\overline{\delta_\lambda X^\lambda}}{\delta \lambda} + O(\delta\lambda^2), \quad \frac{\partial X \cos\varphi}{\partial \varphi} = \frac{\delta_\varphi(\overline{X^\varphi}\cos\varphi)}{\delta\varphi} + O(\delta\varphi^2),$$

$$\frac{\partial XY\cos\varphi}{\partial\varphi} = \frac{\delta_\varphi(\overline{X^\varphi}\,\overline{Y^\varphi}\cos\varphi)}{\delta\varphi} + O(\delta\varphi^2), \quad \frac{\partial XY}{\partial\lambda} = \frac{\delta_\lambda(\overline{X^\lambda}\,\overline{Y^\lambda})}{\delta\lambda} + O(\delta\lambda^2),$$

$$\frac{\partial \omega X}{\partial p} = \frac{\delta_p(\omega \overline{X^p})}{\delta p} + O(\delta p^2).$$

2.6. Time Integration

For time integration of the model equations use is made of a modified Euler iteration scheme proposed in [10],

$$X^* = X^k + \delta t(F_1^k + F_2^k),$$

$$X^{k+1} = X^k + \delta t((1-w_1)F_1^k + w_1 F_1^*) + \delta t((1-w_2)F_2^k + w_2 F_2^*),$$

where k is the number of the time interval, $\delta t$ is the time interval, equal to 15 minutes. [The author expresses appreciation to Doctor I. Kurihara, who directed his attention to this integration method.]

The weights $w_1$ and $w_2$ are equal to 0.506 and 3.0 respectively.

2.7. Filtering

Fourier filtering of the V, T and $p_s$ fields is used in suppressing the parasitic modes arising in the integration of the model equations, especially in the polar regions, which is associated with the closer spacing of the grid points and with a given time interval impairment of the computational stability condition. In the filtering of wind velocity first there is transformation from the spherical components of the velocity vector to the velocity components in the stereographic plane

$$\overline{u} = -u\sin\lambda - v\cos\lambda, \quad \overline{v} = u\cos\lambda - v\sin\lambda.$$

After filtering there is reverse transformation to spherical components. The filtering parameters are similar to those used in [6].

2.8. Physical Processes

2.8.1. Macroturbulence

The macroturbulent exchange of momentum, heat and moisture by small eddies, which cannot be described by the finite-difference scheme in the model, is taken into account on the basis of very simple hypotheses concerning the nature of the macroturbulent regime of the atmosphere and its inclusion in the model was selected in the form described in [8],

$$D_u^H = k_M^u \Delta u, \quad D_v^H = k_M^v \Delta v, \quad D_T^H = k_M^T \Delta T, \quad D_q^H = k_M^q \Delta q,$$

$$k_M^u = k_0|\Delta u|, \quad k_M^v = k_0|\Delta v|, \quad k_M^T = k_0'|\Delta T|, \quad k_M^q = k_0''|\Delta q|,$$

where $k_0 = 10^{15}$ $m^3$, and $k'_0$ and $k''_0$ are selected at each latitude from the condition that the mean value of the corresponding coefficient of macroturbulent exchange at this latitude is equal to the mean value $(k_M^u + k_M^v)/2$.

2.8.2. Vertical Diffusion

The change in momentum, heat and moisture caused by vertical turbulent mixing are determined by the following formulas:

$$D_u^V = \frac{1}{\rho}\frac{\partial}{\partial z}\rho k_V \frac{\partial u}{\partial z}; \quad D_v^V = \frac{1}{\rho}\frac{\partial}{\partial z}\rho k_V \frac{\partial v}{\partial z},$$

$$D_T^V = \frac{1}{\rho}\frac{\partial}{\partial z}\rho k_V \frac{\partial \theta}{\partial z}, \quad D_q^V = \frac{1}{\rho}\frac{\partial}{\partial z}\rho k_V \frac{\partial q}{\partial z},$$

where the coefficient of vertical turbulence $k_V = 10\ m^2/sec$ in the lower troposphere and zero above.

2.8.3. Fluxes at the Underlying Surface

Frictional stress, the fluxes of heat and moisture at the underlying surface are determined using the formulas

$$\tau = -\rho c_{DH}|V_s|V_s,$$

$$\dot{H} = \rho c_D c_p |V_s|(T_s - T_B),$$

[B = air]

$$\dot{E} = \rho c_D |V_s|(q_s(T_s) - q_B)\beta.$$

For determining evaporation the surface mixing ratio of air $q_s$ is determined as:

$$q_s(T_s) \quad q^*(p_s, T_s) \qquad \text{over the ocean}$$

[B = air]

$$q_s(T_s) = q^*(p_s, T_B)\left(1 + \frac{L(T_s - T_B)}{R_v T_B^2}\right) \qquad \text{over the land}$$

and the mixing ratio with a saturation corresponding to a particular pressure and temperature is determined using the Magnus formula

$$q^*(p, T) = \frac{3.7942}{p}\, 10^{\frac{7.63\,T - 2082}{T - 31}}$$

for pressure, expressed in millibars and temperature, expressed in °K. The determination of the $\beta$ coefficient is given in the next section. The drag coefficients $c_{DH}$ and $c_D$ are determined using a scheme proposed in [5].

$$c_{DH} = 0{,}002 + 1{,}2 \cdot 10^{-6} z_0 \qquad \text{over the land}$$

$$c_{DH} = 0{,}001\ (1 + 0{,}07|V_s|) \qquad \text{over the ocean}$$

$$c_D = c_{DH}/(1 - 7\,\delta T\,|V_s|), \quad \text{if} \quad \delta T = T_s - T_{air} < 0,$$

$$c_D = c_{DH}\,(1 + \sqrt{\delta T\,|V_s|}), \quad \text{if} \quad \delta T = T_s - T_{air} > 0.$$

In these formulas $z_0$ is the elevation of the terrain above sea level in meters. Since the drag coefficients are dependent on surface wind velocity and the temperature jump, these values in the computations are taken from the preceding time interval.

The wind velocity, temperature and humidity in the surface layer are determined on the assumption that in the lower layer of the model there is no accumulation of momentum, heat and moisture (see [5]).

2.8.4. Hydrology of the Land

A scheme proposed by M. I. Budyko [1] is used in determining evaporation from the land surface. With a soil moisture content m greater than half the critical value $m_c$ = 150 kg/m$^2$ -- the maximum quantity of water which can be stored in the meter soil layer, evaporation does not differ from the evaporation from the water surface. With lesser m values the evaporation rate decreases, which is determined by the $\beta$ coefficient:

$$\beta = 1 \text{ with } m \geqslant m_c/2, \quad \beta = 2\,m/m_c \text{ with } m < m_c/2.$$

The moisture content of the snow-free soil is determined by integration of the equation for m in the main system of the model. In a case when the soil is covered with snow the change in soil moisture content is determined only by the melting of the snow,

$$\frac{\partial m}{\partial t} = \dot{m},$$

and the coefficient $\beta = 1/2$.

The melting of the snow is dependent on the temperature of the surface air: $\dot{m} = 0$ with $T_{air} < 0°C$ and $\dot{m} = 5 \cdot 10^{-7}\,(T_{air} - 273)$ with $T_{air} > 0°C$.

The surface of an ice-covered ocean is dealt with in the same way. In this case $\beta = 0.25$.

2.8.5. Determination of Temperature of the Underlying Surface

The temperature of the ocean surface is assumed to be stipulated and the temperature of the underlying surface of the land and sea ice is determined from the heat balance condition: $\dot{R} = \dot{H} + L\dot{E}$. Since $\dot{H}$ and $\dot{E}$ are linearly dependent on $T_s$, then

$$T^{k-1} = T_s^k - \frac{\dot{R} - \dot{H}(T_s^k) - L\dot{E}\,(T_s^k)}{T_B^3 + \rho c_p |V_s| c_D \left(1 + \dfrac{q^*(T_B)\,L^2 \beta}{c_p R_v T_B^2}\right)},$$

where k is the number of the time interval.

2.8.6. Macroscale Condensation

Macroscale condensation processes are included in the form of a modification of the following algorithm: condensation occurs in those squares of a spatial grid in which the value of the mixing ratio exceeds some fraction $\varepsilon$ (in the experiments 85%) of the mixing ratio at a saturation corresponding to the pressure p and the temperature $T_0$ in the grid square $q^*(p_0, T_0)$. Assuming that the energy released in this case is expended only on a change in air temperature, then the process itself transpires up to the time when the new temperature $T_N$ and humidity $q_N$ values satisfy the relationship $q_N = \varepsilon q^*(p_0, T_N)$. Thus, in the course of the process the energy released will be equal to $c_p(T_N - T_0)$. Equating this expression to the energy equivalent of the released moisture, we obtain the equation

$$c_p (T_N - T_0) = L (q_0 - \varepsilon q^* (T_N )).$$

For its solution in each time interval use is made of one iteration by the Newton-Rafson method

$$T_N = T_0 - \frac{\frac{L}{c_p} (\varepsilon q^* (T_0) - q_0)/2^k}{1 + \frac{4251,63}{(T_0 - 31)^2} \varepsilon q^* (T_0)},$$

where k is minimum, making it possible to satisfy the condition

$$\dot{C} \delta t \equiv q_0 - \varepsilon q^* (T_N) \geqslant 0.$$

All the condensing moisture falls in the form of liquid precipitation or snow if the mean temperature in the lower layer of the atmosphere with a thickness of 340 m is below 0°C. This temperature is determined by linear interpolation using the temperature values at the lower level of the model and in the surface layer.

2.8.7. Radiation

The heat influxes to a unit air mass as a result of radiation and convective processes are computed by the method described in [4]. At the p level these influxes are determined using the formula

$$\dot{Q}_{RC} = \frac{c_p}{t_r} \left( T^* - T - \frac{1}{p_s} \int_0^{p_s} (T^* - T)\, dp \right) + \frac{g}{p_s} (F_s (1 - \alpha) - F_l - \dot{R}),$$

where $T^* = T_{air} - \gamma_m z$ with $z \leqslant z_T$ and $T^* = T_{air} - \gamma_m z_T$ with $z > z_T$. The altitude of the tropopause is stipulated as dependent on latitude. The relaxation time $t_r$ of the radiation processes is assumed equal to two weeks. The radiation fluxes are computed using the following formulas:

the flux of long-wave radiation passing through the upper boundary of the atmosphere [3]

[B = air] $$F_l = a + bT_B - (a_1 + b_1 T_B) n,$$

where $a = -800$, $b = 4.667$, $a_1 = 810$, $b_1 = 3.333$ are empirical coefficients (the dimensionality of the flux is cal/(cm$^2$·day));

the total short-wave radiation at the underlying surface is

$$F_s^s = 0{,}7\ F_s\,(0{,}29 + 0{,}71\ (1 - n));$$

the effective long-wave radiation of the earth's surface is

[B = air] $$F_i^l = \sigma T_{\text{в}}^3 (4\,(T_s - T_{\text{в}}) + T_{\text{в}}\,((0{,}25 - 0{,}004\ p_s/(q_{\text{в}} + 0{,}623))(1 - cn^2),$$

where c are empirical coefficients dependent on latitude [1].

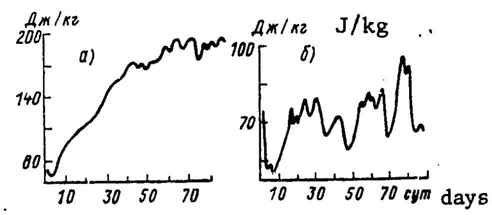


Fig. 2. Temporal change of the mean (for the entire atmosphere) zonal (a) and eddy (b) components of specific kinetic energy.

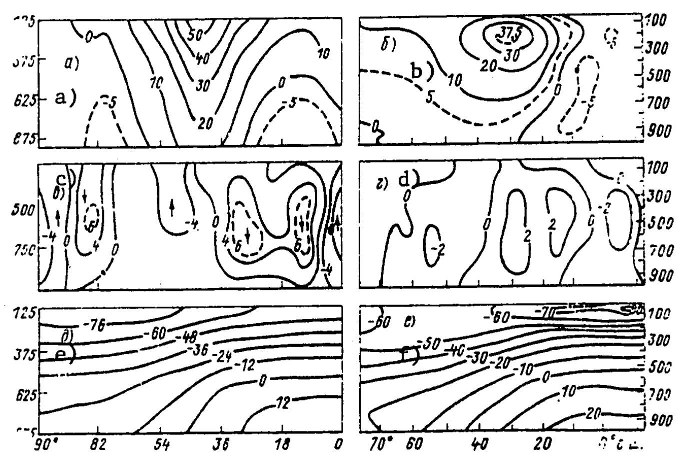


Fig. 3. January mean latitudinal distributions of meteorological elements. a) zonal velocity (m/sec) in model and b) according to [12], c) vertical velocity in model (dimensionless) and d) according to [12] ($10^{-1}$mb/sec), e) temperature (°C) in model and f) according to [12].

3. Numerical Experiment

Below we give some results of modeling of January circulation of the atmosphere in the northern hemisphere. As the initial conditions in the experiment we selected the fields of meteorological elements for 4 November 1969 [7]. The "boundary" conditions were fixed and corresponded to January: temperature of the ocean surface, zonal flux of solar radiation at the upper boundary of the atmosphere, surface albedo and tenths of cloud cover. Thus, the formation of January circulation proceeded from a state of the atmosphere corresponding to autumn conditions and transition to winter required about 1 1/2 months of model time. The presence of two circulation regimes -- transitional and quasistationary -- can be seen in Fig. 2a. It shows the temporal variation of the specific zonal kinetic energy averaged for the entire atmosphere. Its rapid increase during the first 45 days was associated with the transition from autumn to winter circulation. The further small temporal trend is associated with the slow cooling of the upper layers of the polar atmosphere continuing in the experiment. Figure 2b shows the behavior of the eddy part of the kinetic energy. Here one should note the first 20 days, when adaptation to winter conditions took place, after which a cyclogenesis-anticyclogenesis regime was established in the model. One should also note the relatively high level of the ratio of the zonal part of the kinetic energy to the eddy component.

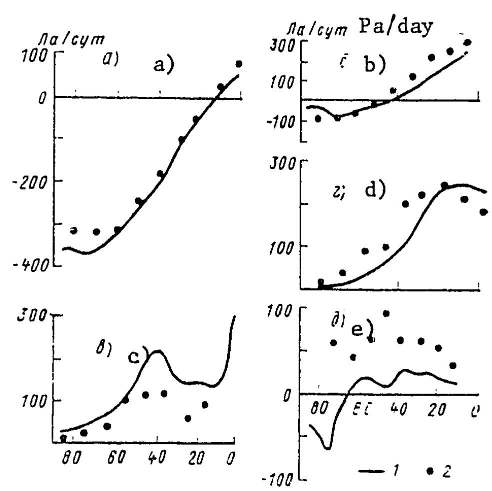


Fig. 4. January mean latitudinal fluxes. a) radiation balance at the upper boundary of the atmosphere according to model (1) and according to [13] (2), b) radiation balance at the surface according to model (1) and according to [1] (2), c) precipitation according to model (1) and according to [1] (2), d) evaporation according to model (1) and according to [1] (2), e) thermal flux according to model (1) and according to [1] (2).

The mean characteristics of January circulation, reproduced by the model, were obtained by 30-day averaging, beginning with the 60th day of model time. Figure 3 shows the mean latitudinal values of zonal velocity (a), vertical velocity (c) and temperature (e). As noted, in this experiment a somewhat reduced temperature was obtained in the upper troposphere of the polar regions, with its exaggeration in the tropics, which in the model led to the formation of a strong jet in the upper atmosphere (see Fig. 3a). Another peculiarity of the zonal flow, distinguishing it from the observed pattern (b), is the inadequate development of easterly winds in the tropical region, which occupy only the lower half of the troposphere. This peculiarity of the circulation is associated with the inadequate spatial resolution of the model. The structure of the circulation cells in the atmosphere (Hadley and Ferrel cells) can be seen in Fig. 3c, which shows the mean latitudinal vertical velocity $\omega$. A comparison with the observed pattern (d) shows a fairly good agreement of the maxima and minima, which indicates a quite precise reproduction of the circulation cells by the model.

Figure 4 shows the mean latitudinal values of the radiation, moisture and heat fluxes. On these graphs the dots represent the observed January values of the corresponding parameters. The comparison indicates a quite precise model reproduction of the peculiarities in the distribution of the radiation and moisture fluxes observed in January. An exception is the heat flux from the surface. However, one should note the considerable uncertainty in the empirical data on the heat fluxes from the land surface for January.

In conclusion the author considers it his duty to note the important role played by the specialists of the Laboratory on Numerical Modeling of General Circulation of the Atmosphere at the USSR Hydrometeorological Center in creating a programmed core of a model of general circulation of the atmosphere in the carrying out and analysis of numerical experiments.

BIBLIOGRAPHY

1. Budyko, M. I., TEPLOVOY BALANS ZEMNOY POVERKHNOSTI (Heat Balance of the Earth's Surface), Leningrad, Gidrometeoizdat, 1956.

2. Budyko, M. I., ATLAS TEPLOVOGO BALANSA ZEMNOGO SHARA (Atlas of the Earth's Heat Balance), Moscow, Mezhduvedomstvennyy Geofizicheskiy Komitet, 1963.

3. Budyko, M. I., IZMENENIYE KLIMATA (Climatic Change), Leningrad, Gidrometeoizdat, 1969.

4. Trosnikov, I. V., Yegorova, Ye. N., "Use of Empirical Formulas for Computing Radiative Energy Influxes in the Modeling of General Circulation of the Atmosphere," TRUDY GIDROMETTSENTRA SSSR (Transactions of the USSR Hydrometeorological Center), No 160, 1975.

5. Arakawa, A., "Design of the UCLA General Circulation Model. Univ. of California, Los Angeles, Dep. of Meteorol.," TECHNICAL REPORT, No 7, 1972.

6. Bengtsson, L., "ECMWF Global Forecasting System European Centre for Medium Range Weather Forecasts," TECHNICAL REPORT, 1978.

7. Carson, D. J., "First Results from the GARP Basic Data Set Project," THE GARP PROGRAMME ON NUMERICAL EXPERIMENTATION, Report No 17, 1978.

8. Gilchrist, A., Corby, G. A., Rowntree, P. R., "United Kingdom Meteorological Office Five-Level General Circulation Model," METHODS IN CO JTATIONAL PHYSICS, Vol 17, 1977.

9. Holloway, J., Leith, Jr., Spellman, M. J., Manabe, S., "Latitude-Longitude Grid Suitable for Numerical Time Integration of a Global Atmospheric Model," MON. WEATHER REV., Vol 101, No 1, 1973.

10. Kurichara, Y., Tripoli, G. J., "An Iterative Time Integration Scheme Designed to Preserve a Low-Frequency Wave," MON. WEATHER REV., Vol 104, No 6, 1976.

11. Miyakoda, K., "Cumulative Results of Testing a Meteorological-Mathematical Model," PROCEEDINGS OF THE ROYAL IRISH ACADEMY, Vol LXXIII, Section A, No 9, 1973.

12. Oort, A. H., Rasmusson, E. M., "Atmospheric Circulation Statistics," NOAA PROFESSIONAL PAPER 5, 1971.

13. Oort, A. H., Vonder Haar, T. H., "On the Observed Annual Cycle in the Ocean-Atmosphere Heat Balance Over the Northern Hemisphere," J. OCEANOGR., Vol 106, No 6, 197ɛ.

UDC 551.(509.313+513)

# USE OF NESTED GRIDS METHOD IN THREE-DIMENSIONAL ATMOSPHERIC MODEL

Moscow METEOROLOGIYA I GIDROLOGIYA in Russian No 11, Nov 80 pp 27-33

[Article by A. I. Degtyarev, USSR Hydrometeorological Scientific Research Center, manuscript submitted 28 May 80]

[Text]

Abstract: A hemispherical finite-difference model of the atmosphere in full equations is considered in a quasistatic approximation. The model makes it possible to use a fine nested grid for improving spatial resolution in a stipulated region. The algorithms employed in carrying out joint computations for two grids are discussed in the article. The author gives the results of control computations based on real data. The results of experiments with the influence of a solution for a nested grid on the solution for a thin grid and without this influence are compared.

In solving problems in the numerical modeling of the atmosphere by the finite-differences method the question inevitably arises of the spatial resolution of the mode. The answer to this question is usually dictated by the capabilities of the electronic computer used. Accordingly, computations in a region comparable to a hemisphere (or sphere) must be made with great spatial intervals which cannot describe the development of atmospheric processes sufficiently well. The errors caused by too thin a grid lead to a distortion of both the amplitudes and the phase velocities of wave components of atmospheric disturbances. An improvement in the spatial resolution model will make it possible to take shorter waves into account, and what is equally important, describe long waves with a greater degree of accuracy.

In order to improve the spatial resolution of the model in some region, a method based on the use of so-called nested grids (NG method) has now come into wide use. The basic idea of the method is that the computations are made using two (or more) grids with a different spatial-temporal interval. The grid with the higher resolution (dense grid) in such a case is stipulated in a definite region, whereas the grid with the poorer resolution (thin grid) covers a greater region, such as a hemisphere.

There are two methods ("two strategies," to use the terminology employed by Phillips and Shukla [12]) for solution of a problem when employing the NG method. Strategy I assumes the stipulation of boundary conditions for the dense network on the basis of a solution for the thin grid. Strategy II, in addition, affords possibility for using the solution in the dense grid in integration for the thin grid ("feedback"). A comparison of these strategies was presented in [12] for different sets of model initial data. The mean square errors, computed over the region with the dense grid for one strategy or the other relative to the control computations for the dense grid in the entire region, indicated the advantage of strategy II for all sets of initial data. However, this strategy, in contrast to the first, requires the carrying out of joint computations for both grids, which leads to additional expenditures of computer memory.

At the present time strategy I has come into wider use and is employed quite successfully in numerical modeling and hydrodynamic short-range weather forecasting [1, 2, 14]. Specific realizations of the NG method differ with respect to the methods for formulating the boundary and initial conditions for the dense grid, methods for eliminating the computational gravitational waves arising in the region of the dense grid and some other details. From this point of view the methodological studies of Chen and Miyakoda [5] and Miyakoda and Rosati [11] are of interest. These studies give a comparison of different methods for formulating the boundary conditions for the dense grid. The results of the experiments indicated that the so-called "sponge" method, based on use of highly dissipative viscous terms for suppressing parasitic waves in the boundary regions, gives excessively smoothed fields of meteorological elements. Then we find that the application of the "radiation" condition at the points of outflow from the region of the dense grid does not completely eliminate the reflected high-frequency waves at the boundaries of the dense grid and requires additional boundary smoothing, as when using the solution for the thin grid at all the boundary points of the dense grid. In addition, the method for stipulation of the boundary condition with "radiation" is by no means trivial with use in a system of full equations.

Strategy II is presently used primarily in the modeling of the development of tropical cyclones. In the studies of Jones [8], Ley and Elsberry [10], the authors examine models consisting of two nested grids with a "feedback." These authors feel that the presence of a feedback does not allow a significant discrepancy in the solutions for the thin and dense grids, which can arise in computations when using strategy I. Therefore, the boundary conditions for the dense grid, obtained from the solution for the thin grid, to a high degree correspond to the solution for the dense grid.

In this article we examine an application of the NG method in a model in full equations and also compare the results obtained when using strategies I and II. The principal mathematical model for the experiments with use of the NG method is a model of general circulation of the atmosphere developed by I. V. Trosnikov [3]. The NG method was realized in a variant of this model without allowance for radiative and phase heat influxes. We will briefly discuss the problem of formulating the problem in a thin grid (a more detailed description of the model is given in

[3]), and then we will examine the principal algorithms for the organization of the computational process in a dense grid.

The system of full equations in hydrothermodynamics is written in a hydrostatic approximation in a spherical coordinate system ($\varphi$ is latitude, $\lambda$ is longitude). A p-coordinate system is used vertically. The state of the atmosphere in the model is determined by the zonal u- and meridional v-components of wind velocity, the analogue of vertical velocity $\omega$, elevation above sea level z, temperature T and surface pressure $P_s$. Then, using the generally employed notations, the system of equations can be written in the form

$$\frac{du}{dt} = -\frac{g}{a\cos\varphi}\frac{\partial z}{\partial \lambda} + \left(f + \frac{\operatorname{tg}\varphi}{a}u\right)v + F_H^u + F_H^w. \quad (1)$$

$$\frac{dv}{dt} = -\frac{g}{a}\frac{\partial z}{\partial \varphi} - \left(f + \frac{\operatorname{tg}\varphi}{a}u\right)u + F_H^v + F_w^v. \quad (2)$$

$$\frac{dT}{dt} = \frac{RT\omega}{c_p p} + F_H^T + F_w^T, \quad (3)$$

$$\frac{\partial p_s}{\partial t} + \frac{1}{a\cos\varphi}\left(\frac{\partial}{\partial \lambda}\int_0^{p_s} u\,dp + \frac{\partial}{\partial \varphi}\int_0^{p_s} v\cos\varphi\,dp\right) = 0, \quad (4)$$

$$\frac{1}{a\cos\varphi}\left(\frac{\partial u}{\partial \lambda} + \frac{\partial v\cos\varphi}{\partial \varphi}\right) + \frac{\partial \omega}{\partial p} = 0, \quad (5)$$

$$\frac{\partial z}{\partial p} = -\frac{RT}{gp}, \quad (6)$$

where f is the Coriolis parameter, a is the earth's mean radius, $c_p$ is specific heat capacity at a constant pressure, R is the specific gas constant of air, $F_H^u$, $F_H^v$, $F_H^T$ are terms for horizontal turbulent diffusion of momentum and heat.

In the model use was made of a simplified method for taking into account the nonlinearity of the diffusion coefficient in dependence on flow deformation proposed in [6]. This coefficient is assumed to be proportional to the modulus of the Laplacian of the corresponding value. The terms for vertical turbulent diffusion $F_w^u$, $F_w^v$, $F_w^T$ determine vertical turbulent movement.

The solution of system (1)-(6) will be sought in a hemisphere (region G with the boundaries $\Gamma$) and in a region (region e with the boundaries d). We have $e + d \in G$. In the hemisphere the boundary conditions are stipulated similar to [3], with the single difference that the surface temperature at the present time is considered fixed. This is attributable to the fact that in the experiments carried out the nonadiabatic influxes are not taken into account and the computations are made for a time up to 3 days. The formulation of boundary conditions for a dense grid will be discussed below.

With conversion to the difference problem in the region $G + \Gamma$ there is stipulation of a grid $\overline{\psi}_{tg}$ with the interval H, and in the region e + d -- the grid $\overline{\psi}_{dg}$ with the interval h in such a way that H = Kh. In these experiments K = 2. Both grids are latitudinal-longitudinal. In writing the system of equations (1)-(6) in finite-difference form use was made of the scheme employed in [7]. As is well known, such a scheme makes it possible to conserve the mass of the atmosphere and also the total energy of atmospheric movements under the condition of adiabaticity and absence of friction.

When using a latitude-longitude grid in the near-polar latitudes the horizontal spatial interval becomes small and therefore Fourier filtering is applied to the main prognostic functions for maintaining computational stability in these latitudes.

For time integration in the model use is made of a modified Euler scheme with the scaling proposed in [9],

$$X^* = X^\tau + \Delta\tau\,(F_1^\tau + F_2^\tau),$$
$$X^{\tau+1} = X^\tau + \Delta\tau\,((1-w_1)\,F_1^\tau + w_1 F_1^*) + \Delta\tau\,((1-w_2)\,F_2^\tau + w_2 F_2^*). \qquad (7)$$

In (7), in the second half-interval, the terms on the right-hand sides are divided into advective terms $F_1$ and all the remaining terms $F_2$. The values of the weights $w_1 = w_2 = 1$ give the known Euler scheme with scaling. Scheme (7) with $w_1 = 0.506$ and $w_2 = 3$ differs from the Euler scheme by scaling with considerably lesser dissipativity in the region of long waves.

Now we will examine the principal algorithms determining the characteristics of integration in the dense grid. As a convenience we will represent the set of points of intersection of a thin grid

$$\bar{\varphi}_{tg} = \varphi^B_{tg} + \gamma_{tg} + \varphi^\Phi_{tg},$$

where $\varphi_{tg}$ are the grid points of intersection within the e region, $\gamma_{tg}$ are the grid points of intersection lying on the boundary d, $\varphi^\Phi_{tg}$ are the grid points of intersection outside the region e + d.

The dense grid $\bar{\varphi}_{dg}$ consists of the boundary points of intersection $\gamma_{dg}$, a series of points of intersection $\gamma 1_{dg}$ adjacent to the boundary points of intersection, and the remaining internal points of intersection $\varphi_{dg}$, that is

$$\bar{\varphi}_{dg} = \gamma_{dg} + \gamma 1_{dg} + \varphi_{dg}.$$

The solution of the problem in the dense grid is dependent on the solution in the thin grid in the sense that for each time interval in the dense grid it is necessary to stipulate the boundary values at the grid points of intersection $\gamma_{dg}$. The seeking of the missing values at these points of intersection is accomplished by parabolic interpolation. As the control points for the interpolation we use the values at the points of intersection of the thin grid $\gamma_{tg}$.

In the model we used an algorithm for the partial change in the spatial computation region with interpolation in time in accordance with scheme (7) in the first and second half-intervals. This algorithm was tested by the author using a one-dimensional model. It is easy to clarify the effect of this model, examining the time integration scheme (7). The computations in the first half-interval are made at the points of intersection $\gamma 1_{dg} + \psi_{dg}$, using the boundary points of intersection $\gamma_{dg}$. The results of these computations are the $X^*$ values at the points of intersection $\gamma 1_{dg} + \psi_{dg}$. In order to obtain the $X^{\tau+1}$ values at these points of intersection it is necessary to have the $X^*$ values at the points of intersection $\gamma_{dg}$. In general, the $X^*$ values have only an auxiliary character in the iteration scheme (7). It is therefore not entirely correct to obtain them by interpolation of the corresponding values from the points of intersection of a thin grid, or, as in the first half-interval, use the X values. Accordingly, the computation region in the second half-interval is narrowed and the $X^{\tau+1}$ values are computed only at the points of intersection $\psi_{dg}$ with the use of $\gamma 1_{dg}$ as boundary points. The $X^{\tau+1}$ values at the points of intersection $\gamma 1_{dg}$ are found using parabolic interpolation.

Since the solution for the dense grid in principle should give a lesser error, associated with the spatial resolution, in calculations for the thin grid at the points of intersection $\psi^B_{tg}$ it is possible to use the results of computations in the dense grid. This operation is carried out using a nine-point Shuman operator [13]. The $X_0$ value at each of the points of intersection $\psi^B_{tg}$ in the thin grid is determined from the value for $X_0$ at the corresponding point of intersection $\psi_{dg}$ in the dense grid and the values at the 8 surrounding points of intersection.

$$\overline{X}_0 = X_0 + \frac{1}{2}\nu(1-\nu)(X_2 + X_4 + X_6 + X_8 - 4X_0) + \quad (8)$$
$$+ \frac{1}{4}\nu^2(X_1 + X_3 + X_5 + X_7 - 4X_0).$$

The operator (8) with $\nu = 1/2$ best eliminates two-step perturbations.

For a better correspondence of the computational solution for the dense grid to the boundary conditions obtained from the solution for the thin grid and for suppressing the high-frequency computational modes, in the model use is made of boundary smoothing, which is employed for only one row of points of intersection $\gamma 1_{dg}$ along the boundary of the dense grid. A three-point smoothing operator, frequently employed for these purposes, is used

$$\overline{X}(\gamma 1_{dg}) = 0.5\, X(\gamma 1_{dg}) + 0.25\, (X(\gamma_{tg}) + X(\psi^1_{dg})),$$

where $\psi^1_{dg}$ is the row of points of intersection in the region $\psi_{dg}$ adjacent to $\gamma 1_{dg}$.

As the initial data for testing the model we used the GARP BDS set of data in [4]. These data represent an analysis of the wind velocity and temperature fields and the pressure field at sea level.

In these experiments the thin grid was determined in the northern hemisphere with a meridional interval $\Delta\varphi = 5°$ and along the circles of latitude -- $\Delta\lambda = 11.25°$. The dense grid has half the horizontal spatial interval and is superposed on the eastern hemisphere from 82.5° to 42.5°N. In the central part of this region, and specifically over the northeastern part of the European USSR, there is a cyclone accompanied by a deep trough at $H_{500}$ which moves in an easterly direction. During the first two days the generation of this low takes place and then it is gradually filled. The nested grid method is employed in order to ascertain the movement of this low more precisely and also the movement of pressure formations associated with it.

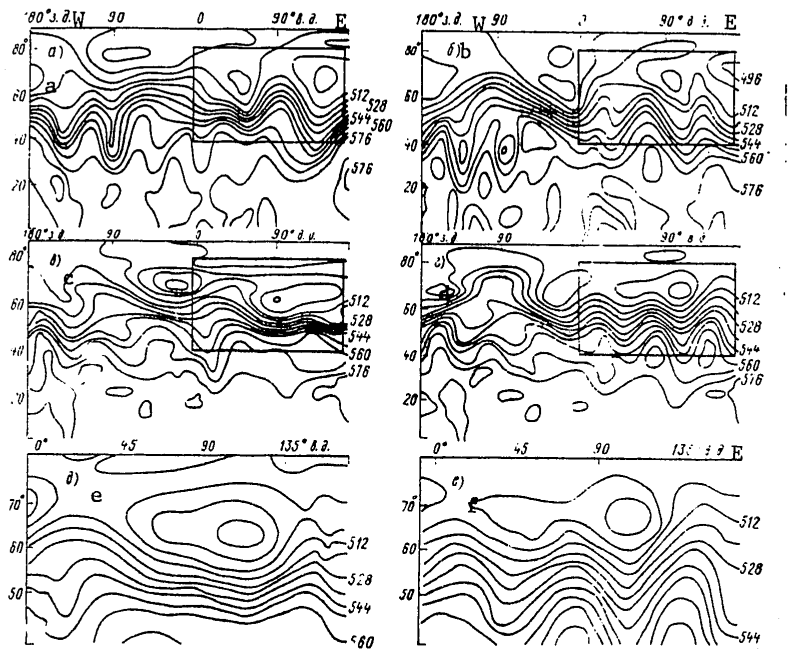


Fig. 1. Fields of heights of isobaric surface $H_{500}$. a) initial, b) actual, after 3 days, c) result of computations for 3 days in experiment B1 for thin grid, d) same, in experiment B1 for dense grid, e) in experiment B2 for thin grid, f) B2 for dense grid.

| Day | Experiment B1 | | | | | | | | Experiment B2 | | | | | | | |
|---|---|---|---|---|---|---|---|---|---|---|---|---|---|---|---|---|
| | thin grid | | | | dense grid | | | | thin grid | | | | dense grid | | | |
| | σ | k | ε | ρ | σ | k | ε | ρ | σ | k | ε | ρ | σ | k | ε | ρ |
| 1 | 11,3 | 0,69 | 0,77 | 0.40 | 10,6 | 0,75 | 0,70 | 0,34 | 9,7 | 0,79 | 0,66 | 0,42 | 9,6 | 0,83 | 0,65 | 0,42 |
| 2 | 15,8 | 0,66 | 0,98 | 0,33 | 14,3 | 0,73 | 0,80 | 0,37 | 12,8 | 0,31 | 0,75 | 0,33 | 11,7 | 0.82 | 0,76 | 0,45 |
| 3 | 18.8 | 0.56 | 1.24 | 0,27 | 17,4 | 0,65 | 1,02 | 0,45 | 14.9 | 0,71 | 0,99 | 0,27 | 14.9 | 0.70 | 0,96 | 0,36 |

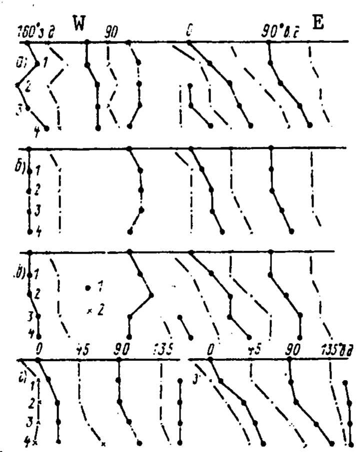


Fig. 2. Longitude-time diagram of position of ridges (1) and troughs (2) of geopotential $H_{55}$ along parallel 50° for 1-4 days. a) actual position, b) in experiment B1 for thin grid, c) B2 for thin grid, d) B1 for dense grid, e) B2 for dense grid.

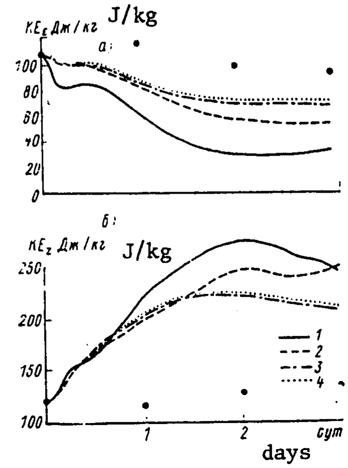


Fig. 3. Temporal variation of eddy (a) and westerly (b) components of kinetic energy, computed for region of nested grid in experiments B1 for thin (1), B1 for dense (2), B2 for thin (3) and B2 for dense (4) grids.

We carried out two experiments using BDS data: an experiment without allowance for feedback (B1) and with allowance for the latter (B2). Figure 1 shows the fields of heights of the $H_{500}$ isobaric surface -- the result of computations in the experiments B1 and B2 for a time of 3 days, and also the actual field for this time interval and the initial field $H_{500}$. Figure 1c shows that the field in the region of the nested grid in experiment B1 has a virtually zonal character. Computations for the dense grid in this experiment somewhat increase meridionality. In experiment B2 there is clear manifestation of a system of troughs and ridges, as in real data.

Longitude-time diagrams (Hovmuller diagrams) of the position of ridges and troughs of geopotential at the 500-mb level along the parallel 50°N are represented in Fig. 2. The experiment B1 gives too slow a movement of pressure formations to the east. In experiment B2 in the region of the nested grid the position of troughs and ridges is considerably closer to the actual position. Figure 3 shows the temporal variation of the zonal and eddy components of kinetic energy in experiments B1 and B2 for the thin and dense grids, computed for the central part of the nested grid. Both experiments give an exaggerated level of the zonal and a reduced level of the eddy components of kinetic energy. However, the corresponding values in B2 are closer to the actual values, which in the figure are represented by dots.

The table gives standard evaluations computed for the central part of the region of the nested grid (66 points). In order to evaluate the quality of computation of geopotential we computed the mean square error in decameters $\sigma$, the mean relative error $\varepsilon$, the correlation coefficient k and the guaranteed prediction of the signs of trend $\rho$.

Thus, it can be noted that in experiment B1 for a thin grid in the region of the nested grid there is a very weak azonality, associated with poor spatial resolution. In addition, the movement of the troughs and ridges was slowed. The use of a nested grid in this experiment somewhat decreases both the mentioned shortcomings. The presence of a feedback substantially favors both an increase in the meridionality of the flow in this region and a better agreement of the phase velocities of large-scale disturbances with the actual values. A comparison of strategies I and II by the BC method in the interpretation described above in a single example is of a preliminary character, and of course requires the implementation of a broader range of experiments. However, the results give a right to hope for good possibilities of use of a nested grid with a feedback.

In conclusion the author takes the opportunity to express appreciation to I. V. Trosnikov for valuable advice in the carrying out of the work.

BIBLIOGRAPHY

1. Kalenkovich, Ye. Ye., "One Method for Refining Difference Solutions in Forecasting Using Nested Grids," METEOROLOGIYA I GIDROLOGIYA (Meteorology and Hydrology), No 8, 1979.

2. Prager, T., "Numerical Model of Hydrodynamic Forecasting Using the Integral Laws of Conservation of Quasistatic Atmospheric Processes," METEOROLOGIYA I GIDROLOGIYA, No 11, 1978.

3. Trosnikov, I. V., "Model of General Circulation of the Atmosphere Developed at the USSR Hydrometeorological Center," METEOROLOGIYA I GIDROLOGIYA, No 11, 1980.

4. Carson, D. J., "First Results From the GARP Basic Data Set Project," THE GARP PROGRAMME ON NUMERICAL EXPERIMENTATION, Report N 17, 1978.

5. Chen, J. H., Mijakoda, K., "A Nested Grid Computation for the Barotropic Free Surface Atmosphere," MON. WEATHER REV., Vol 102, No 2, 1974.

6. Corby, G. A., Gilchrist, A., Newson, R. L., "A General Circulation Model of the Atmosphere Suitable for Long Period Integration," QUART. J. ROY. METEOROL. SOC., Vol 98, No 418, 1972.

7. Holloway, J. L., Spellman M. J., Manabe, S., "Latitude-Longitude Grid Suitable for Numerical Time Integration of a Global Atmospheric Model," MON. WEATHER REV., Vol 101, No 1, 1973.

8. Jones, R. W., "A Nested Grid for a Three-Dimensional Model of a Tropical Cyclone," J. ATMOS. SCI., Vol 34, 1977.

9. Kurihara, Y., Tripoli, G. J., "An Iterative Time Integration Scheme Designed to Preserve a Low-Frequency Wave," MON. WEATHER REV., Vol 104, No 6, 1976.

10. Ley, G. W., Elsberry, R. L., "Forecasts of Typhoon Irma Using a Nested Grid Model," MON. WEATHER REV., Vol 104, No 6, 1976.

11. Miyakoda, K., Rosati, A., "One-Way Nested Grid Models: the Interface Conditions and the Numerical Accuracy," MON. WEATHER REV., Vol 105, 1977.

12. Phillips, N. A., Shukla, J., "On the Strategy of Combining Coarse and Fine Grid Meshes in Numerical Weather Prediction," J. APPL. METEOROL., Vol 12, No 5, 1973.

13. Shuman, F. G., "Numerical Methods in Weather Prediction: II. Smoothing and Filtering," MON. WEATHER REV., Vol 85, 1957.

14. Williamson, D. L., Browning, G. L., "Formulation of the Lateral Boundary Conditions for the NCAR Limited-Area Model," J. APPL. METEOROL., Vol 13, 1974.

UDC 551.509.314

MEDIUM-RANGE PREDICTION OF $H_{500}$ BY A PHYSICOSTATISTICAL METHOD

Moscow METEOROLOGIYA I GIDROLOGIYA in Russian No 11, Nov 80 pp 34-41

[Article by R. P. Repinskaya, candidate of physical and mathematical sciences, Leningrad Hydrometeorological Institute, manuscript submitted 5 May 80]

[Text]

Abstract: The article examines the results of prediction of geopotential $H_{500}$ for the third, sixth and ninth days using a physicostatistical method. The predictants and test predictors are selected from among the parameters of expansion of the hydrometeorological fields in empirical orthogonal functions. The following are taken into account: the large-scale properties of the fields of empirical orthogonal functions; fraction of dispersion of initial information described by natural fluctuations and their relaxation time. The author compares evaluations of the success of the predictions made with evaluations of statistical and hydrodynamic predictions. The possibilities of improvement of the prognostic method are discussed.

In many physicostatistical weather forecasting schemes the predictants used are the parameters of expansion of hydrometeorological fields into a series in orthogonal base functions. In this case there is a fundamental possibility, by means of numerical experiments, to clarify for what times this method can be used in predicting the generalized characteristics of processes of different spatial and temporal scales. Some results of such experiments, directed to clarification of the possibilities of physicostatistical medium-range prediction of the surface pressure $P_0$ fields for the area of the North Atlantic, were published in [11]. The predictants used in three variants of the prognostic scheme were 4-6 coefficients of expansion of the $P_0$ fields in empirical (natural) orthogonal functions (EOF) [1].

In this investigation, being a methodological continuation of [11], we discuss the results of application of the method of medium-range physicostatistical prediction applicable to prediction of the geopotential $H_{500}$ for the third, sixth and ninth days for the spring months over the Atlantic sector of the northern hemisphere. Information on the predictant was stipulated at 20 points of an irregular grid. which covered the mentioned region (see Fig. 1). All the points coincide with the observation stations and weather ships, which ensures more precise stipulation of the initial data on the predictant, which were taken from special microfilms. The observational data were collected for 0000 GMT each three days for 1960-1971. The volume of the sample for each month was 120-130 records of a 20-dimensional vector of geopotential $H_{500}$. In developing the prediction method [11] we used as a point of departure the physical hypotheses on the basis of which the physicostatistical method for long-range weather forecasts created at the Main Geophysical Observatory [14] was constructed and recommendations obtained as a result of its introduction into operational practice [12, 17]. In particular, the choice of the virtual predictors was made taking into account the following fundamental physical concepts: 1) the atmosphere is a unified physical system, all parts of which strongly interact with one another. As a result of the interaction the evolution of one part of the atmosphere is determined by the state of all its parts and prehistory of development of the processes [9, 14]; 2) the atmosphere is not a closed system, but part of the unified physical system "atmosphere - active layer of the underlying surface" [9, 14]; 3) "the totality of the predictors should characterize all the principal peculiarities of the initial state of the unified physical system in which the macroprocesses develop" [14].

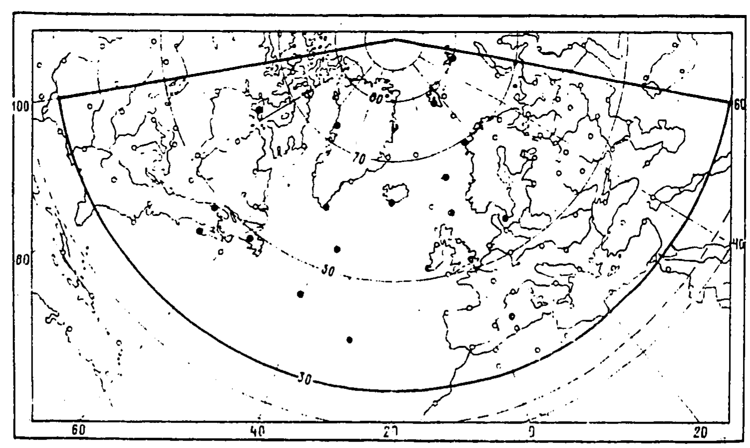


Fig. 1. Network of computation points.

Proceeding on the basis of these basic concepts, in the set of test predictors we included the generalized characteristics of processes developing both over the region of the forecast at different altitudes and over a hemisphere. We also took into account the influence of the underlying surface. The virtual predictors used were: surface pressure, geopotential $AT_{700}$ and $AT_{500}$ and the three-hour pressure trends at 66, 29, 20 and 28 points respectively in the Atlantic Ocean situated approximately from 20 to 82°N; surface pressure and geopotential $AT_{500}$ at 55 and 50 points respectively, situated in dynamically significant regions of the northern hemisphere determined using the pressure-thermal characteristics of macroprocesses [13]; the temperature of the water surface in the Atlantic Ocean on the basis of data from nine weather ships. Information on the fields of all the virtual predictors was stipulated for February, March, April and May for the above-mentioned 12-year series.

Predictor space was minimized in two stages. In the first stage the set of fields of each virtual predictor and predictant was subjected to expansion into a series in empirical orthogonal functions [1]. The expansion was carried out for each month along its base. The fields of virtual predictors, stipulated at more than 35 points, were divided into two sectors, which was dictated by the possibilities of the operational memory of the "BESM-4" electronic computer which was used in making all the computations. The sectors were discriminated taking into account the recommendations made on the basis of climatological and synoptic investigations. Finally, the total number of fields of virtual predictors (n) was 10.

Thus, as the transformed information on the fields of virtual predictors (and the predictant) use is made of the coefficients of their expansion into a series in EOF. Henceforth the mentioned coefficients (main components) will be denoted $a_j(t_{k,m}) = a_j$. Here j = 1, 2,... is the sequence number of the EOF for a particular field; $t_{k,m}$ are time reference points within the sample; m is the number of the year; k is the date in the particular month.

Table 1

Evaluation of Accuracy of Convergence of Expansion of EOF Fields in EOF

| $j$ | February | | March | | April | | May | |
|---|---|---|---|---|---|---|---|---|
| | $\alpha_j$ | $\beta_j$ | $\alpha_j$ | $\beta_j$ | $\alpha_j$ | $\beta_j$ | $\alpha_j$ | $\beta_j$ |
| 1 | 18,60 | 18,60 | 17,[illegible] | 17,96 | 17,70 | 17,70 | 19,68 | 19,68 |
| 2 | 17,56 | 36,16 | 15,23 | 33,19 | 14,60 | 32,30 | 15,79 | 35,47 |
| 3 | 11,94 | 48,10 | 12,98 | 46,17 | 10,63 | 42,93 | 10,62 | 46,09 |
| 4 | 9,87 | 57,97 | 9,65 | 55,82 | 9,13 | 52,06 | 9,34 | 55,43 |
| 5 | 7,53 | 65,50 | 7,74 | 63,56 | 8,28 | 60,34 | 7,71 | 63,14 |
| 6 | 6,15 | 71,65 | 5,94 | 69,50 | 6,24 | 66,58 | 5,91 | 69,05 |
| 7 | 5,03 | 76,68 | 5,41 | 74,91 | 5,61 | 72,19 | 5,23 | 74,28 |
| 8 | 3,83 | 80,51 | 4,37 | 79,28 | 4,59 | 76,77 | 4,41 | 78,69 |
| 9 | 3,23 | 83,74 | 3,62 | 82,90 | 3,63 | 80,40 | 3,82 | 82,51 |
| 10 | 3,01 | 86,75 | 3,39 | 86,29 | 3,38 | 83,78 | 2,97 | 85,48 |

Note. $\alpha_j$ is the contribution (in %) of the j-th natural fluctuation to the total dispersion of the initial information; $\beta_j$ is the increasing sum $\alpha_j$.

The following factors are taken into account: large-scale properties of the fields of empirical orthogonal functions; fraction of dispersion of initial information $\alpha_j$ described by a particular natural fluctuation and its relaxation time $t_r$, determined using the normalized time autocorrelation functions of the parameters $a_j$ [18]. In particular, it was required that two conditions be satisfied without fail: 1) $\alpha_j \geqslant 5\%$; 2) $t_r \geqslant \tau_{min}$, where $\tau_{min}$ is the minimum advance time of the forecast, in our problem equal to three days.

Table 2

Evaluation of $H_{500}$ Predictions for Three, Six and Nine Days

| Month | Forecast time, days | α | δ | ρ | r | N | m |
|---|---|---|---|---|---|---|---|
| March | 3 | 9,7 | 0,93 | 0,26 | 0,564 | 11 | 4 |
| | | 8,3 | 0,92 | 0,28 | 0,653 | 11 | 5 |
| | | 6,4 | 0,88 | 0,32 | 0,670 | 11 | 6 |
| | 6 | 11,2 | 0,85 | 0,21 | 0,646 | 13 | 4 |
| | | 9,2 | 0,87 | 0,24 | 0,668 | 13 | 5 |
| | | 7,6 | 0,85 | 0,26 | 0,658 | 13 | 6 |
| | 9 | 10,9 | 0,72 | 0,22 | 0,583 | 16 | 4 |
| | | 9,7 | 0,76 | 0,23 | 0,588 | 15 | 5 |
| | | 10,0 | 0,79 | 0,22 | 0,577 | 16 | 6 |
| April | 3 | 10,8 | 0,98 | 0,34 | 0,637 | 11 | 4 |
| | | 8,7 | 0,95 | 0,35 | 0,667 | 11 | 5 |
| | | 6,9 | 0,92 | 0,35 | 0,672 | 11 | 6 |
| | 6 | 11,9 | 0,88 | 0,25 | 0,615 | 11 | 4 |
| | | 10,1 | 0,90 | 0,25 | 0,652 | 11 | 5 |
| | | 10,4 | 0,94 | 0,23 | 0,637 | 11 | 6 |
| | 9 | 12,2 | 0,89 | 0,21 | 0,681 | 12 | 4 |
| | | 9,5 | 0,84 | 0,26 | 0,663 | 12 | 5 |
| | | 10,1 | 0,87 | 0,23 | 0,654 | 12 | 6 |
| May | 3 | 11,5 | 0,97 | 0,27 | 0,531 | 10 | 4 |
| | | 9,1 | 0,96 | 0,31 | 0,598 | 10 | 5 |
| | | 7,7 | 0,88 | 0,33 | 0,628 | 10 | 6 |
| | 6 | 12,3 | 0,98 | 0,23 | 0,579 | 11 | 4 |
| | | 9,6 | 0,93 | 0,27 | 0,621 | 11 | 5 |
| | | 8,8 | 0,91 | 0,30 | 0,631 | 11 | 6 |
| | 9 | 12,0 | 0,96 | 0,19 | 0,656 | 15 | 4 |
| | | 10,2 | 0,91 | 0,21 | 0,656 | 15 | 5 |
| | | 9,7 | 0,88 | 0,25 | 0,665 | 15 | 6 |
| June | 3 | 10,7 | 0,96 | 0,29 | 0,577 | | 4 |
| | | 8,7 | 0,95 | 0,31 | 0,639 | | 5 |
| | | 7,0 | 0,89 | 0,33 | 0,657 | | 6 |
| | 6 | 11,8 | 0,91 | 0,21 | 0,613 | | 4 |
| | | 9,6 | 0,90 | 0,25 | 0,647 | | 5 |
| | | 8,9 | 0,90 | 0,26 | 0,642 | | 6 |
| | 9 | 11,7 | 0,86 | 0,21 | 0,640 | | 4 |
| | | 9,8 | 0,84 | 0,23 | 0,636 | | 5 |
| | | 9,9 | 0,85 | 0,23 | 0,632 | | 6 |

Note. N -- number of prepared predictions; m -- number of EOF taken into account.

Table 1 gives an evaluation of the accuracy of convergence of series of expansion of the $H_{500}$ fields in EOF. It follows from this table that proceeding on the basis of the first condition adopted as a basis for the forming of a set of predictants in each month it is possible to predict not less than seven $a_j$ parameters. In the three variants of the scheme which we developed there was successive prediction of four, five and six expansion coefficients containing information on the most spatially extensive long-lived and energetically strongest natural fluctuations over the forecast region. We feel that such a "stepped" approach has definite advantages since it makes it possible, by a direct evaluation of the results of the forecast, to draw a conclusion concerning the desirability of including some expansion parameter among the predictants.

In the archives of the test predictors in all the variants of the prognostic scheme we included the four first expansion coefficients in a series of EOF for the set of fields of each precursor of the future weather, in individual cases describing up to 90% of the total dispersion of the initial samples. Thus, the archives of the test predictors for each month contains 40 coefficients $a_j$ (j = 1-4, n = 10).

Then, for each predictant for a particular month from the archives of the test predictors we select the most informative. This procedure is carried out using an evaluation of the regression of the main components of the vector-predictors on the main components of the vector-predictant by the sifting method. The selection method is continued until a further increase in the number of predictors does not lead to a substantial decrease in the mean square error of the "composite" multiple linear regression coefficient R. In our problem the "saturation" of R for all the predictants was attained when 7-12 predictors were taken into account. Accordingly, 10 was selected as the "optimum" number of predictors. At the end of this stage, for each of the six main components of the predictant in March, April and May there are sets of regression coefficients, making use of which it is possible to compute the future value of these components with an advance period of three, six and nine days. We wrote a total of $\ell \times q \times g = 54$ regression equations, where $\ell = 6$ is the maximum number of prediction coefficients $a_j$ in each month; q = 3 is the number of variants of the prognostic scheme, differing with respect to the advance time of the forecast; g = 3 is the number of months for which the equations were written. The $H_{500}$ prognostic fields are obtained using the known "restoration" procedure [11, 12, 14] with the use of the determined expansion coefficients and EOF corresponding with respect to the j index. It is evident that the latter in this case serve as "weighting" functions.

The most informative predictors entering into virtually all the regression equations were as follows -- geopotential $AT_{500}$ over the forecast region, surface pressure and geopotential $AT_{500}$ in dynamically significant regions of the hemisphere and in the prediction for the ninth day -- temperature of the ocean water surface. The three-hour pressure trend is a predictor carrying little information and is included in only four regression equations: for prediction on the third day of the fifth and sixth natural oscillations in March and the sixth in April and May.

Testing of these regression equations was carried out using data for 1972 and 1973. We prepared a total of 32, 35 and 43 forecasts for the third, sixth and ninth days respectively with the use of four, five and six EOF. For evaluating the success of the forecasts we employed the generally accepted synoptic-statistical characteristics: mean absolute error a; mean relative error $\delta$ (as a "test" we used the climatological forecast); the correlation coefficient r between the predicted and the actual fields; the criterion of similarity of the actual and predicted fields with respect to the sign of the anomalies $\rho$, being a measure of the geometrical similarity of the compared fields.

The mean values of all the enumerated characteristics of quality of the prepared forecasts are given in Table 3. Its analysis shows that with respect to the parameters $\delta$, $\rho$ and r all three types of forecasts in all the months are entirely satisfactory. Allowance for the fifth natural oscillation, whose relaxation time varies in the course of the spring in the range 9 (March) - 15 (April, May) days, makes possible a considerable improvement in the quality of the forecasts for all times, especially with respect to the mean absolute error and the correlation coefficient. The relaxation time for the sixth natural oscillation is in March 6, in April 3 and in May 9 days.

Table 2 shows that it is undesirable to take this oscillation into account in March when forecasting for the ninth day and in April for the ninth and sixth days since this will lead to some deterioration of the quality of the forecasts.

Now we will compare the results with the results obtained by other authors. For example, A. V. Borodina [4] for December, January and February prepared three- and five-day statistical forecasts of $H_{500}$ for a territory taking in Europe, the Arctic, Western and Eastern Siberia and the Far East. A prognostic scheme was developed on the basis of a combination of the empirical orthogonal functions method and a classification of macroprocesses in dependence on the position of the circumpolar vortex in the stratosphere. The following values of the forecast quality characteristics were obtained: $\delta_3$ = 0.81-0.84, $\delta_5$ = 0.80-0.83, $\rho_3$ = 0.24-0.25, $\rho_5$ = 0.14-0.17; $r_3$ = 0.59-0.62; $r_5$ = 0.57-0.60, where the subscripts 3 and 5 on the $\delta$, $\rho$ and r parameters denote the advance time of the forecasts. It can be seen from a comparison of these results with the data in Table 2 that the physico-statistical forecasts even for the ninth day have a somewhat better quality than five-day forecasts [4].

Table 3

Evaluations of Hydrodynamic Forecasts $H_{500}$ for 72 Hours

| Model | a | $\delta$ | $\rho$ |
|---|---|---|---|
| Belousov | | 0.91 | |
| Berkovich | | 0.93 | |
| Kalenkovich-Penenko | 4.5 | 0.82 | 0.39 |
| Pressman | | 0.82 | |

It is generally known that hydrodynamic forecasts for 24-28 hours are quite successful. However, with an increase in the advance time to 72 hours the relative error in the forecast at all levels increases appreciably and approaches unity. This means that methodological forecasts degenerate into a trivial test forecast. Table 3 gives some results of routine tests of hydrodynamic models [2, 3, 6, 10], published in [5, 7]. Here reference is only to the guaranteed probability of three-day forecasts of $H_{500}$ for a region including the North Atlantic and Western Europe. A study was made of both quasigeostrophic models [2] and models based on a solution of the full equations of atmospheric dynamics [3, 6, 10].

It follows from an analysis of Tables 2 and 3 that physicostatistical forecasts for the third day, taking into account six natural oscillations with respect to the $\delta$ and $\rho$ parameters, for all practical purposes are at the level of errors in forecasting $H_{500}$ by hydrodynamic models [2, 3, 6, 10]. With respect to the mean absolute error they are inferior only to hydrodynamic forecasts [6]. However, it must be remembered that the errors given in Table 3 were obtained for a region including not only the North Atlantic, but also the territory of Europe, which is well covered by meteorological observations. We, however, are dealing with a very thin network of observation stations for which there is a loss of information not only about processes whose characteristic scales are equal to two or three grid intervals, usually used in numerical models, but also about larger atmospheric disturbances, allowance for which is important in forecasts for several days. Thus, the initial field of the predictant in numerical schemes is stipulated more precisely, which unquestionably has an effect on the quality of the forecasts.

In our scheme it is possibly necessary to take into account a great number of main components. In any case, for the third day it makes sense to predict the seventh and eighth natural oscillations, since their relaxation time is equal to 6 and 18, 3 and 12, 15 and 3 days respectively in March, April and May. However, we feel that for a reliable determination of the forms of EOF describing such small-scale oscillations in the field of the predictant it is necessary to have, first of all, considerably greater samples, and second, there must be better coverage of the investigated region with initial data, that is, a denser grid of points. In our country a definite source of forecasting errors was also the replacement of data missing on the microfilms by norms. Evidently it would be better to use the data read from isolines on synoptic charts.

It is important to note that with an increase in the advance time to nine days the guaranteed probability of physicostatistical forecasts of $H_{500}$ making use of the $\delta$, $\rho$ and r parameters in general was no worse than for the third day. The attained results indicate, in our opinion, that it is necessary to continue experiments directed to improvement of the method and clarification of the possibilities for physicostatistical forecasting for intermediate times on the basis of large samples. We intended to carry out the first objective within the framework of the physicostatistical long-range forecasting method [12, 14, 17], having considerable possibilities. We have in mind primarily the possibilities of improving the method for selecting informative statistical correlations [15], and in addition, the possibility for a more complete and precise description of the initial state of the atmosphere-underlying surface system by supplementing the archives of test predictors with conservative carriers of the "meteorological memory" and its physical enrichment. In particular, investigations of the relaxation time of natural oscillations in the fields of different meteorological elements indicated that extremely small-scale atmospheric disturbances, describing less than 5% of the total dispersion of the initial samples, often exist far longer than large-scale atmospheric disturbances.

As indicated by the results of this study and study [11], the $a_j$ coefficients, carrying information on the behavior of such long-lived localized processes, must be included in the predictants and test predictors in developing schemes for medium- and long-range weather forecasts. These results to a definite degree also confirm the conclusions drawn earlier in hydrodynamic theory on the basis of conjugate equations relative to the prognostic significance of different types of information [8, 16].

It appears that using the indicated possibilities it is possible to achieve a further increase in the quality of physicostatistical forecasts of geopotential $H_{500}$ for intermediate times.

BIBLIOGRAPHY

1. Bagrov, N. A., "Analytical Representation of a Series of Meteorological Fields Using Natural Orthogonal Components," TRUDY TsIP (Transactions of the Central Institute of Forecasts), No 74, 1959.

2. Belousov, S. L., MNOGOUROVENNYYE KVAZIGEOSTROFICHESKIYE MODELI PROGNOZA: LEKTSII PO CHISLENNYM METODAM KRATKOSROCHNOGO PROGNOZA POGODY (Multilevel Quasi-geostrophic Forecasting Models: Lectures on Numerical Short-Range Weather Forecasting), Leningrad, Gidrometeoizdat, 1969.

3. Berkovich, L. V., "Six-Level Scheme for Forecasting Using Full Equations for a Large Territory," TRUDY GIDROMETTSENTRA SSSR (Transactions of the USSR Hydrometeorological Center), No 100, 1972.

4. Borodina, A. V., "Use of Natural Components for Objective Classification of $H_{500}$ Fields," METEOROLOGIYA I GIDROLOGIYA (Meteorology and Hydrology), No 8, 1967.

5. Kalenkovich, Ye. Ye., Kaminskaya, L. Ye., Petrova, M. G., "Results of Testing of a Numerical Scheme for Predicting the Pressure Field of the Northern Hemisphere," INFORMATSIONNYY SBORNIK GIDROMETTSENTRA SSSR (Informative Collection of Articles of the USSR Hydrometeorological Center), No 4, 1975.

6. Kalenkovich, Ye. Ye., Penenko, V. V., "Numerical Model for Predicting the Fields of Meteorological Elements for the Northern Hemisphere," CHISLENNYYE METODY RESHENIYA ZADACH PROGNOZA POGODY I OBSHCHEY TSIRKULYATSII ATMOSFERY (Numerical Methods for Solving Problems in Predicting Weather and General Circulation of the Atmosphere), Novosibirsk, Nauka, 1970.

7. Luzhnaya, N. P., "Results of Testing of Schemes for Numerical Forecasting of the Pressure Field Over the Northern Hemisphere for 24, 48 and 72 Hours Developed at the USSR Hydrometeorological Center," INFORMATSIONNYY SBORNIK GIDROMETTSENTRA SSSR, No 4, 1975.

8. Marchuk, G. I., Skiba, Yu. N., "Numerical Computation of the Conjugate Problem for a Model of Thermal Interaction of the Atmosphere and Ocean and the Continents," IZV. AN SSSR, FIZIKA ATMOSFERY I OKEANA (News of the USSR Academy of Sciences: Physics of the Atmosphere and Ocean), Vol 12, 1976.

9. Monin, A. S., PROGNOZ POGODY KAK ZADACHA FIZIKI (Weather Forecasting as a Problem in Physics), Moscow, Nauka, 1969.

10. Pressman, D. Ya., "Six-Level Scheme for Short-Range Weather Forecasting Using Full Equations," TRUDY VSESOYUZN. KONF. MOLODYKH UCHENYKH GIDROMETSLUZHBY SSSR (Transactions of the All-Union Conference of Young Scientists of the USSR Hydrometeorological Service), Leningrad, Gidrometeoizdat, 1971.

11. Repinskaya, R. P., "Prediction of the Surface Pressure Field for Several Days," METEOROLOGIYA I GIDROLOGIYA, No 11, 1978.

12. RUKOVODSTVO PO MESYACHNYM PROGNOZAM POGODY (Manual on Monthly Weather Forecasts), Leningrad, Gidrometeoizdat, 1971.

13. Savichev, A. I., "On the Problem of Prediction of the Pressure Field Over the North Atlantic in July," TRUDY LGMI (Transactions of the Leningrad Hydrometeorological Institute), No 32, 1970.

14. Yudin, M. I., FIZIKO-STATISTICHESKIY METOD DOLGOSROCHNYKH PROGNOZOV POGODY (Physicostatistical Method for Long-Range Weather Forecasting), Leningrad, Gidrometeoizdat, 1968.

15. Yudin, M. I., "The Problem of a Multiaspect Statistical Evaluation of the Information Yield of Prognostic Relationships," TRUDY GGO (Transactions of the Main Geophysical Observatory), No 329, 1975.

16. Yudin, M. I., "Significance of Different Types of Information in the Long-Range Weather-Forecasting Problem," METEOROLOGIYA I GIDROLOGIYA, No 3, 1979.

17. Yudin, M. I., Meshcherskaya, A. V., "Complex Physicostatistical Method for Predicting Weather for a Long Time in Advance," METEOROLOGIYA I GIDROLOGIYA (Meteorology and Hydrology), No 1, 1977.

18. Yakovleva, N. I., Repinskaya, R. P., Gurleva, K. A., "Determination of the Coherence of Processes in Time and its Seasonal Characteristics," TRUDY GGO, No 201, 1968.

UDC 551.583

SIMPLE CLIMATIC MODEL OF THE LATITUDINAL DISTRIBUTION OF ATMOSPHERIC PRECIPITATION

Moscow METEOROLOGIYA I GIDROLOGIYA in Russian No 11, Nov 80 pp 42-48

[Article by A. S. Kabanov, candidate of physical and mathematical sciences, Institute of Experimental Meteorology, manuscript submitted 25 Jan 80]

[Text]

Abstract: An attempt is made to supplement simple models of the thermal regime of the atmosphere by still another climatic parameter -- precipitation. In formulating the model use is made of the postulated correlation between the quantity of atmospheric water vapor and surface air temperature, averaged in time and along a circle of latitude. An expression is derived for the averaged intensity of precipitation, which includes the local evaporation of water vapor from the underlying surface, the local rate of change in air temperature and the meridional transfer of water vapor, regulated by the meridional transport of heat. The computed mean annual distribution of precipitation by latitude for the M. I. Budyko variant of the model agrees qualitatively with the variation of the measured distribution of precipitation outside the tropical zone of the atmosphere. The possible reasons for the discrepancy between theory and experiment in the tropical zone of the atmosphere are indicated.

Introduction. At the present time an active search is being made for ways to create methods for predicting climatic changes. Great hopes are being laid on simple climatic models based on the balance of solar energy, the long-wave energy escaping into space and on the modeling of heat transfer in the atmosphere and hydrosphere [1, 12, 14, 15]. Naturally, these models cannot replace more detailed models, which in principle can solve many problems going beyond the content of simple models. Nevertheless, the use of semi-empirical models even now has made it possible to clarify many important climatic aspects, in particular, possible reasons for climatic change in the geological past and in the present epoch [2, 3].

The possibilities of simple models can be increased if within the framework of these same approximations an allowance is made for the moisture balance in the atmosphere. The objective of our study was to supplement simple models of the thermal regime of the atmosphere by still another climatic parameter -- precipitation -- and clarify possible ways to obtain a closed system of equations for computing the mean latitudinal distributions of air temperature at the earth's surface and precipitation. An attempt to integrate the moisture cycle in a simple climatic model was made for the first time by Sellers in [15]; after introducing a whole series of rather arbitrary hypotheses it was possible to achieve a rather good agreement between the computed and observed mean latitudinal distributions of temperature, but it was not possible to achieve satisfactory results for precipitation.

Principal equations of model. We will assume that all the climatic variables are averaged along a circle of latitude and for a time interval considerably exceeding the characteristic time during which it is possible to construct vertical profiles of temperature and humidity under the corresponding boundary conditions. Then, within the framework of a one-dimensional model of the thermal regime it is deemed possible to use the air temperature T at the earth's surface as a climatic variable [1, 2].

We will introduce another climatic variable q -- the quantity of water vapor in a vertical column of the atmosphere with a unit cross section. Climatic data [9, 13] indicate that precipitation exists at any circles of latitude. This means that the value of the q parameter, averaged along a circle of latitude and in time, is regulated by phase transitions, which should lead to a correlation between q and T. A review of investigations of the activation of feedbacks between T and the quantity of water vapor in the atmosphere for a study of the earth's climate was presented in [11].

Assuming that there is a correlation between T and q, it is possible to write equations for T, q and the W values (W is the quantity of liquid (or crystalline) water in a vertical column of air with a unit cross-sectional area; W is averaged in the same sense as q and T) by analogy with the system of equations used in describing cloud processes [5, 7, 10]:

$$\frac{\partial T}{\partial t} + \frac{1}{Mc_p} \hat{L} Q_T = \frac{\varepsilon}{Mc_p} + \frac{L}{Mc_p} (m - E) + \frac{L}{Mc_p} \mu, \quad (1)$$

$$\frac{\partial q}{\partial t} + \hat{L} Q_q = E - m - \mu, \quad (2)$$

$$\frac{\partial W}{\partial t} + \hat{L} Q_w = m + \mu - I, \quad (3)$$

where $\hat{L} = \frac{1}{R \sin\varphi} \frac{\partial}{\partial\varphi} \sin\varphi$ is an operator, R is the earth's radius; $\varphi$ is the complement to latitude to 90°; M is the mass of a vertical column of air with a unit cross-sectional area; $c_p$ is the specific heat capacity of air at a constant pressure; $Q_T$, $Q_q$ and $Q_W$ are the quantities of heat, water vapor and liquid (or crystalline) moisture flowing in a meridional direction through an area of a unit thickness in a unit time; L is the specific latent heat of condensation (sublimation); E is the quantity of water evaporating from a unit surface in a unit time; I is the quantity of water which falls on a unit surface area in a unit time;

$$\varepsilon = r_s + r_0;$$

$r_s$ is the influx of radiant energy in a unit time through the upper boundary of the atmosphere (an expression for $r_s$ is cited, for example, in [2]); $r_0$ is the rate of exchange of energy through a unit area of surface between the ocean and the atmosphere; m is the quantity of water vapor which is condensed (or evaporated) in clouds in a unit time in a vertical column of air with a unit cross-sectional area as a result of action of the source of energy $\varepsilon$ and evaporating from the underlying surface.

The appearance of terms with $\mu$ in (1)-(3) is associated with the additional release or absorption of heat (moisture) due to phase transitions during the mixing of air masses containing clouds. When cloud cover is present the mixing of air masses moving horizontally with the surrounding air leads to an adjustment of their temperature to the temperature of the surrounding medium; in this process there will be additional release or absorption of heat (moisture) due to phase transitions. In other words, in the derivation of the transfer equations (1)-(3) horizontal mixing in the atmosphere is seemingly taken into account in two stages: first in the atmosphere there is an exchange of air masses (without mixing) through the vertical boundaries (this transfer is described by the second terms in (1)-(3); then, after intensive exchange, creating great local gradients (which can be interpreted as the formation of frontal zones), an equalization occurs due to mesoscale processes. The phase transitions occurring in the second stage of mixing were taken into account by means of introducing the source $\mu$.

In the presence of the correlation q(T) the $Q_q$ flux is expressed unambiguously through $Q_T$ and equation (2) for q is transformed into an equation for temperature, but with (1) taken into account it should be transformed into identity. This condition makes it possible to determine that

$$\mu = \frac{Q_T}{L} \frac{1}{R\alpha} \frac{\partial \alpha}{\partial \varphi}, \quad \alpha = \frac{1}{1 + \frac{L}{c_p M} \frac{dq}{dT}}, \tag{4}$$

$$m - E = -\beta \frac{\varepsilon}{c_p}, \quad \beta = (1 - \alpha) \frac{c_p}{L}, \tag{5}$$

$$Q_q = \frac{(1 - \alpha)}{L\alpha} Q_T. \tag{6}$$

It must be remembered that without introduction of the source $\mu$ it is impossible to achieve transformations of equation (2) into identity and the problem of determining the parameters in (4)-(6) becomes insoluble. The $\alpha$ and $\mu$ parameters were used earlier in the theory of cloud processes [5, 7, 10].

In the atmosphere the quantity of water in liquid and crystalline states is always much less than the quantity of water vapor. We will also take into account that the geographical variability of q exceeds the latitudinal changes of W. In addition, estimates show that during times greater than the time of mixing of the entire atmosphere, everywhere except possibly in the tropical zone, there is satisfaction of the condition $\partial q/\partial t \gg \partial W/\partial t$. All this makes it possible, in describing the global distribution of precipitation, to use the well-known hypothesis [6] that all the condensed moisture falls as precipitation. Then

$$\frac{\partial q}{\partial t} + \hat{L}Q_q \gg \frac{\partial W}{\partial t} + \hat{L}Q_w,$$

and it follows from (2) and (3) that

$$I = m + \mu. \tag{7}$$

With (4)-(6) taken into account, expressions (1) and (7) are transformed to the form

$$\frac{Mc_p}{\alpha}\frac{\partial T}{\partial t} + \hat{L}\frac{Q_T}{\alpha} = \varepsilon, \tag{8}$$

$$I = E - \frac{dq}{dt}\frac{\partial T}{\partial t} - \frac{1}{L}\hat{L}\frac{1-\alpha}{\alpha}Q_T. \tag{9}$$

Expressions (8) and (9) represent the principal result of the work.

It follows from (8) that the value $\alpha < 1$ characterizes the expenditures of energy from the source $\varepsilon$ on phase transitions in the adjustment of the water vapor content to the q(T) value. The $c_p^* = c_p/\alpha$ value can be interpreted as the effective specific heat capacity of an atmosphere with a cloud cover at a constant pressure. In this case $c_p^* > c_p$, since the heat introduced into such a system is expended not only on heating, but also on phase transitions. It is important that $c_p^*$ can be essentially dependent on temperature.

As an example, we will assume that

[H = sat]

$$\frac{q}{M} = k\frac{\rho_H(T)}{\rho},$$

where k is a dimensionless value less than unity, $\rho_{sat}(T)$ is the density of the saturated vapor at the temperature T, $\rho$ is air density at the underlying surface.

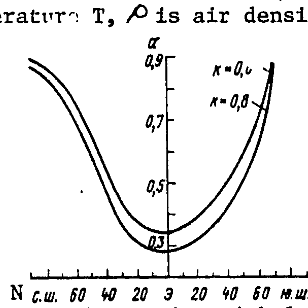


Fig. 1. Change in $\alpha$ value with latitude.

This assumption makes it possible to compute the $\alpha$ value at different latitudes which correspond to the observed latitudinal distribution of mean annual temperatures. The results of such computations for different k = 0.8-0.6 are represented in Fig. 1. It can be seen that the effective heat capacity in the southern latitudes can be two or three times greater than in the northern latitudes. It can be concluded from this that fluctuations of the energy source $\varepsilon$ identical in intensity will lead to fluctuations of temperature greater in value in the northern and temperate latitudes in comparison with temperature fluctuations in the southern latitudes.

It follows from (9) that the intensity of precipitation is determined by local evaporation E, the local rate of change in atmospheric temperature and the meridional transfer of water vapor, which is regulated by heat transfer and which is described by the last term in (9).

It is important that the averaged intensity of precipitation was not sensitive to different variations of cloud cover. This conclusion is a result of the fact that after spatial averaging along the circles of latitude and for time intervals exceeding the time of atmospheric relaxation that part of the condensed moisture which is expended on an increase in the size or liquid-water content of clouds is a small fraction in comparison with the total quantity of condensed moisture.

It should also be noted that it was possible to match the heat and moisture balances by the introduction of only one additional parameter dq/dT. Such an approach made it possible to exclude precipitation and evaporation from the underlying surface in explicit form from the thermal regime equation (8) and make equation (8) independent of (9). It goes without saying that (8) will nevertheless be dependent on (9) if one takes into account the possible influence of precipitation on the zonally averaged albedo and the intensity of long-wave radiation.

Variant of model formulated by M. I. Budyko. We will use the M. I. Budyko hypothesis [1] in which

$$L \frac{Q_T}{\alpha} - r_0 = \gamma (T - T_p), \tag{10}$$

where $T_p$ is the mean planetary temperature of the lower air layer. For modern conditions $T_p$ = 288 K. This relationship was confirmed by materials from satellite observations for the mean annual conditions of the radiation balance of the earth-atmosphere system [3]. The following is obtained

$$\gamma \approx 2.784 \text{ Cal/(cm}^2\cdot\text{degree}\cdot\text{year)}$$

We will examine a case when $r_0 \sim (T - T_p)$. Then expression (10) makes it possible to represent the flux $Q_T$ by a nonlocal expression through the temperature field

$$Q_T = \gamma_* \alpha \frac{R}{\sin\varphi} \int\limits_0^{\varphi} [T(\varphi') - T_p] \sin\varphi' \, d\varphi', \tag{11}$$

where $\gamma - \gamma_*$ determines the fraction of heat transported by ocean currents. The physical sense of the nonlocal parameterization of the flux (11) is explained in [4].

The representation of the flux in form (11) makes it possible to write equations (8) and (9) in the form

$$\frac{Mc_p}{a}\frac{\partial T}{\partial t} + \gamma (T - T_p) = r_s, \qquad (12)$$

$$l = E - \frac{dq}{dT}\frac{\partial T}{\partial t} - (1-a)\frac{\gamma_*}{L}(T - T_p) + \frac{\partial a}{\partial \varphi}\frac{\gamma_*}{L}\frac{1}{\sin\varphi}\int_0^{\varphi}(T - T_p)\sin\varphi' \, d\varphi'. \qquad (13)$$

The semiempirical equation (12), except for the nonstationary term, retained the same form which was proposed in the initial M. I. Budyko variant [1]. Using formula (13) it is possible to compute the mean annual latitudinal distribution of precipitation corresponding to the latitudinal distribution of mean temperature obtained from solution of equation (12) [13] (with $\partial T/\partial t = 0$) and by means of measurement. As the mean latitudinal distribution of evaporation E use was made of the data published by Sellers [9, 13]. As an example it was assumed that $q/M = k\,\rho_{sat}(T)/\rho$.

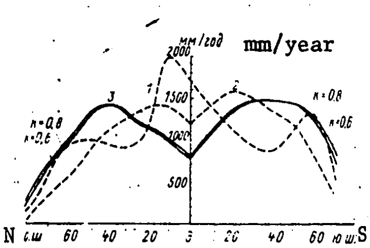


Fig. 2. Experimental curves of the mean annual distribution of precipitation (1) and evaporation (2) [9], and also computed distributions of precipitation (3) on earth.

The results of such computations with k = 0.8-0.6 and $\gamma_* = \gamma$ are represented in Fig. 2. Here also for comparison we give the experimental curve for the mean annual distribution of precipitation on the earth [9].

The computed curves of the distribution of precipitation virtually coincide (Fig. 2) for cases of temperature distributions measured and obtained from solution of equations (12). The dependence of the distribution of precipitation on the parameter k in the range of its values 1-0.6 is weak. There is a qualitative agreement of the computed and measured distributions of precipitation in the high and temperate latitudes. However, there is a considerable noncorrespondence between theory and experimental data for the low latitudes. This discrepancy is attributable, in particular, to the fact that the considered mechanism of meridional transport of heat and moisture does not apply in the tropical zone of the atmosphere. Moreover, it follows from (13) that this mechanism gives an incorrect direction of the transfer of moisture in the tropical zone from the equator to the pole.

In actuality, however, the transfer of moisture by the Trade winds occurs here in the opposite direction, which also leads to the appearance of heavy precipitation in the ICZ. However, in this model heavy precipitation does not appear in the ICZ.

It can be concluded from this that the region of Hadley circulation is not satisfactorily described within the framework of one-dimensional models, which can be used correctly only in those cases when movement in the troposphere has a quasi-two-dimensional character and the transfer of heat and moisture along the meridian is accomplished by macroscale atmospheric eddies and not by regular currents, as in the region of the Trades.

Next we note that on the basis of equations (12) and (13) it is possible to solve self-consistent problems if the E value is determined. According to the schematization cited in [2], $E = ft_w$, where $t_w$ is the temperature of the surface of ocean waters in degrees Celsius. Since the change in $t_w$ with latitude qualitatively coincides with the variation $E(\varphi)$, using the correlation between E and $t_w$ and in a definite way carefully selecting the proportionality factor f, we qualitatively obtain the same results for the distribution of precipitation as shown in Fig. 2.

The correlation $E = ft_w$ was obtained with neglecting of the dependence of E on wind velocity variations. This is justified by the fact that in the computations in [2] use was made only of the mean latitudinal and mean seasonal values of the parameters for which different variations of wind velocity possibly are real but play a small role.

In a general case, however, it is usually assumed that E and $r_0$ are dependent on wind velocity. Then for the closing of equation (9) it is necessary to have dynamic equations. Such equations within the framework of a one-layer model, with allowance for the mechanism of interaction between moving atmospheric eddies and the main flow of the atmosphere, were proposed in [8].

In conclusion the author expresses appreciation to N. S. Okhrimenko for assistance in carrying out the computations.

BIBLIOGRAPHY

1. Budyko, M. I., "Origin of Glacial Epochs," METEOROLOGIYA I GIDROLOGIYA (Meteorology and Hydrology), No 11, 1968.

2. Budyko, M. I., IZMENENIYE KLIMATA (Climatic Change), Leningrad, Gidrometeoizdat, 1974.

3. Budyko, M. I., "Semiempirical Model of the Thermal Regime of the Atmosphere and Real Climate," METEOROLOGIYA I GIDROLOGIYA (Meteorology and Hydrology), No 4, 1979.

4. Voloshchuk, V. M., Svirkunov, P. N., "On the Problem of Nonlocal Parameterization of Turbulent Flows," METEOROLOGIYA I GIDROLOGIYA, No 7, 1980.

5. Voloshchuk, V. M., Sedunov, Yu. S., "Kinetic Equation for Evolution of the Spectrum of Droplets in a Turbulent Medium in the Condensation Stage of Cloud Development," METEOROLOGIYA I GIDROLOGIYA, No 3, 1977.

6. Gandin, L. S., Dubov, A. S., CHISLENNYYE METODY KRATKOSROCHNOGO PROGNOZA POGODY (Numerical Methods for Short-Range Weather Forecasting), Leningrad, Gidrometeoizdat, 1968.

7. Kabanov, A. S., Sedunov, Yu. S., "On the Equations for the Transfer of Heat and Moisture in Clouds," TRUDY IEM (Transactions of the Institute of Experimental Meteorology), No 30, 1972.

8. Kabanov, A. S., Shmerlin, B. Ya., "On Allowance for the Influence of Rotation and Movement of Eddies in the Main Flow of a Fluid," METEOROLOGIYA I GIDROLOGIYA, No 10, 1979.

9. Pal'men, E., N'yuton, Ch., TSIRKULYATSIONNYYE SISTEMY ATMOSFERY (Circulation Systems in the Atmosphere), Leningrad, Gidrometeoizdat, 1973.

10. Stepanov, A. S., "Condensation Growth of Cloud Droplets in a Turbulent Atmosphere," IZV. AN SSSR, FIZIKA ATMOSFERY I OKEANA (News of the USSR Academy of Sciences: Physics of the Atmosphere and Ocean), Vol 11, No 1, 1975.

11. Coakley, J. A., "Climate Modeling Radiative-Convective Model," REV. GEOPHYS. SPACE PHYS., Vol 16, No 4, 1978.

12. North, G., "Analytical Solution to a Simple Climate Model With Diffusive Heat Transport," J. ATMOS. SCI., Vol 32, No 6, 1975.

13. Sellers, W. D., PHYSICAL CLIMATOLOGY, Univ. of Chicago Press, Chicago, Illinois, 1965.

14. Sellers, W. D., "A Global Climatic Model Based on the Energy Balance of the Earth-Atmosphere System," J. APPL. METEOROL., No 8, 1969.

15. Sellers, W. D., "A New Global Climatic Model," J. APPL. METEOROL., Vol 12, No 2, 1973.

UDC 551.558(575.4)

# EXPERIMENTAL INVESTIGATIONS OF OROGRAPHIC WAVES AND VERTICAL MOVEMENTS IN THE NEIGHBORHOOD OF KRASNOVODSK AIRPORT

Moscow METEOROLOGIYA I GIDROLOGIYA in Russian No 11, Nov 80 pp 49-53

[Article by O. A. Lyapina and Ye. I. Sofiyev, candidate of physical and mathematical sciences, Central Asiatic Regional Scientific Research Institute, manuscript submitted 7 Apr 80]

[Text]

Abstract: This study was carried out in connection with the complex conditions involved in the landing of aircraft during presence of strong northerly winds. Orographic waves were investigated using constant-level pilot balloons tracked by theodolite. Vertical movements were investigated using conventional pilot balloons. The parameters of waves are given, the conditions for their development are described and their influence on a landing aircraft is discussed.

Krasnovodsk airport is situated on a plateau which drops off steeply (at an angle of 45°) to Krasnovodskiy Gulf. The dropoff extends latitudinally and at the edge there are highlands with a small (about 50 m) relative relief.

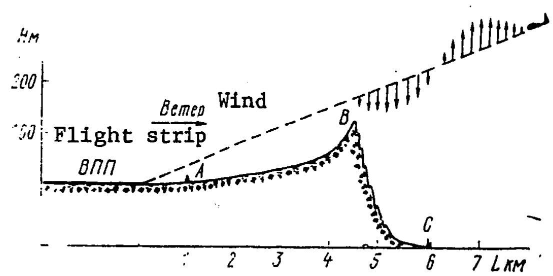


Fig. 1. Orographic waves near Krasnovodsk airport.

Figure 1 schematically shows the vertical profile of the terrain along the landing beam when an approach is made from the north.

In an investigation of the orographic deformation of the flow in the case of northerly winds we released constant-level pilot balloons from point B, situated at the edge of the dropoff. The trajectories of the pilot balloons were tracked by two optical theodolites set up along the shores of Krasnovodskiy Gulf (point C, Fig. 1).

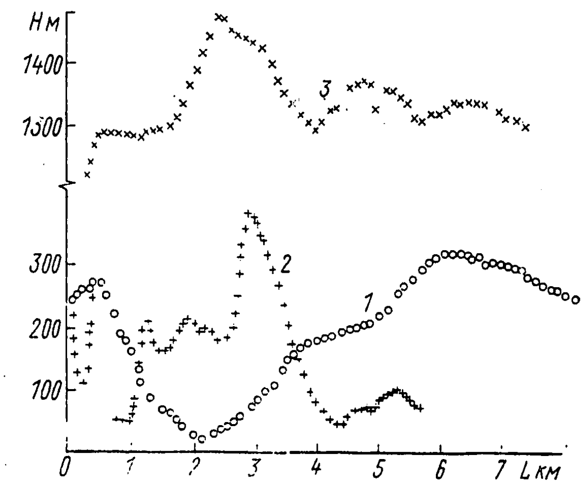


Fig. 2. Trajectories of constant-level pilot balloons for different temperature gradients. October 1978. 1) $\gamma$ = 0.6°C/100 m (24 Oct, 1130 hours), 2) $\gamma$ = 1.0°C/100 m (24 Oct, 1430 hours), 3) $\gamma$ = 1.1°C/100 m (14 Oct, 1130 hours).

In addition, at points A and C ordinary (non-constant level) pilot balloons were launched for measuring the vertical wind profiles and these were tracked by theodolite. All the pilot balloons (both constant-level and ordinary) were released each hour. The coordinates were reckoned with a discreteness of 15 sec with AShT theodolites (accuracy of readings 0.01°). The observations were processed on a "Minsk-22" electronic computer using a specially formulated algorithm [1], making it possible to compute the coordinates with any arrangement of the pilot balloons relative to the base (in particular, when the pilot balloon is at the zenith, in the vertical plane of the base, and also at the same level with or even below the observation points).

The temperature stratification was evaluated by making measurements of temperature at point C and on the landing strip (difference in elevations 120 m), and also using data from aircraft soundings and radiosonde measurements.

Wave movements were observed when there were northerly winds exceeding 6 m/sec and a stable thermal stratification. These conditions are evidently necessary for the appearance of waves, that is, are always observed when waves are present. For the time being it is not clear whether they are also adequate, that is, whether they inevitably lead to waves. The vertical wind profile measured at point A, despite expectations [3,4], did not exhibit a significant correlation with the presence of waves. It is easy to trace the development and destruction of waves during the course of one northerly intrusion when they developed during a stable stratification and were destroyed when the stratification was unstable (for example, on 17 and 24 October 1978). The waves usually have a lifetime of 0.5-2 hours; their frequency of appearance is relatively small: in 50 cases of observations of constant-level balloons waves were noted in only 11.

The vertical extent of the wave disturbances is dependent on the thickness of the inversion layer. According to data from research flights it usually is 800-1,000 m, that is, exceeds the height of the obstacle by a factor of 10. The horizontal extent of the waves can exceed 10 km.

Table 1

Characteristic Parameters of Lee Waves. October, 1978

| Number | Time | $\gamma$°C/100 m | $\bar{u}$ m/sec | $\bar{H}$ km | $\lambda$ km | $A_{max}$ | $\vert W_{max} \vert$ |
|---|---|---|---|---|---|---|---|
| 2 | $17^h27^m$ | 1.2 | 5.0 | 0.25 | 1.7 | 500 | 2.7 |
| 8 | $14^h10^m$ | --- | 8.1 | 0.3 | 2.1 | 200 | 3.4 |
| 10 | $9^h38^m$ | --- | 5.2 | 0.6 | 1.9 | 100 | 1.3 |
| 10 | $10^h30^m$ | --- | 6.3 | 0.5 | 3.0 | 130 | 0.8 |

$\bar{H}$ -- mean wave height; $A_{max}$ -- maximum wave amplitude

Figure 2 shows the projections of the trajectories of constant-level pilot balloons entering into waves onto the vertical plane. The trajectories 1, 2, 3 relate to stable, neutral and unstable stratifications respectively. Trajectory 3 merits special mention. The stratification in the lower 100-m layer at the time of observation was unstable and no waves were observed here. The constant-level pilot balloon rose monotonically. At an altitude of 1300 m it entered into a clearly expressed attenuating wave, probably arising on the boundary of an inversion.

The characteristic parameters of some waves are given in the table.

The length of the waves in kilometers can be roughly estimated using the formula $\lambda \approx \sqrt{\bar{u}}$, where $\bar{u}$ is the wind velocity at the level of the waves in m/sec, that is, half as great as computed using the approximate Dorodnitsyn formula [2]. The modulus of the vertical velocity can be from 0.1 to 0.3 of the horizontal velocity at the level of the waves or from 0.2 to 0.4 of the wind velocity at the level of the landing strip.

Thus, with great wind velocities (15-20 m/sec) the vertical velocity components in the waves can attain 5-7 m/sec, which is not safe for an aircraft coming in for a landing.

Another danger of the waves is as follows. An aircraft on the descent path alternately enters into the ascending and descending branches of the wave. Upon entering into the ascending branch the pilot parries its effect using the elevators and as a result (after 8-12 sec) the aircraft can be in the descending branch with a negative pitching angle. Such a situation is especially dangerous directly near elevations where the descending flows are most intensive and overcoming them may be beyond the technical capabilities of the aircraft.

The descending flows on the lee side of a steep dropoff are well known to the experienced pilots of Krasnovodsk airport. A spontaneous loss of altitude, which here is called an "indraft," appears at a distance of 1-2 km from the edge of the steep scarp, which agrees well with the lengths of the waves cited in the table. The "indraft" is observed both against the background of calm flight and when there is bumping of different intensity.

According to our observations, a stable stratification, favoring the formation of waves at the time of northerly and northwesterly intrusions, does not exist for a long time, 0.5-2 hours, and is replaced by an equally brief period of instability. This circumstance, evidently, imposes definite limitations on the maximum possible advance time for predicting waves, limiting it to 1-2 hours.

Vertical fluctuations of the wind were computed using data from base pilot balloon observations made on the windward (point A, Fig. 1) and leeward (point C) sides using the formula

$$W_i' = \overline{W} - W_i,$$

where $\overline{W}$ is the vertical velocity of the pilot balloon, averaged for the entire ascent, $W_i$ is the vertical velocity of the pilot balloon in the i-th layer. The thickness of the i-th layer, with a discreteness of observations of 15 sec, was 30-100 m.

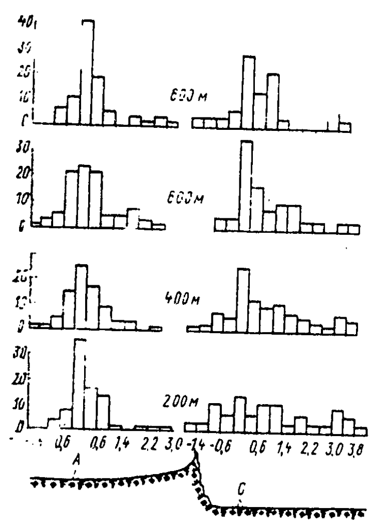


Fig. 3. Frequency of recurrence of vertical gusts at different altitudes over windward and leeward sides of obstacles (with winds of northerly directions).

Figure 3 sh. s the frequency of recurrence of vertical fluctuations of the wind over the windward ard leeward sides of topographic rises when there are strong winds of northerly directions. The figure shows that over the leeward side the vertical fluctuations are two or three times stronger than over the windward side. We note a considerable distc..tion of the histogram of the frequency of recurrence after the passage of an air flow over topographic rises. On the leeward side there is a sharp increase in the fraction of high values of the fluctuations (the histogram is "blurred"). In addition, the nearly normal distribution of frequency of recurrences on the windward sides becomes bimodal on the leeward side. All these differences are smoothed with an increase in altitude.

The appreciable asymmetry of the histogram at an altitude of 200 m over the windward side is evidently associated with the ordered rising of air along the slope.

As might be expected, bumping is much more probable and intense on the leeward side of the topographic rises. Instrumental measurements of vertical accelerations of the AN-24 aircraft in the case of northerly winds registered accelerations up to 1 g on the leeward side. At the same time, on the windward side the accelerations did not exceed 0.1 g.

Bumping has a sharply defined limit: regardless of intensity, when coming in for a landing it ceases 1-0.5 km from the edge of the topographic rise.

In all probability, on the leeward side considerable vertical gusts are attributable either to waves or to eddies with a horizontal axis which become detached from the edge of the steep rise. Judging from the oscillogram of accelerations, the horizontal dimensions of eddies are about 500 m. Flight on the leeward side is usually accompanied by considerable fluctuations of air velocity. According to communications of pilots, there were cases when the amplitude of fluctuations of air velocity attained up to 200 km/hour. This is possible when the aircraft passes through eddies in which the linear velocity is close to 30 m/sec and seems entirely real, since at point B (Fig. 1) velocities of 22-25 m/sec were repeatedly observed.

It is usually assumed that the reason for turbulence on the leeward side of the topographic rise is the hills situated at its very edge (Fig. 1). Our observations for the time being have not confirmed this. The flights made over a part of the scarp where there were no rises revealed that here bumping of the same intensity is encountered.

Conclusions

In the region of southern rises near Krasnovodsk airport, when there are strong winds of northerly directions, waves create the "indraft" effect -- a spontaneous dropping of the aircraft when coming in for a landing. The waves, experiencing breakdown, lead to bumping. Orographic bumping on the leeward side has a limited localization: when coming in for a landing it ceases 0.5-1 km in front of the edge of the topographic rise.

Vertical wind fluctuations on the leeward side of the topographic rise can attain 0.4 of the velocity measured on the landing strip.

In order to predict waves and aircraft bumping it is necessary that thermal stratification be taken into account. The advance time of a forecast cannot exceed 1-2 hours due to the great time variability of the phenomenon.

BIBLIOGRAPHY

1. Denisov, Yu. M., Sofiyev, Ye. I., "New Algorithm for Computing the Coordinates of a Pilot in Base Observations," TRUDY SARNIGMI (Transactions of the Central Asian Regional Scientific Research Hydrometeorological Institute), No 38(119), 1976.

2. Dorodnitsyn, A. A., "Some Problems in the Flow of Air Currents Around Irregularities of the Earth's Surface," TRUDY GGO (Transactions of the Main Geophysical Observatory), No 31, 1940.

3. Musayelyan, Sh., VOLNY PREPYATSTVIY V ATMOSFERE (Obstacle Waves in the Atmosphere), Leningrad, Gidrometeoizdat, 1962.

4. Scorer, R. S., "Airflow Over Mountains: II -- The Flow Over a Ridge," QUART. J. ROY. METEOROL. SOC., Vol 79, 1953.

UDC 551.324.51

# ON THE PROBLEM OF THE MOVEMENT OF CONTINENTAL ICE

Moscow METEOROLOGIYA I GIDROLOGIYA in Russian No 11, Nov 80 pp 54-62

[Article by N. A. Bagrov, professor, USSR Hydrometeorological Scientific Research Center, manuscript submitted 28 May 80]

[Text]

Abstract: A study was made of the problem of movement of continental ice on the assumption of linearity in the resistance to movement. In this case the rate of movement is proportional to the surface slope of the glacier. A model of a circular glacier was formulated applicable to the Antarctic glacier. The results of the computations agree rather well with available data with stipulation of one constant -- the resistance coefficient.

At the present time most scientists acknowledge that during the Tertiary the earth's temperature decreased almost monotonically. At the end of this period and during the entire period which followed, the Quaternary, this weak decrease began to be accompanied by great variations with an alternation of cold glacial and relatively warm interglacial epochs. The last glacial epoch, evidently, was one of the longest and most severe [5, 11].

A. I. Voyeykov was one of the first to bring attention to the fact that the snow and ice covers are not only a result of cooling, but themselves are responsible for their own existence because of their cooling effect. This point of view was further developed in the studies of Brooks [2].

In his studies on the theory of climate Budyko [4] and other scientists made a detailed examination of the influence of ice on climate. It was gradually clarified that ice is the principal factor in the instability of Quaternary climate. Climatic variations were absent in the course of the Tertiary and a large part of the Cenozoic era because a warm climate, especially warm polar regions, do not arise in the presence of an ice cover. But by no means everything is clear here. One of the unsolved problems concerning climatic variations is that more or less significant coolings or warmings are evidently associated with some important restructurings of the entire atmospheric circulation, which are accompanied by changes in the properties of macroturbulence.

In actuality, for example, cooling is reflected primarily in the polar regions, which causes an increase in the equator-pole gradient. It would seem that in this case there should be a substantial increase in the influx of advective heat from the equator. But this for some reason or another does not occur, but there is a further cooling, the formation of continental ice, a decrease of the ocean level, and accordingly, a decrease in oceanic advection.

Evidently, with an increase in the equator-pole thermal gradient there is an increase in the intensity of zonal circulation and circulation itself becomes more stable. The latter can be attributed to the fact that with a decrease in temperature and the ocean level there is an increase in dryness of the air; this results in a decrease in cyclonic activity and the latter in turn reduces meridional exchange.

Finally, the propagation of ice is stopped at some latitudes (provided it does not cross a critical latitude). But this position will also not be stable, and the less stable the closer the ice approaches the critical latitude. Should there be a random variation in the direction of a warming which is quite significant, the entire process can go in the opposite direction, that is, in the direction of a further warming. However, for such a reverse process there must be some exceeding of the temperature conditions in comparison with the conditions for advance of the ice.

In any case, according to the computations made by Budyko [4], whereas a decrease in the mean temperature by several tenths of a degree makes it possible for the ice to propagate southward by 10 or more degrees of latitude, the reverse temperature increase to the initial value still does not ensure retreat of the glacier. The ice advances easily but retreats with difficulty.

What about the ice itself? The ice has many properties of a solid brittle body relative to rapidly changing stresses. It is capable of retaining its form for a long time almost unchanged and is capable of withstanding some dilatation. The elasticity of ice is very small. Under the influence of relatively small long-persisting and slowly changing stresses the ice is capable of being slowly deformed, flow and change its form. In this property it resembles a very viscous fluid. However, the tensor of stresses in the ice mass is related very complexly to the tensor of deformation and this relationship is very highly dependent on temperature and the type of ice and the degree of nonlinearity increases with an increase in the stresses. More or less rigorous solutions of the equations for the flow of ice have been derived only for extremely schematic conditions and they are ill-suited for practical computations of the regime of glaciers. For this reason it makes sense to use the simplest assumptions for studying the movement of glaciers. The simplest assumption here will be the hypothesis of linearity of the correlation between resistance and the rate of movement. Using the equation for movement of a fluid in which all the terms on the left-hand side are dropped, we write equations for the movement of ice in rectangular coordinates:

$$0 = -\frac{1}{\rho}\frac{\partial p}{\partial x} - \frac{g}{k}u + X, \qquad (1)$$
$$0 = -\frac{1}{\rho}\frac{\partial p}{\partial y} - \frac{g}{k}v + Y,$$

$$0 = -\frac{1}{\rho}\frac{\partial p}{\partial z} - \frac{g}{k} w + z,$$
$$\frac{\partial u}{\partial x} + \frac{\partial v}{\partial y} + \frac{\partial w}{\partial z} = 0. \quad (1)$$

Here k is some coefficient having the dimensionality of velocity; X, Y, Z are the projections of mass forces (gravitational forces) onto the coordinate axes, $\rho$ is density, p is pressure.

The use of these equations for ice seems extremely unrealistic. There is a definite difficulty in their interpretation. But their application to definite situations is easily interpreted and gives acceptable results.

Now we will examine a very broad glacier on a bed having a common slope with the nonuniformities (see Fig. 1). By selecting the x-axis along the slope and the y-axis in an upward sloping direction, we obtain

$$u = -\frac{k}{\rho g}\frac{\partial p}{\partial x} + k \sin \varepsilon,$$
$$v = -\frac{k}{\rho g}\frac{\partial p}{\partial y} - k \sin \varepsilon. \quad (2)$$

Obviously, the rate of movement along the y-axis can be neglected if the nonuniformities of the bed are small and the glacier surface is slightly slanting along the x-axis.

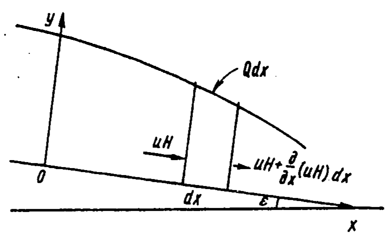


Fig. 1. Diagram of movement of glacier along sloping surface. ε is the slope of the glacier bed to the horizon, H is glacier thickness, u is the rate of movement along the x-axis, Q(x,t) is the rate of growth of ice on the surface due to the precipitation - evaporation difference.

By integrating the continuity equation along y we obtain:

$$\frac{\partial}{\partial x}(\bar{u}H) + v_H = 0, \quad (3)$$

where $\bar{u}$ is the mean rate of movement of the glacier in the cross section, $v_H$ is the rate of movement at the glacier surface.

For the rate $v_H$ we have the obvious expression

$$v_H = \frac{\partial H}{\partial t} + u\frac{\partial H}{\partial x} - Q(x, t). \quad (4)$$

Here Q(x,t) is the layer of growth of the glacier from above as a result of the falling of precipitation. The second term for $v_H$ can be dropped as a result of its smallness.

Integrating the second equation (2), we find that

$$\frac{k}{\rho g} p = k \cos \varepsilon H.$$

Introducing this result into the first equation, we will have

$$u = -k\left(\frac{\partial H}{\partial x} - \sin \varepsilon\right). \quad (5)$$

It therefore can be seen that the rate u is not dependent on y, that is, it remains constant for the entire cross section. This means that the glacier seemingly slides along its bed, being drawn out and becoming slightly deformed.

Collecting the results of (4) and (5), and introducing them into (3), we obtain finally an equation of motion in the following form:

$$\frac{\partial H}{\partial t} = \frac{\partial}{\partial x}\left(kH \frac{\partial H}{\partial x}\right) - \frac{\partial kH}{\partial x} \sin \varepsilon + Q(x, t). \quad (6)$$

This equation can be derived by another, more graphic method. According to the figure shown above, a mass of ice flows into a defined elementary volume with a mean rate of movement u, equal to uH, whereas the outflow is $uH + \partial/\partial x\,(uH)dx$. The difference, equal to $-\partial/\partial x\,(uH)dx$, arises due to the increase of the surface $\partial H/\partial t\, dx$ and falling precipitation Qdx. Comparing these values, we obtain the continuity equation in the following form:

$$\frac{\partial H}{\partial t} + \frac{\partial}{\partial x}(uH) = Q(x, t).$$

The principal hypothesis now is that there is assumed to be a proportionality between the rate of movement u and the slope of the glacier surface, that is, it is assumed that

$$u = -k\left(\frac{\partial H}{\partial x} - \sin \varepsilon\right),$$

where $\varepsilon$ is the slope of the x-axis to the horizon. Introducing this expression into the continuity equation, we again obtain the equation (6).

We will examine the simplest case of a plane horizontal bed. Assume that the accumulation of precipitation Q = const. Then equation (5) in the case of steady movement assumes the form

$$\frac{\partial}{\partial x}\left(H \frac{\partial H}{\partial x}\right) + \frac{Q}{k} = 0.$$

Integrating this expression once, we obtain

$$H \frac{\partial H}{\partial x} + \frac{Q}{k} x = \text{const}.$$

If with x = 0 $\partial H/\partial x = 0$, the constant will be equal to zero.

Integrating the derived equation once again, we obtain

$$H^2 + \frac{Q}{k} x^2 = H_0^2. \quad (7)$$

The surface of such a glacier is an ellipse whose minor axis is $b = H_0$ and whose major axis is $\sqrt{k/Q}$ times greater.

The point $x = H_0 \sqrt{Q/k}$ is the runoff point. This is a singularity: here $H(x) = 0$. In its neighborhood our assumption of smallness of the derivative $\partial H/\partial x$ is substantially impaired. However, this condition comes close to the conditions when the glacier descends from the land to the sea and its end is constantly broken off and seemingly becomes vertical. It is easy to confirm that at the end of the glacier its "discharge" of ice is equal precisely to the entire quantity of accumulation of precipitation on the glacier surface.

In the case of steady movement and a sloping bed equation (6) allows one integral in the form

$$H \frac{\partial H}{\partial x} - \varepsilon H + \frac{1}{k} \int \frac{Q(x)}{k} \, dx = \text{const.}$$

We will examine the simplest case Q = const and write the preceding equation in the form

$$\gamma x = C + \varepsilon H - HH'. \qquad (8)$$

Here $\gamma = Q/k$, and $H'$ is used in denoting the derivative $dH/dx$.

We will differentiate this equation for H. We will have

$$\gamma \frac{1}{H'} = \varepsilon - H' - H \frac{dH'}{dH}.$$

This equation allows the separation of variables (if $H'$ is assumed to be some new variable). Obviously, we will have

$$\frac{dH}{H} = \frac{H'\,dH'}{H'^2 - \varepsilon H' + \gamma} = \frac{H'\,dH'}{\left(H' - \frac{\varepsilon}{2}\right)^2 + \frac{1}{4}(4\gamma - \varepsilon^2)}.$$

The integral of this equation in the case $4\gamma - \varepsilon^2 > 0$ can be written in the form

$$\ln H = \frac{1}{2} \ln (H'^2 - \varepsilon H' + \gamma) + \frac{\varepsilon}{\sqrt{4\gamma - \varepsilon^2}} \operatorname{arctg} \frac{2H' + \varepsilon}{\sqrt{4\gamma - \varepsilon^2}} + \text{const.} \qquad (9)$$

In the case $4\gamma - \varepsilon^2 < 0$ in formula (9) it is only necessary to change the sign of the integrand, that is, under the sign write $\varepsilon^2 - 4\gamma$ and replace the trigonometric arc tangent by the hyperbolic arc tangent.

Suitably determining the constants in equations (8) and (9) in a valid manner, we can, using the variable $H'$ as a parameter, use (9) to compute the H value and using (8) — the corresponding value of the x variable. It is possible to obtain a more graphic solution of equation (8) if the $\gamma$ parameter is assumed to be small and if the solution is sought in the form of a series in powers of this parameter.

$$H(x) = h_0 + \gamma h_1(x) + \gamma^2 h_2(x) + \ldots$$

Then as a zero approximation, for determining the initial conditions we could obtain the surface of the glacier again in the form of an ellipse.

Now we will examine a circular glacier lying on a circular cone with a small slope of the generatrix. This will be a model of the Antarctic glacier.

We will write the continuity equation in cylindrical coordinates:

$$\frac{\partial}{\partial r}(rV_r) + \frac{1}{r}\frac{\partial V_\theta}{\partial \theta} + r\frac{\partial V_z}{\partial z} = 0. \qquad (11)$$

Integrating this equation vertically and introducing the mean radial $V_r$ and mean transversal $V_\theta$ velocities

$$u = \frac{1}{H}\int_\xi^H V_r\, dz; \qquad v = \frac{1}{H}\int_\xi^H V_\theta\, dz,$$

we obtain the equation

$$\frac{\partial}{\partial r}(ruH) + \frac{1}{r}\frac{\partial}{\partial \theta}(vH) + r\left(\frac{\partial H}{\partial t} - Q - w_\xi\right) = 0.$$

If the slope of the generatrix of the glacier bed is equal to $\varepsilon$, then $w_\xi = -\varepsilon u$. From the equations of motion or in accordance with the main hypothesis of ice movement we write the rates of ice movement:

$$u = -k\frac{\partial H}{\partial r}; \quad v = -\frac{k}{r}\frac{\partial H}{\partial \theta}. \qquad (12)$$

We obtain a fundamental equation by introducing these expressions into the continuity equation. For purely radial movement we will have

$$\frac{\partial}{\partial r}\left(rH\frac{\partial H}{\partial r}\right) + \varepsilon r\frac{\partial H}{\partial r} + \frac{r}{k}\left(Q - \frac{\partial H}{\partial t}\right) = 0. \qquad (12)$$

Unfortunately, this equation with $\varepsilon \neq 0$ cannot be integrated in quadratures even for steady movement.

We will examine the simplest case of steady movement in the case of a horizontal bed. The equation for such movement will be

$$\frac{\partial}{\partial r}\left(rH\frac{\partial H}{\partial x}\right) + \frac{r}{k}Q(r) = 0. \qquad (13)$$

We will first examine the case of constant accumulation of ice. In this case we obtain

$$rH\frac{\partial H}{\partial r} + \frac{Q}{2k}r^2 = \text{const.}$$

The integration constant will be equal to zero if with $r = 0$ $\partial H/\partial r = 0$. Once again integrating the derived expression, we obtain

$$H^2 + \frac{Q}{2k} r^2 = \frac{Q}{2k} R^2. \tag{14}$$

The constant on the right-hand side was given such a form for convenience in interpretation. Here R is the radius of the glacier -- the major semiaxis of the ellipse (14). The minor semiaxis will be $H_0 = R\sqrt{Q/2k}$ is the thickness of the glacier at the center.

The major axis of the ellipse (14) for the surface of a circular glacier with radial movement is greater by a factor of $\sqrt{2}$ than the major axis of an ellipse (7) for a surface with plane-parallel movement.

Some ice "sources" are necessary for the existence of a stationary glacier. Such a source can be the stipulated constant thickness $H_0$ in some section. Then, downstream, the surface slope increases, the rate of movement increases until the ice discharge is equal to the entire mass of ice accumulation at the surface. Here there is a break in continuity and the glacier breaks off. Analytically this is expressed by the vertical boundary of the glacier at its end. We note that in nature a sharp breakoff of the glacier at its end is evidently characteristic. The discontinuous accumulations of morainal deposits can be evidence of this.

In this entire theory it is noteworthy that if somewhere in the initial section a constant thickness of the glacier is maintained, it will progress downstream only a finite distance, despite the fact that hypothetically conditions exist at its surface for the accumulation of ice.

According to data published by P. A. Shumskiy [12], the most suitable dimensions of an ellipse approximating the Antarctic glacier will be R - 1903 km, $H_0$ = 3.63 km.

However, for a more realistic picture the accumulation of precipitation cannot be considered constant, not dependent on r. Numerous observations show that at the edges of the glacier there is considerably more precipitation than at the center. For precipitation we will take the linear expression

$$Q(\rho) = \alpha(1 + \beta\rho), \tag{15}$$

where $\rho$ = r/R. Equation (13), after the introduction of $\rho$ instead of r, will have the form

$$\frac{\partial}{\partial \rho}\left(\rho H \frac{\partial H}{\partial \rho}\right) + \alpha \frac{R^2}{k} \rho (1 + \beta\rho),$$

and after integration

$$\rho H \frac{\partial H}{\partial \rho} + \alpha \frac{R^2}{2k}\left(\rho^2 + \frac{2\beta}{3}\rho^3\right) = 0.$$

Integrating once again, we obtain

$$H^2 + \frac{\alpha R^2}{2k}\left(\rho^2 + \frac{4\beta}{9}\rho^3\right) = \frac{\alpha R^2}{2k}\left(1 + \frac{4\beta}{9}\right) \tag{16}$$

or

$$\frac{2kH^2}{aR^2} - (1 - \rho^2) - \frac{4a\xi}{9}(1 - \rho^3) = 0. \tag{17}$$

Thus, in the particular case the glacier surface is described by a third-order curve. It is evident that the curve for the glacier surface lies above the ellipse determined by the first two terms of equation (17) without taking into account the increase in precipitation toward the edges of the glacier.

If for the conditions of Antarctica it is assumed that $Q = Q_0(1 + 9\rho)$, that is, that the precipitation increases from the center to the coast by a factor of 10, the total volume of ice accumulation will be determined by the expression $2\pi Q_0 \cdot 3.5R_0^2$, where $R_0$ is the radius of the Antarctic continent stylized as a circle. Then assuming $R_0$ = 1900 km, $Q_0$ = 0.025 m/year, which in general coincides with the estimates of V. A. Bugayev [3] and V. N. Petrov [9], we obtain the ice accumulation of about 1900 $km^3$/year.

In the case of steady movement of glaciers there will be an equivalent discharge of ice into the ocean in the form of floating ice and icebergs.

However, modern data on the earth's water balance make it necessary to postulate that the discharge of ice must be 350-400 $km^3$ greater than the quantity cited above. The fact is that according to data published by R. K. Klige [6], the level of the world ocean during recent decades has been rising 1-1.5 (or even 2) mm/year. And for this the ocean must receive 400-600 $km^3$ of water annually. It is assumed that about 75% of this quantity enters the ocean from Antarctica.

Thus, at the present time Antarctic glaciers have a slightly unsteady character because the total volume of Antarctic ice is estimated at $(25-27)\cdot 10^6$ $km^3$.

This agrees well with modern estimates of the ice balance in Antarctica.

It can be seen clearly from equations (6) and (14) that the form of the glacier surface, and accordingly, other characteristics, are essentially dependent on the dimensionless parameter Q/k. Using Shumskiy's data, we find that in application to a glacier of a circular configuration

$$\sqrt{\frac{2k}{Q}} = \frac{R_0}{H_0} = 524{,}2.$$

Hence $k \approx 1.4Q\cdot 10^5$ cm/year, if Q, the quantity of precipitation, is expressed in cm/year. The rates of movement of glacial masses in Antarctica vary greatly and range from 0 to 1250 m/year. Assuming the mean slope to be equal to $H_0/R_0 = 0.002$, we obtain the mean rate of glacier movement:

$$u = 1{,}4Q\cdot 10^5\cdot 2\cdot 10^{-3} = 2{,}8\cdot Q\cdot 10^2.$$

For estimating the rate we thus obtain

$$\bar{u} \approx (40\text{–}50)\ \text{m/year},$$

which fully agrees with Shumskiy's estimates.

The discharge of ice into the ocean is about 2200 $km^3$, which is 300-400 $km^3$ greater than the total volume of falling precipitation on the entire continent.

It should be noted that the hypotheses used here in the derivation of equations (6), (12) and others, are not new and original. Such hypotheses have long served as the basis of the theory of movement of a fluid (water, petroleum) in porous media.

Moreover, it has been proposed that these hypotheses also be used for the theory of movement of glaciers. A brief exposition (half-page of small print) of such a proposal is given in a book by Paterson [8]. In a book by Badd [1] there is exposition of other, more complex proposals. Nevertheless, glaciologists evidently make no use of the linear theory of movement. As an example, Shumskiy, already cited here, working with all kinds of ellipses and hyperbolas, uses them purely formally for approximation of the type of surface.

It is possible that for ice science itself this theory scarcely can be of great importance. But for the modeling of climate and allowance for the influence of continental ice on climate the procedures set forth here may be of some use. In most cases, evidently, it is possible to use steady movement, that is, it is possible to discard the glacier thickness time derivative $\partial H/\partial t$. In this case time will be taken into account parametrically, through the dependence of the quantity of precipitation Q(x, t) on time.

It seems to me that the model of movement of glaciers described here is considerably more precise than the model used in the book by Sergin and Sergin [10]. It is true that for the Sergin model the retention of the $\partial H/\partial t$ derivative and reduction of glacier movement to a linear equation was extremely important.

In any case, in the modeling of atmospheric circulation, especially in the modeling of the climatic conditions of different epochs, it must be remembered tha' the boundary of the glacial cover can be displaced far to the south (in general, toward the equator) by virtue of the capacity of ice for mechanical movement. As a result, the thawing of ice occurs almost always far from the place where it was formed. It is easy to understand that this capacity for mechanical movement in space, the capacity to creep, slows and limits ice accumulation in thickness in the epoch of the process of its increase and accelerates the thawing of the ice in an epoch of warming, even in a case when the thawing of ice on the glacier surface almost does not occur.

For a more complete analysis of all these characteristics it would be extremely interesting to carry out a numerical analysis and solve the equation of motion for a glacier (6) in full form, stipulating the external parameters in the form of the quantity of ice accumulation at the surface, with precise formulation of the boundary conditions at the end of the glacier, for example, applicable to the last Valday glaciation.

BIBLIOGRAPHY

1. Badd, U. F., DINAMIKA MASS L'DA (Dynamics of Ice Masses), Leningrad, Gidrometeoizdat, 1975.

2. Brooks, Ch., KLIMATY PROSHLOGO (Climates of the Past), Moscow, IL, 1952.

3. Bugayev, V. A., "Atmospheric Processes in Antarctica," OSNOVNYYE ITOGI IZUCHENIYA ANTARKTIKI ZA 10 LET (Principal Results of Study of Antarctica in 10 Years), Moscow, Nauka, 1967.

4. Budyko, M. I., IZMENENIYE KLIMATA (Climatic Change), Leningrad, Gidrometeoizdat, 1974.

5. Gerasimov, I. P., "Climates of Past Geological Epochs," METEOROLOGIYA I GIDROLOGIYA (Meteorology and Hydrology), No 7, 1979.

6. Klige, R. K., SOVREMENNYYE IZMENENIYA UROVNYA MIROVOGO OKEANA (Modern Changes in Level of the World Ocean), Moscow, Nauka, 1978.

7. Monin, A. S., Shishkov, Yu. A., ISTORIYA KLIMATA (History of Climate), Leningrad, Gidrometeoizdat, 1979.

8. Paterson, U., FIZIKA LEDNIKOV (Physics of Glaciers), Moscow, Mir, 1972.

9. Petrov, V. N., ATMOSFERNOYE PITANIYE LEDNIKOVOGO POKROVA ANTARKTIDY (Atmospheric Feeding of the Glacial Cover of Antarctica), Leningrad, Gidrometeoizdat, 1975.

10. Sergin, V. Ya., Sergin, S. Ya., SISTEMNYY ANALIZ PROBLEMY BOL'SHIKH KOLEBANIY KLIMATA I OLEDENENIYE ZEMLI (Systemic Analysis of the Problem of Major Variations of Climate and the Earth's Glaciation), Leningrad, Gidrometeoizdat, 1978.

11. Flen, G., "History and Intransivity of Climate," FIZICHESKIYE OSNOVY TEORII KLIMATA I YEGO MODELIROVANIYA. (TRUDY MEZHDUNARODNOY NAUCHNOY KONFERENTSII. STOKGOL'M, 1974) (Physical Principles of the Theory of Climate and its Modeling. (Transactions of the International Scientific Conference. Stockholm, 1974)), Leningrad, Gidrometeoizdat, 1977.

12. Shumskiy, P. A., "Antarctic Glaciation," OSNOVNYYE ITOGI IZUCHENIYA ANTARKTIDY ZA 10 LET, Moscow, Nauka, 1967.

UDC 551.466

# BISPECTRAL ANALYSIS OF SEA LEVEL FLUCTUATIONS

Moscow METEOROLOGIYA I GIDROLOGIYA in Russian No 11, Nov 80 pp 63-70

[Article by V. Kh. German, candidate of technical sciences, S. P. Levikov, candidate of physical and mathematical sciences, A. S. Tsvetsinskiy, State Oceanographic Institute, manuscript submitted 21 May 80]

[Text]

Abstract: Some theoretical aspects of bispectral analysis are examined. It is shown that in the case of a Gaussian process and weak nonlinearity it is possible, using one output function of the system, to determine the relative contribution of a nonlinear element. A bispectral analysis of the total levels was made, making it possible to evaluate the role of nonlinear interactions in the formation of shallow-water tidal waves.

In shallow-water regions of tidal seas during a period of storms the free surface experiences changes caused by the complex process of interaction between the tide and surge. Here, evidently, the total level differs from a value equal to the linear superposing of the surge and tide, created independently. A study of the interaction between the tide and surge is of great importance for practical purposes. For example, according to an estimate made by Prandle and Walf [7], the height of the surge due to nonlinear interaction with the tide can be increased by 25%. The mechanism of interaction of two types of waves is explained by Rossiter [9] in the following way: during a surge the advance of the full water occurs sooner because the velocity of propagation of the free tidal wave increases and the influence of bottom friction decreases. In addition to interaction between the surge and tide in the seas there are nonlinear interactions between the tidal waves themselves.

In our article the process of nonlinear interactions in level fluctuations will be investigated using bispectral analysis.

The term "bispectrum" was evidently used for the first time by Tick [10], who applied it to a third-order Fourier transform of a centered correlation function. An analysis of a specific geophysical process -- wind waves -- was made using this approach in a study by Hasselman, et al. [3]. The principal properties of bispectral curves are given. We will examine some of them.

If x(t) is a rigorously stationary random process with a mathematical expectation equal to zero, its bispectrum $B(f_1, f_2)$ is determined using the formula

$$B(f_1, f_2) = \frac{1}{(2\pi)^2} \iint\limits_{-\infty}^{\infty} R(\tau_1, \tau_2) \exp[-i(f_1\tau_1 + f_2\tau_2)]\, d\tau_1\, d\tau_2, \tag{1}$$

where

$$R(\tau_1, \tau_2) = \langle x(t)\, x(t+\tau_1)\, x(t+\tau_2) \rangle \tag{2}$$

is a third-order correlation function. The symbol $\langle\,\rangle$ denotes averaging for the set.

If, in addition, x(t) is a real random process, then

$$B(f_1, f_2) = B(-f_1, -f_2)^*. \tag{3}$$

Here the sign* denotes a complexly conjugate value. From the stationarity of the process we have the symmetry relationship

$$\begin{aligned} B(f_1, f_2) &= B(f_2, f_1) = B(f_1, -f_1 - f_2) = B(-f_1 - f_2, f_1) = \\ &= B(f_2, -f_1 - f_2) = B(-f_1 - f_2, f_2). \end{aligned} \tag{4}$$

These relationships show that the bispectrum need only be determined for $f_1$ and $f_2$ values satisfying the condition $0 \leqslant f_1 \leqslant f_2 < \infty$.

We will examine the Kramer representation for a stationary random process

$$x(t) = \int\limits_{-\infty}^{\infty} e^{ift}\, dz(f),$$

where dz(f) is an uncorrelated rando. measure.

Then it is possible to write the following expressions: $\langle dz(f) \rangle = 0,$

$$\langle dz(f_1)\, dz(f_2) \rangle = S(f_1)\, \delta(f_1 + f_2)\, df_1,$$

$$\langle dz(f_1)\, dz(f_2)\, dz(f_3) \rangle = B(f_1, f_2)\, \delta(f_1 + f_2 + f_3)\, df_1 df_2,$$

where $\delta$ (f) is the delta function.

Thus, if the spectrum represents the contribution to the mean square, that is, the dispersion of the process due to the two Fourier components, whose frequencies together equal zero, the bispectrum gives the contribution to the mean cube, that is, the asymmetry due to the product of the components whose frequencies together are equal to zero.

As is well known, for a Gaussian process the third moment (asymmetry) is equal to zero. In this case

$$\langle x^3(t) \rangle = R(0,0) = 0 \tag{5}$$

and it follows from (1) that

$$B(f_1, f_2) = 0.$$

Thus, the bispectrum shows how the deviations of the process from a Gaussian process are "expanded" in frequency, that is, arise due to some frequencies which exist under synchronism conditions,

$$f_1 + f_2 + f_3 = 0. \quad (6)$$

On the other hand, if it is assumed that some investigated process x(t) is Gaussian at the initial moment or that it was formed due to the passage of some Gaussian process through a nonlinear system, then the bispectrum becomes a characteristic of the nonlinearity of this system. [Between the linearity of the wave field and the Gaussian distribution there is some dependence established by a theorem (Hasselman [1]) which asserts that in a linear approximation the random homogeneous field of waves with dispersion asymptotically tends to a Gaussian state, even if at the initial moment it was not Gaussian.] In this case it is possible to speak of the interaction between some frequencies.

Now we will examine two examples illustrating the need to use bispectral characteristics.

Example 1. We will assume that the record (for example, level) x(t) is known. This was formed as a result of transformation of some input real stationary function $x_0(t)$ in the case of passage of an inertialess system with quadratic nonlinearity:

$$x(t) = ax_0(t) + \varepsilon bx_0^2(t), \quad (7)$$

where a, b, $\varepsilon$ are real constants.

In a real case this can correspond to the process of transformation of a tidal wave as a result of friction against the bottom.

We will raise the question as to whether it is possible to determine the values of the coefficients a and $\varepsilon b$ or the relative contribution of a nonlinear element relative to the linear element on the basis of the characteristics of the input and output of the system (a simple nonlinear "black box" variant). This problem is broken down into two variants: a) the input function $x_0$ is not known; b) it is known.

Here we will be interested in the first variant, when the function at the input is not known (as a rule, we do not know the characteristics of the tidal wave at the input, that is, in deep water). However, if it is assumed that:
-- the input function $x_0(t)$ is a real rigorously stationary Gaussian random process with a zero mean (a Gaussian state is essential).
-- the nonlinearity of the system is small ($\varepsilon \ll 1$), then in this case it is possible to obtain some approximate solution of the problem, to be more precise, determine the relative contribution of the nonlinear term. Taking into account that the third moment of the Gaussian process is equal to zero, from (7) we obtain

$$<x^2(t)> = a^2 < x_0^2(t)> + \varepsilon^2 b^2 < x_0^4(t)>, \quad (8)$$

$$<x(t)\, x_0(t)> = \varepsilon b < x_0^4(t)>. \quad (9)$$

But

$$x(t) = a x_0(t) + O(\varepsilon), \quad \text{that is,} \quad x_0(t) = \frac{1}{a}\, x(t) + O(\varepsilon),$$

$$\frac{1}{a^2} < x^3(t)> + O(\varepsilon) = \frac{\varepsilon b}{a^4} < x^4(t)>, \quad (10)$$

$$\frac{\varepsilon b}{a^2} \approx < x^3(t)> / < x^4(t)>.$$

The relative contribution of the nonlinear term relative to the linear term is determined as follows:

$$\frac{\varepsilon^2 b^2 < x_0^4(t)>}{a^2 < x_0^2(t)>} \approx \frac{\varepsilon^2 b^2 < x^4(t)>}{a^4 < x^2(t)>} = \frac{(< x^3(t)>)^2}{< x^4(t)> < x^2(t)>}. \quad (11)$$

Thus, in the case of an input Gaussian process and weak nonlinearity it is possible, using one output function, to determine (approximately) the relative contribution of the nonlinear element (but not the value of the coefficients a and $\varepsilon$ b, because a full solution can be obtained with known input and output processes).

Example 2. We will examine the system

$$x(t) = \int a(\tau)\, x_0(t-\tau)\, d\tau + \varepsilon \iint K(\tau_1, \tau_2)\, x_0(t-\tau) \times \times x_0(t-\tau_1)\, d\tau_1\, d\tau_2. \quad (12)$$

We will assume, first, that $x_0(t)$ is a real rigorously stationary random Gaussian process with a zero mean, and second, that the nonlinearity of the system is weak ($\varepsilon \ll 1$). We know only the process at the system output x(t). As in the preceding example, it is possible to solve two problems:

a) determination of the ratio of the contributions to the spectrum of the process x(t) from the nonlinear and linear parts of the system for each frequency f on the basis of the statistics of the output function $<\{x(t)\}>$, that is

$$\alpha(f) = \varphi(<\{x(t)\}>);$$

b) determination of the Z(f, f') value through the statistics of the function at the output $<\{x(t)\}>$ (known) and the coefficients a(f) (unknown). Here Z(f, f') is the double Fourier transform of the transfer function $K(\tau_1, \tau_2)$; the Z(f, f') value is usually called the interaction or biadmittance coefficient. [The term "biadmittance," having the sense of a two-frequency transfer function, was taken from a study by Cartwright [2].]

For brevity we will cite the final expressions. The solution of the second problem is as follows:

$$\varepsilon Z(f, f') = \hat{a}(f)\, \hat{a}(f') \frac{B(f, f)}{2 S_x(f)\, S_x(f')}, \quad (13)$$

where a(f) is the Fourier transform of $a(\tau)$, $S_x(f)$ is the spectrum of the process x(t), B.f, f') is the bispectrum of the process x(t).

The first problem has the following solution:

$$\alpha(f) = \int \frac{|B(f', f'-f)|^2}{S_x(f)\, S_x(f')\, S_x(f'-f)}\, df'. \quad (14)$$

Thus, with the assumptions made above it is possible to determine (approximately) the relative contribution of nonlinear interactions to the spectrum of level fluctuations on the basis of only one characteristic of the output function.

Below, when we speak of interaction between individual frequencies, it will always be understood that the investigated system conforms to the assumptions made above: a Gaussian state of the input process and the weak nonlinearity of the system. Otherwise the reasonings concerning the interaction of frequencies can lose sense. For example, when a non-Gaussian process is fed to the input of the linear system an investigation of the bispectral characteristics of the output process does not give any information concerning the nonlinearity of the system but determines the internal structure of the output process, distorted by the linear system.

It follows from what has been stated above that the characteristics of nonlinearity of geophysical processes can be obtained on the basis of a bispectral analysis of the corresponding time series. In an evaluation of the interaction between the frequencies use is made of the real part of the bispectrum $Re[B(f_1, f_2]$, which is a complex function, and the bicoherence function:

$$\gamma^2(f_1, f_2) = \frac{|B(f_1, f_2)|^2}{S_x(f_1)\, S_x(f_2)\, S_x(f_1+f_2)}. \quad (15)$$

At the present time in solving practical problems use is made of the following method for computing the bispectrum [2, 4]. The initial time series x(t) is divided into n segments, each with the length N. The Fourier transform is computed for each segment.

$$X_j(f) = \frac{1}{(2\pi N)^{1/2}} \sum_{t'=1}^{N} e^{-ift'}\, x_j(t')\, W_n(t');$$
$$j = 1, 2, \ldots, n; \quad t' = 1, 2, \ldots, N, \quad (16)$$

where $W_n(t')$ is the weighting function.

Then the bispectrum is computed using the formula

$$B(f_1, f_2) = \frac{1}{n} \sum_{j=1}^{n} X_j(f_1)\, X_j(f_2)\, X_j^*(f_1+f_2). \quad (17)$$

The bicoherence is computed using the formula

$$\gamma^2(f_1, f_2) = \frac{n^3 |B(f_1, f_2)|^2}{\sum_{j=1}^{n} |X_j(f_1)|^2 \sum_{j=1}^{n} |X_j(f_2)|^2 \sum_{j=1}^{n} |X_j(f_1+f_2)|^2}. \tag{18}$$

It is usually assumed that if the bicoherence is equal to 1, a nonlinear interaction exists between the frequencies, whereas if the bicoherence is equal to zero, interaction is absent [8]. Usually the bispectrum and bicoherence are represented in the plane of the frequencies $f_1$ and $f_2$ in the form of a triangle whose vertices have the coordinates

$$(0,\ 0)\ (f_N,\ 0) \text{ and } (1/2\ f_N,\ 1/2\ f_N),$$

where $f_N = 1/2\Delta t$ is the Nyquist frequency, $\Delta t$ is the discreteness of observations.

Now, adhering to Cartwright [2], we will determine the numerical algorithm for computing the interaction coefficient $Z(f_1, f_2)$. Assume that $X_{r1}$, $X_{r2}$, $X_{r3}$ are evaluations of the level spectrum for three frequencies. The sea level spectrum $X_r$ is computed using the formula

$$X_r = \frac{1}{N} \sum_{j=-N}^{N} \left(1 + \cos\frac{\pi j}{N}\right) \exp(2\pi i r j/N)\ x(j\Delta t - t_0), \quad \left(r = 1, 2, \ldots, \frac{1}{2}N - 1\right). \tag{19}$$

In most cases in an analysis of the level of tidal seas $N\Delta t = 29.5$ days (in order that $\Delta f$ be less than 1 cycle/month). Here $r_1$ corresponds to the arbitrary nontidal frequency $2\pi r_1 \Delta f$, $r_2$ corresponds to the frequency of the main semidiurnal tidal wave 2 cycles/lunar day, $r_3 = r_2 - r_1$ for convenience will be assumed positive. $X_{r3}$ contains the element $h_3$, which reflects the interaction between $X_{r1}$ and $X_{r2}$, and the residual element $h'_3$, which is unrelated to $h_3$. Similarly, $X_{r1} = h + h^1$, where h reflects the interaction between $X_{r2}$ and $X_{r3}$. Thus, it can be written that

$$h_3 = Z(-f_1, f_2)\ X_{r_1}\ X_{r_2}; \qquad h_1 = Z(-f_3, f_2)\ X_{r_3}\ X_{r_2}, \tag{20}$$

where $f_k$ are frequencies proportional to $r_k$.

We will examine the mean product for the set

$$(X^*_{r_2} X_{r_2})\ X^*_{r_3} = (X^*_{r_3} X_{r_2})\ X^*_{r_1} = X^*_{r_1} X^*_{r_3} X_{r_2}.$$

Assuming that the product of the incoherent components is equal to zero,

$$X_{r_2} X^*_{r_2} [Z(-f_1, f_2)\ h'_1 h'^*_1 + Z(-f_3, f_2)\ h'_3 h'^*_3],$$

we obtain

$$Z(-f_1, f_2) \approx \langle X^*_{r_1} X^*_{r_3} X_{r_2} \rangle / \langle |X_{r_2}|^2 |X_{r_1}|^2 \rangle. \tag{21}$$

It can be seen that in its structure this relationship agrees with expression (13) for the interaction coefficient in a model case.

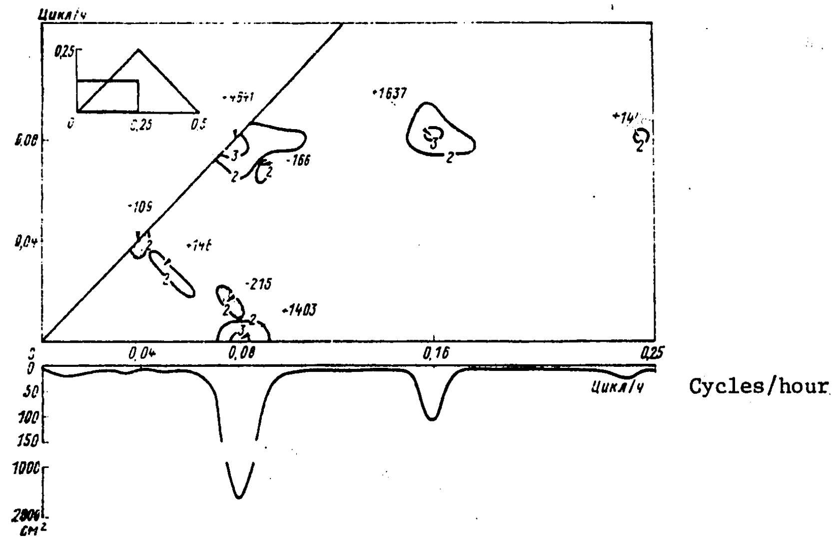


Fig. 1. Bispectrum of total level fluctuations. White Sea, level post Kandalaksha, 1 July-13 September 1972. Discreteness of observations 1 hour. Dimensionality of bispectrum [cm3]. The graph shows all the values exceeding 100 cm3. The figures on the isolines are exponents of a base 10. The regions of negative values of the bispectrum are shaded. The figures at the ends of the arrows are the extremal values of the bispectrum. In the upper left corner of the bispectrum -- the full region of determination of the bispectrum; the thick line indicates the analyzed part of the bispectrum. The energy spectrum is shown in the lower part of the figure. The y-axis is broken.

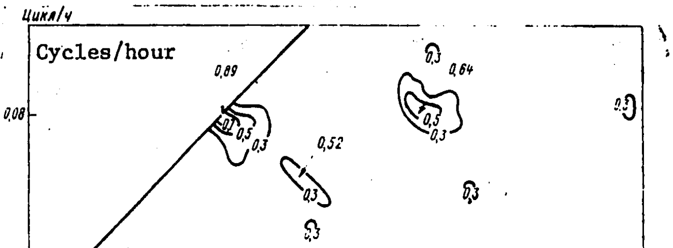


Fig. 2. Bicoherence of total level fluctuations. White Sea, level post Kandalaksha, 1 July - 13 September 1972. Discreteness of observations 1 hour. The extremal values are indicated by the figures at the end of the arrows.

The method described above was used in computing the bispectra and the bicoherence of sea level fluctuations. The initial data used were observations at the level post Kandalaksha (White Sea) for two periods: ice period (1 January - 15 March

1972) and ice-free (1 July-13 September 1972). The duration of each record was 75 days with a discreteness of 1 hour.

Table 1

Principal Interacting Frequencies and Corresponding Values of Bispectrum and Bicoherence

| Interacting frequencies, cycles/hour | | Resultant frequency, cycles/hour | Ice period | | Ice-free period | |
|---|---|---|---|---|---|---|
| | | | bispectrum $cm^3$ | bicoherence | bispectrum $cm^3$ | bicoherence |
| 0.08; 0.08 | 0.16 | 0.16 | 940 | 0.80 | 4641 | 0.89 |
| 0.08; 0.16 | 0.24 | 0.24 | 994 | 0.80 | 1637 | 0.64 |
| 0.08; 0.24 | 0.32 | 0.32 | --- | ---- | 144 | 0.31 |

Figure 1 shows the bispectrum and energy spectrum of variations of sea level for an ice-free period. The energy spectrum was computed by applying the Fourier transform to successive nc ıoverlapping segments of the initial series (9 segments with 200 ordinates in each) and with subsequent averaging of the periodograms. The periodograms were smoothed using the Tukey-Henning filter [2]. The resolution of the bispectrum and the energy spectrum was 0.005 cycle/hour. In both bispectra (the bispectrum for the ice period is not given in this article but in appearance it is similar to the bispectrum for the ice-free period) it is possible to trace a number of well-expressed maxima and the frequencies of the most significant of them are multiples of the frequency of the semidiurnal tide (see Table 1).

In the interpretation of the bispectra it is assumed [3, 8] that positive values of the bispectrum correspond to interaction with frequencies equal to the fundamental frequency or are greater than it, whereas negative values correspond to interaction of the low frequencies with the fundamental frequency. As noted above, a quantitative measure of the nonlinear interaction between two frequencies is the bicoherence function. If the bicoherence value is equal to 1, there is a nonlinear interaction between the particular frequencies, otherwise (the bicoherence is equal to 0) there is no interaction. It follows from Fig. 2 and the table that such an interaction is not characteristic for all maxima of the bispectrum. For example, for the ice-free period significant bicoherence values and bispectrum maxima corresponding to them are observed only for the following pairs of frequencies: (0.08; 0.08), (0.08; 0.16) and (0.08; 0.24).

The position of the particular maxima, and also the maxima in the level spectrum, indicates that in this region there is a rather significant interaction in the system of semidiurnal tidal waves, the result of which is the formation of more high-frequency 1/4-day and 1/6-day shallow-water waves. Evidently, the peak of the level spectrum at a frequency 0.16 cycle/hour is a result of interaction of the semidiurnal fluctuations with one another, the presence of which is specifically indicated by the bispectrum maximum having coordinates in the frequency region equal to 0.08 and 0.08 respectively. In turn, the peak in the level spectrum at a frequency 0.24 owes its origin to the interaction between the semidiurnal and six-hour peaks, which on the bispectrum and bicoherence graph correspond to the maxima

$B(0.08; 0.16) = 1637\ cm^3$, $\gamma^2(0.08; 0.16) = 0.64$ (see Table 1).

It should be noted that the bicoherence for the interaction between the semidiurnal and six-hour frequencies during the winter is substantially greater than in summer (0.80 and 0.64 respectively, see Table 1). It can be assumed that the increase in the degree of nonlinear interactions during winter is attributable to the fact that in addition to bottom friction [6] at this time there is friction against the ice cover commensurable with it. Another interesting peculiarity is the lesser absolute values of the bispectrum in winter, which evidently is associated with the fact that the amplitude of the semidiurnal tidal fluctuations predominating here in winter is approximately 85% of the summer amplitude.

Conclusions

1. It was demonstrated in model examples that in the case of a Gaussian process and a weak nonlinearity the contribution to the spectrum due to nonlinear interactions can be evaluated using exclusively the characteristics of the output function.

2. A bispectral analysis was made of level fluctuations at Kandalaksha station (White Sea). It was established that a bispectral analysis correctly reflects the principal characteristics of nonlinear interactions in a system of tidal waves propagating along a relatively shallow-water bay. This can serve as a basis for investigating nonlinear interactions within the framework of other physical systems whose character (in contrast to a tide) is unknown in advance.

BIBLIOGRAPHY

1. Khassel'man, K., "Description of Nonlinear Interactions by the Methods of Theoretical Physics (With Application to the Formation of Wind Waves)," NELINEYNYYE VOLNY (Nonlinear Waves), Moscow, Mir, 1970.

2. Cartwright, D. E., "A Unified Analysis of Tides and Surges Around North and East Britain," PHIL. TRANS. ROY. SOC. LOND., Vol 263, No 1134 [year not given].

3. Hasselman, K., Munk, W., MacDonald, G. J., "Bispectra of Ocean Waves," TIME SERIES ANALYSIS, edited by M. Rosenblatt, N. Y., Wiley, 1963.

4. Haubrich, R. A., "Earth Noise 5 to 500 Millicycles per Second. I. Spectral Stationarity, Normality and Nonlinearity," JOURNAL OF GEOPHYSICAL RESEARCH, Vol 70, No 6, 1965.

5. Imasato, N., Kunishi, H., "Bispectra of Wind Waves and Wave-Wave Interaction," J. OCEAN. SOC. JAP., Vol 33, 1972.

6. Prandle, D., Walf, J., "Interaction of Surge and Tide in the North Sea and the River Thames," GEOPH. J. ROY. ASTR. SOC., Vol 55, 1975.

7. Prandle, D., Walf, J., "Surge-Tide Interaction in the Southern North Sea," HYDRODYN. ESTUAR. AND FJORDS. PROC. 9th INT. LIEGE COLL. OCEAN HYDRODYN., 1977, Amsterdam, 1978.

8. Roden, G. J., "Low-Frequency Sea Level Oscillations Along the Pacific Coast of North America," JOURNAL OF GEOPHYSICAL RESEARCH, Vol 71, No 20, 1966.

9. Rossiter, J. R., "Interaction Between Tide and Surge in the Thames," GEOPHYSICAL JOURNAL, Vol 6, No 1, 1961.

10. Tick, L. J., "The Estimation 'Transfer Function' of Quadratic Systems," TECHNOMETRICS, Vol 3, No 4, 1961.



APPROVED FOR RELEASE: 2007/02/08: CIA-RDP82-00850R000300100013-3

UDC 556.(06+536+537)

PREDICTION OF THE CHANNEL PROCESS AND SOLUTIONS OF THE PROBLEM

Moscow METEOROLOGIYA I GIDROLOGIYA in Russian No 11, Nov 80 pp 71-78

[Article by B. F. Snishchenko, candidate of technical sciences, State Hydrological Institute, manuscript submitted 24 Apr 80]

[Text]

Abstract: The need for developing a system of predictions of channel processes is substantiated. The author proposes a classification of predictions. It is noted that the most important condition for the successful development of such predictions is the organization of systematic channel observations in the network of the State Committee on Hydrometeorology.

One of the most important problems in science is prediction. In emphasizing this thesis, the well-known Soviet hydrologist V. G. Glushkov wrote: "In essence, it is predictions and only predictions which are required from hydrology" [2].

Hydrological forecasts long ago were transformed into one of the principal branches of applied hydrology; they have traditionally been directed to the prediction of elements of the water and ice regimes [4, 6]. During recent years, in connection with the broad economic activity in river basins, the tasks of monitoring and preserving the environment and creating a unified system for the inventorying of waters, an insistent need has arisen for the development of methods for predicting other elements of the hydrological regime, in particular, the channel process.

Each year new structures are built on rivers. In their construction it is necessary to foresee possible changes in channels and floodplains. The intensity of these changes is dependent on the degree of the effect of engineering work on the factors determining the channel process -- fluid runoff, solid runoff and limiting conditions. In the case of implementation of work not involving channel-forming factors (for example, the erection of supports in the channel for overhead power lines) the problem arises of foreseeing the natural course of the channel process during the time of operation of the structure. If the implementation of engineering measures leads to a change in the characteristics of the determining factors (as happens, for example, in the erection of hydraulic structures), the reformation of the river can assume the most unexpected direction and its prediction acquires an extremely complex character.

In the first case the result of prediction is intended for solution of a unique problem -- evaluation of the stability of a planned structure, and the success of the prediction itself is dependent on a knowledge of the regularities of deformations of the natural channel.

In the second case in order to prepare a prediction it is necessary to ascertain new regularities of the channel process and the prediction itself must lead to the solution of not one, but many problems, such as:

-- evaluation of the degree of change of the river as an element of the natural landscape;

-- evaluation of the change in the flow regime and channel and the possibility of its reverse influence on the conditions for operation of the planned structure;

-- evaluation of the influence of the modified water and channel regimes on other structures falling in the zone to be affected by the planned structure;

-- evaluation of the representativeness of regime observations made in the network of the State Committee on Hydrometeorology after erecting the planned structure, etc.

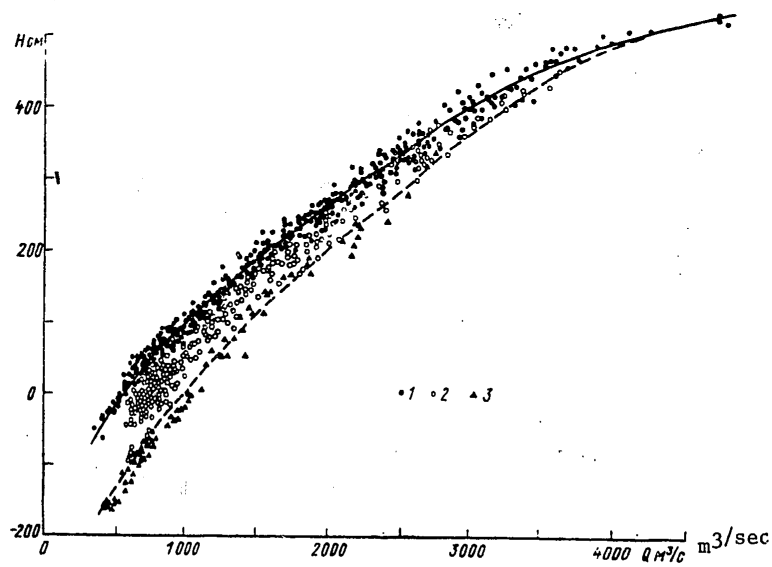


Fig. 1. Nat... e of change of curve of correlation between discharges and levels under conditions of intensive excavation of river alluvium. 1) 1936-1955, 2) 1956-1974, 3) 1975-1978.

Modern economic activity, ca...ed out on rivers or in their basins, is characterized by great volumes of work and intensity. Its results are frequently commensurable with the activity of flowing water during periods measured on a geological time scale.

Thus, during the last two or three decades there has been an appreciable degradation of small and intermediate rivers in the southern part of the European USSR. Their channels have filled with shoals and their floodplains have become swampy and saline as a result of a marked increase in solid runoff received from cultivated watersheds [4]. It is clear that in the future the exploitation and upgrading of these watercourses can be accomplished only on the basis of predictions of channel and floodplain processes.

Equally acute is the problem of predicting channel processes when artificially deepening river channels -- a massive phenomenon observed on many rivers with the excavation of alluvium from them for construction purposes. We will cite an example of such work on the Irtysh in the Omsk region.

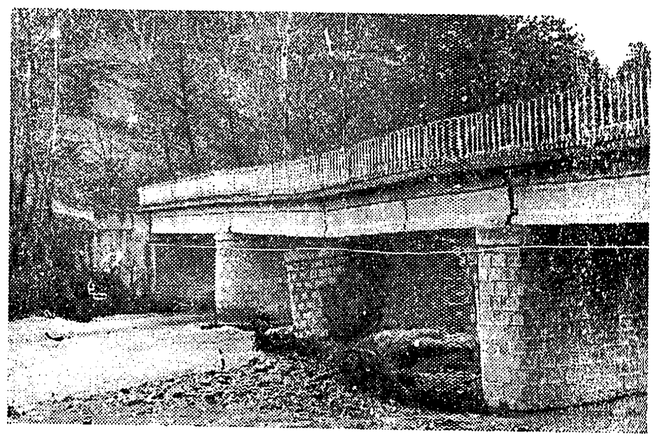

Fig. 2. Initial stage in destruction of bridge situated below excavations of river alluvium.

About 30 million cubic meters of bottom material were excavated in a river reach with a length of 50 km in 15 years; this considerably exceeded the natural receipt of sediments. The evolution of the morphological elements of the channel (bars, beaches, etc.), serving as local erosional bases, led to a falling of water levels in the river. The unambiguous correlation between discharges and levels at the reference gaging station was impaired (Fig. 1), as, however, was the correlation between other regime elements. The carrying out of engineering work in the neighborhood of the gaging station itself introduced substantial errors into measurements of water discharge and turbidity. In order to restore the representativeness of the results of observations it was necessary to take serious organizational-technical measures -- the opening of new gaging stations, changes in the methods for carrying out hydrometric work, etc.

The deficit of transported alluvium below the reach where channel excavations take place always leads to a change in the regime of channel deformations in the lower-lying reaches for a considerable distance. All the engineering structures situated both below and above the excavations, as well in the actual area of the excavations, fall within the zone of influence of such changes. In the event that these engineering structures were built without allowance for possible changes in the channel process their stability will be impaired. Figure 2 shows the initial stage in destruction of a bridge built across a small river above the point where alluvium has been excavated from the channel.

The cited examples indicate the extremely complex cause-and-effect relationships arising as a result of the reciprocal influence of engineering work and the channel process. Taking into account the enormous number of structures and their varieties and the diversity of types of channel regime, it becomes obvious that it is possible to take into account all the forms of their interaction only by use of a special system of channel predictions which would be able to take in all possible manifestations of the channel process, all types of engineering activity on rivers, the entire diversity of forms of their mutual influence.

We note in passing that during recent years artificial watercourses, the large canals which play the main role in the redistribution of water resources, have also become objects of channel predictions. A prediction of the channel process in canals is necessary for selecting their dimensions, handling capacity, magnitude of capital and operational expenditures, and frequently also solution of the problem of the very feasibility of their construction. The common laws of channel formation characteristic for all watercourses transporting sediments enable us to analyze the problem of predicting channel processes in rivers and canals.

At the present time, due to a number of objective factors, a system of predictions of the channel process has not been created. However, individual predictions of channel deformations have long been made. Some prediction methods, such as the hydromorphological analysis method [6], have been developed and are being used successfully.

However, modern practical needs in water management construction no longer are being met by individual, however apt, developments in the field of channel predictions. It is necessary to create such a system of channel predictions which would take in the overwhelming majority of practical problems. And in this period this problem is one of the most important, if not the most important, in the theory of channel processes.

Known studies in the field of hydrological predictions [1, 5], the needs of science for a general prediction method -- a prognostic scheme [9], and also accumulated experience in the prediction of changes in river channels all indicate that success in the development of predictions is dependent on two conditions: availability of a method for developing predictions and a theory of the phenomenon to be predicted. First we will discuss the first condition.

By "prediction" is meant a scientifically validated concept of the future, in the terms of some branch of knowledge pertaining to an unobserved event and giving an indication of the space or time interval within which the predicted event will take place [9].

An important and the first condition in the method for formulating predictions is the defining of criteria or principles. Prediction criteria can be defined on the basis of concepts concerning the practical needs for the prediction of channel

processes, use of the experience in defining criteria in hydrological forecasts and in forecasting work generalizing the experience of all sciences in this field. At the present time it is desirable to define the following prediction criteria, which, it appears, have a general methodological character for channel processes:
-- purpose;
-- origin of watercourse;
-- nature of interaction of a channel process and a structure;
-- nature of interaction of a channel process and the hydrological regime;
-- precomputation time;
-- precomputation methods;
-- form of expression of results;
-- accuracy of precomputation.

If now, using each criterion, we define the types of forecasts, their combination can form a system or classification of forecasts. A truly scientific classification of forecasts must be based on laws and patterns characteristic of the predicted object, that is, the channel process. Theory establishes the patterns and laws. As noted above, the presence of a theory is the second condition for the successful development of forecasts. We will now examine this condition.

The hydromorphological approach is beginning to play the leading role in the channel process theory. It is being developed most actively at the State Hydrological Institute. The fundamental principles (postulates) adopted in it made it possible to lay the basis for a hydromorphological theory of the channel process [3]. These principles established some basic, general properties of the channel process, such as its discreteness, the nature of the direction of channel deformations, the forms of sediment transport, etc. The channel process theory is developing its laws and patterns, taking the established properties into account.

The scientific classification of channel forecasts must take into account these properties of the channel process as a genetic basis. Each of the types of forecasts must be developed not only with allowance for the general methodological criteria, but also on the basis of the properties of the channel process. These processes, in essence, are also the criteria for defining the types of forecasts, but criteria of a special, internal order, characteristic only of the hydromorphological theory of the channel process. However, since the properties of the channel process are common for all channel process phenomena, obviously it is more reasonable not to define additional types of forecasts, but to set as a necessary condition of the classification allowance for the principal properties of the channel in each forecast.

We will recall briefly some of the principal properties of the channel process defined in hydromorphological theory.

In accordance with discrete representations, in hydromorphological theory all manifestations of the channel process are considered at different structural levels. At these levels particular laws, particular correlations and ratios, particular determining factors and particular research methods are operative. Each level has its genetically homogeneous forms of channel relief whose movement is a complexly organized form of transport of sediments and expresses channel deformations.

In accordance with the complication of forms of transport of sediment, the structural levels should desirably be represented in the following order: individual particles of channel sediment, channel microforms, channel mesoforms, river macroforms, river morphologically homogeneous reaches, entire river. To the five levels usually considered by theory, a sixth has been added: the entire river.

Each of the types of forecasts defined below also must be considered at the mentioned structural levels of the channel process.

It was established in hydromorphological theory that a change in river channels can occur in two fundamentally different ways: as a result of unidirectional irreversible deformations and as a result of differently directed, sign-variable reversible channel reformations not changing the statistical characteristics of the channels. In some river reaches subjected to intensive economic activity, for example, in the lower pools at hydroelectric power complexes, these deformations are manifested simultaneously, jointly. Accordingly, it is necessary to define a third type of deformations -- joint.

The direction of channel deformations must also be taken into account in each type of forecasts.

An important property of the channel process is the nature of the interaction between discrete channel forms. The interaction can have a uniform character, applicable to channel forms of one structural level, for example, the level of macroforms between meanders. Its character may be diverse when there is a mutual influence of the channel forms considered at different levels, for example, the interaction between an underwater bar and the small ridges (microforms) situated on it. All types of forecasts must also be made with allowance for this property of the channel process.

The cited description of some properties of the channel process gives some idea concerning its essence and now makes it possible to proceed to the defining of types of channel forecasts on the basis of their general methodological criteria.

With respect to the "purpose" criterion, it is possible to distinguish gnosiological and engineering forecasts. The first are prepared for the purpose of developing our knowledge of the natural process without regard to specific practical needs. Engineering forecasts take into account the specific requirements of users related to the implementation of engineering-economic measures on rivers.

The "origin of watercourse" criterion was introduced primarily for the purpose of distinguishing forecasts made for rivers and canals. Depending on the morphological characteristics of watercourses it is possible to carry out a further breakdown of the forecasts: for example, for lowland and mountain rivers, rivers in the permafrost zone; for canals dug in embankments and excavations, in alluvial deposits and in sedimentary rocks.

With respect to the nature of the interaction between the channel process and structures, as already follows from the examples cited at the beginning of the article, it is necessary to distinguish forecasts in engineering work, exerting an influence on definite channel process factors and with structures not capable of acting on them, but experiencing a reverse influence on the channel process. In a detailed classification of engineering structures [7], using the mentioned criterion structures of the first type are called active and those of the second type are called passive structures. These forecasts must then be more detailed, for example, forecasts for bridges, structures to prevent avalanches, water intakes, river petroleum pipeline crossings, etc.

With respect to the character of the interaction between the channel process and hydrological regime it is possible to discriminate forecasts for a natural hydrological regime and forecasts for a modified regime.

With respect to the precomputation or advance time of precomputation of the elements of the hydrological regime in hydrology it is possible to distinguish short-, medium- and long-range forecasts, assigning absolute values of the time interval. With respect to the channel process such a division is incorrect because in this case the theoretical basis of the division is not determined. Accordingly, in actuality, in absolute expression the time of transpiring of channel process phenomena at different structural levels is extremely different. For example, the time required for a sand ridge to move its own length varies from minutes to tens of days; the corresponding duration for mesoforms is an interval from 24 hours to several years, and the time for the development of phenomena at the macroform level (cycle of development of meanders) may be hundreds of days and hundreds of years. The indicated time intervals of the genetic cycles are also dependent on the characteristics of the hydrological cycles.

Accordingly, as a basis for dividing channel forecasts with respect to time it is desirable to use the time of a full genetic cycle of development of a channel form or phenomenon at a definite structural level and also the time of development of these channel regime elements during the period of a hydrological cycle. Thus, time channel forecasts are classified as cyclic genetic and cyclic hydrological forecasts.

The preparation of forecasts using the "precomputation method" criterion must be accomplished taking into account general scientific research methods and the specific conditions of the problem, the stage of the project, type of structure, complexity of the predicted phenomenon, required accuracy of the forecast, etc. The different forecasting methods existing in channel process theory can be reduced to three principal methods: hydromorphological, hydraulic-morphometric and modeling.

Each of the cited types of forecast can be subdivided into subtypes. For example, in the hydraulic-morphometric methods it is possible to discriminate the sediment balance method and the movement of channel forms method. In modeling it is possible to discriminate mathematical and hydraulic models. The latter are subdivided into air and water. Water models can be made rigid or erodable, etc.

With respect to the form of expression of the results, forecasts can be subdivided into qualitative and quantitative, and with respect to accuracy -- as approximate and precise. These forecasts are commonplace and require no clarification.

The proposed classification of forecasts is of a preliminary character. In the future it can be supplemented and made more detailed.

The forecasts defined in the classification are still far from final form and most of them have only been entered into the classification. Nevertheless, it appears that it corresponds to the modern practical requirements and has an entirely purposeful significance -- outline and make more specific the ways to develop channel forecasts. This work must evidently be carried out in three directions:

1) by the accumulation of in situ data on channel process phenomena;
2) by the further revelation of channel process laws and patterns -- as the physical basis for forecasts;
3) by the development of forecasting methods.

Now we will clarify these.

In hydrometeorological forecasts there is a direct relationship between the quantity of initial information and the quality of the forecast. It is also known that the existing rather well-branched network of stations for systematic observations is nevertheless inadequate for obtaining the necessary accuracy or advance time of the forecasts.

The network of the State Committee on Hydrometeorology does not make systematic observations of reformations of river channels and floodplains. Other departments do not make these observations.

Most Administrations of the Hydrometeorological Service during recent years have proceeded to individual, sporadic observations under the methodological direction of the State Hydrological Institute. However, they are made by an extremely few people and this does not make it possible to obtain the information necessary for making channel forecasts.

At the same time, the experience of a number of Administrations of the Hydrometeorological Service is evidence of the great interest of national economic organizations in channel information and the capability of the Administrations of the Hydrometeorological Service to supply such information. For example, the observations of the Kutaisskaya Hydrometeorological Observatory of the Georgian Republic Administration of the Hydrometeorological Service, for ascertaining the channel regime of the Rioni River, make it possible to introduce an important contribution to the project for exploitation of the Kolkhidskaya Lowland; the studies of the Volga and Krasnodarsk Hydrometeorological Observatories of the Northern Caucasus Administration of the Hydrometeorological Service have already made possible a sounder approach to forecasting the reformations of the lower pools of the Volgogradskoye and Krasnodarskoye Reservoirs. The observations of the Western Siberian Scientific Research Institute not only led to solution of a number of practical problems -- validation of the projects for agricultural and industrial water intakes, prediction of changes in the channel of the Ob' in the lower pool of the Novosibirskaya Hydroelectric Power Station, but also made it possible to obtain a series of new scientific results. Important practical results were obtained at the Omsk and Northern Administrations of the Hydrometeorological Service, the Far

Eastern Scientific Research Institute, and elsewhere, on the basis of data from channel observations.

The problems involved in developing some branches of the national economy -- navigation, water supply, melioration, production of nonore construction materials, etc. require the further formulation of systematic observations of the channel process in the network of the State Committee on Hydrometeorology, for the time being, of individual river reaches, especially in urbanized areas [8]. In the not distant future they will make it possible to proceed to the preparation of not only sporadic, but also operational forecasts of channel processes. For this reason there should be immediate expansion of network channel observations and they must be given the status of regime hydrological observations.

With respect to the prospects for development of channel process theory, they also are determined to a great extent by the presence of in situ information, especially for river reaches with a modified hydrological regime. The classification of forecasts makes it possible to be oriented in the priority of those aspects of theory which will be required, in particular, for the further development of these types of forecasts.

Without in situ information it is difficult to hope for a rapid improvement of forecasting methods. For example, the theoretical models which are now being actively developed are frequently fruitless once again due to the lack of reliable in situ information for validating the boundary conditions, evaluation of the representativeness of laboratory data, etc.

BIBLIOGRAPHY

1. Appolov, B. A., Kalinin, G. P., Komarov, V. D., KURS GIDROLOGICHESKIKH PROGNOZOV (Course on Hydrological Forecasts), Leningrad, Gidrometeoizdat, 1974.

2. Glushkov, V. G., VOPROSY TEORII I METODY GIDROLOGICHESKIKH ISSLEDOVANIY (Problems in the Theory and Methods of Hydrological Investigations), Moscow, Izd-vo AN SSSR, 1961.

3. Kondrat'yev, N. Ye., et al., RUSLOVOY PROTSESS (Channel Process), Leningrad, Gidrometeoizdat, 1959.

4. Lapshenkov, V. S., GIDROTEKHNICHESKAYA REKUL'TIVATSIYA MALYKH I SREDNIKH REK V BASSEYNE DONA (Hydrotechnical Upgrading of Small and Intermediate Rivers in the Don Basin), Rostov, Knizhnoye Izdatel'stvo, 1979.

5. Popov, Ye. G., GIDROLOGICHESKIYE PROGNOZY (Hydrological Forecasts), Leningrad, Gidrometeoizdat, 1957.

6. Popov, I. V., DEFORMATSII RECHNYKH RUSEL I GIDROTEKHNICHESKOYE STROITEL'STVO (River Channel Deformations and Hydrotechnical Construction), Leningrad, Gidrometeoizdat, 1969.

7. Snishchenko, B. F., "Methods for Solving Practical Problems on the Basis of the Hydromorphological Theory of the Channel Process," TRUDY IV VSESOYUZNOGO GIDROLOGICHESKOGO S"YEZDA (Transactions of the Fourth All-Union Hydrological Congress), Leningrad, Vol 10, 1976.

8. Snishchenko, B. F., "The Channel Process in Urbanized River Reaches," GIDROLOGICHESKIYE ASPEKTY URBANIZATSII (Hydrological Aspects of Urbanization), Moscow, MFGO, 1978.

9. Yampol'skiy, S. M., Zhilyuk, F. M., Lisichkin, V. A., PROBLEMY NAUCHNO-TEKHNICHESKOGO PROGNOZIROVANIYA (Problems of Scientific-Technical Forecasting), Moscow, Ekonomika, 1969.

UDC 556.(048+16)

RELIABILITY OF CHOICE OF PARAMETERS OF A GAMMA DISTRIBUTION IN THE PROCESSING OF RUNOFF DATA

Moscow METEOROLOGIYA I GIDROLOGIYA in Russian No 11, Nov 80 pp 79-86

[Article by A. V. Khristoforov, candidate of geographical sciences, Moscow State University, manuscript submitted 27 May 80]

[Text]

Abstract: In computations of runoff guaranteed probability curves the relationship between the asymmetry coefficient and the variation coefficient, determining the type of gamma distribution curve, is assumed to be the same for the entire region. The problem arises of checking the correspondence of the selected type of guaranteed probability curves to each of the generalized series and the entire region as a whole. An optimum variant of the "$\chi^2$" test is proposed for solution of this problem. It is shown that the asymptotic theory of the "$\chi^2$" test is applicable in hydrological computations. Formulas are proposed for determining the reliability of choice of the type of guaranteed probability curves in regional generalizations of data on runoff with allowance for their spatial coherence.

In computations of annual, maximum and minimum river runoff used in water management and hydroengineering construction and in constructing guaranteed probability curves which establish the relationship between the value of the investigated runoff characteristic and the annual probability of its excess the most widespread use has been made of a three-parameter gamma distribution proposed in 1946 by S. N. Kritskiy and M. F. Menkel' and introduced into the current USSR norms [4, 7]. The parameters participating in this distribution are the mean value (norm) of the computed characteristic $X_0$, the variation coefficient $C_V$ and the ratio of the asymmetry coefficient to the variation coefficient $C_S/C_V$, determining the type of gamma-distribution curve ($C_S/C_V$ = 1; 2;...). With the availability of a series of hydrometric observations the parameters $X_0$ and $C_V$ are evaluated by the moments method, approximate maximum probability method or graph analysis method [7]. A satisfactory evaluation of the third parameter of the guaranteed probability curve $C_S/C_V$ can be obtained from an individual series only with the presence of an extremely long period of runoff observations for a particular river [1, 6]. As a rule, the choice of the type of gamma distribution curve (selection of the $C_s/C_v$ value) is accomplished on the basis of spatial-temporal generalizations of runoff data for several rivers. Thus, the value of the $C_s/C_v$ parameter is assumed to be common for the rivers of the entire region within which only the $X_0$ and $C_v$ parameters are subject to an individual sample evaluation and all the guaranteed probability curves correspond to a single type of gamma distribution [4, 7]. The problem arises of checking the correspondence between the $C_s/C_v$ value of each specific series of observations and the series as a whole. This article is devoted to an investigation of the possibilities of solving this problem.

Different variants of the Pearson chi-square test have come into the widest use in solving such problems [3, 5].

Assume that there is a sample $x_1,\ldots,x_n$, whose elements are essentially independent random values having a three-parameter gamma distribution with the density $f(x, \theta_1, \theta_2, \theta_3)$, where $\theta_1 = X_0$; $\theta_2 = C_v$; $\theta_3^0 = C_s/C_v$. Then the statistical hypothesis is checked: $H_0: \theta_3 = \theta_3^0$, where $\theta_3^0$ is some value of the $C_s/C_v$ parameter. The region of values $(0, \infty)$ is broken down into k intervals $A_1,\ldots,A_k$ and the frequencies $\nu_1,\ldots,\nu_k$ of falling in the corresponding intervals are determined from the sample. The t statistics are computed using the formula

$$t = n \min_{\theta_1, \theta_2} \sum_{i=1}^{k} \frac{[\nu_i - p_i(\theta_1, \theta_2, \theta_3^0)]^2}{p_i(\theta_1, \theta_2, \theta_3^0)}, \tag{1}$$

where $p_i(\theta_1, \theta_2, \theta_3^0)$ are the probabilities of falling into $A_i$ intervals corresponding to the distribution $f(x; \theta_1, \theta_2, \theta_3^0)$.

If the $H_0$ hypothesis is correct, the t statistics asymptotically have the distribution $\chi^2_{k-3}$ (central distribution of chi-square with k - 3 degrees of freedom) [3]. If the hypothesis $H_0$: $\theta_3 = \theta_3^0$ is incorrect and the elements of the sample $x_1,\ldots,x_n$ have the alternative distribution $f(x; \theta_1', \theta_2', \theta_3')$ (alternative to $H_1$), the t statistics have a noncentral distribution $\chi^2_{k-3,\ n\delta_0}$ with the noncentrality parameter $n\delta_0$. Here

$$\delta_0 = \min_{\theta_1, \theta_2} \sum_{i=1}^{k} \frac{[p_i(\theta_1', \theta_2', \theta_3') - p_i(\theta_1, \theta_2, \theta_3^0)]^2}{p_i(\theta_1, \theta_2, \theta_3^0)}, \tag{2}$$

where $p_i(\theta_1', \theta_2', \theta_3')$ are the true probabilities of falling in the intervals $A_i$, $i = 1,\ldots,k$ [3,5].

Stipulating the $\alpha$ criterion (the probability of refuting the $H_0$ hypothesis when it is true) with the significance level, we refute the checked hypothesis if the t statistics exceed the quantile $\chi^2_{k-3}(\alpha)$ of the probability $1-\alpha$ of a chi-square distribution with k - 3 degrees of freedom. Thus, the strength of this criterion (the probability of refuting the hypothesis $H_0$: $\theta_3 = \theta_3^0$, when it is untrue, but the alternative $H_1: (\theta_1', \theta_2', \theta_3')$ is true, is found asymptotically as the probability of exceeding of a random value having the distribution $\chi^2_{k-3,\ n\delta_0}$, that is, in excess of $\chi^2_{k-3}(\alpha)$:

$$\mu(\alpha) = P\{\chi^2_{k-3,\ n\delta_0} > \chi^2_{k-3}(\alpha)\}. \tag{3}$$

This criterion does not take into account the fact that the alternatives to the $H_0$ hypothesis also correspond to a three-parameter gamma distribution and also can be called the general $\chi^2$ test. Since in the investigated problem the alternatives to the $H_0$ hypothesis also belong to a gamma distribution, the optimum $\chi^2$ test, using the $t_0$ statistics

$$t_0 = t - n \min_{\theta_1, \theta_2, \theta_3} \sum_{i=1}^{k} \frac{[\nu_i - p_i(\theta_1, \theta_2, \theta_3)]^2}{p_i(\theta_1, \theta_2, \theta_3)}. \tag{4}$$

will have a considerably greater value.

The $t_0$ statistics have the distribution $\chi_1^2$ if the $H_0$ hypothesis is true and $\chi^2_{1,\, n\delta_0}$ if the alternative $H_1$ is true [3, 5]. The $\mu_0(\alpha)$ value of the optimum test ($\chi^2$) considerably exceeds the value of the general test and asymptotically is equal to

$$\mu_0(\alpha) = P\{\chi^2_{1,\, n\delta_0} > \chi_1^2(\alpha)\}, \tag{5}$$

where $\chi_1^2(\alpha)$ is the quantile of the probability $1-\alpha$ of a central $\chi^2$ distribution with one degree of freedom [3, 5].

The value of the optimum and general Pearson test is dependent on the parameter $\delta_0$, characterizing the degree of difference between the hypothesis $H_0$: $\theta_3 = \theta_3^0$ and the true alternative $H_1$:($\theta_1$, $\theta_2$, $\theta_3$).

An investigation of more than 50 different variants of the combination of the hypothetical value $\theta_3^0$ of the parameter $C_s/C_v$ and the true values $C_v = \theta_2'$ and $C_s/C_v = \theta_3'$, and also the general theoretical analysis, using the results cited in [1, 3, 6], makes it possible to propose the following approximation formula for computing the $\delta_0$ values with breakdown into $k > 3$ intervals, equiprobable from the $H_1$ point of view:

$$\delta_0 = 10^{-3}\sqrt{k-3}\,(\theta_3^0 - \theta_3')^2\,[0{,}70 + 0{,}25\,\theta_2'\,(6 - \theta_3')], \tag{6}$$

and with $\theta_3' > 6$ in formula (6) in place of $\theta_3'$ it is necessary to substitute the value 6. This dependence makes it possible to compute the value of the general and optimum $\chi^2$ tests with a relative error not exceeding 10-15%.

In actual hydrological computations it is customary to use only the general $\chi^2$ test and in order to avoid minimizing the statistical test in formula (1) it is necessary to compute the $\tilde{t}$ statistics:

$$\tilde{t} = n \sum_{i=1}^{k} \frac{[\nu_i - p_i(\theta_1^*, \theta_2^*, \theta_3^0)]^2}{p_i(\theta_1^*, \theta_2^*, \theta_3^0)}, \tag{7}$$

where $\theta_1^*$ and $\theta_2^*$ are evaluations of the parameters $\theta_1 = X_0$ and $\theta_2 = C_v$ by the moments method. If the hypothesis $H_0$: $\theta_3 = \theta_3^0$ is true, the $\tilde{t}$ statistics have a central $\chi^2$ distribution $\chi_l^2$, with $l$ degrees of freedom, $k - 3 \leqslant l \leqslant k - 1$. If the alternative $H_1$:($\theta_1$, $\theta_2$, $\theta_3$) is correct, the $\tilde{t}$ statistics have a noncentral distribution $\chi^2_{l,\, n\delta}$, where

$$\delta = \sum_{i=1}^{k} \frac{[p_i(\theta_1', \theta_2', \theta_3') - p_i(\theta_1', \theta_2', \theta_3^0)]^2}{p_i(\theta_1', \theta_2', \theta_3^0)}. \qquad (8)$$

Since for the $\ell$ value it is only possible to indicate the (k − 3, k − 1) interval of possible values, this test can be called the approximate general $\chi^2$ test. By analogy with the preceding precise case the approximate optimum test can be determined using the $\tilde{t}_0$ statistics:

$$\tilde{t}_0 = \tilde{t} - n \min_{\theta_3} \sum_{i=1}^{k} \frac{[\nu_i - p_i(\theta_1^*, \theta_2^*, \theta_3)]^2}{p_i(\theta_1^*, \theta_2^*, \theta_3)}. \qquad (9)$$

The $\tilde{t}_0$ statistics have the distribution $\chi^2_{1,n\delta}$, and the value of the approximate optimim test, refuting the $H_0$ hypothesis with $\tilde{t}_0 > \chi^2_1(\alpha)$, is determined by formula (5) with the replacement of $\delta_0$ by $\delta$.

The approximate $\chi^2$ test accurately corresponds only to the case of checking of the simple hypothesis $H_0$: $\theta_1 = \theta_1^*$; $\theta_2 = \theta_2^*$; $\theta_3 = \theta_3^0$ versus the complex alternative $H_1$: $\theta_1' = \theta_1^*$; $\theta_2' = \theta_2^*$; $\theta_3' \neq \theta_3^0$. Its application for checking complex hypotheses of the type $H_0$: $\theta_3 = \theta_3^*$ is conditional and leads, as will be demonstrated below, to a substantial exaggeration of the value.

The following formula is proposed for computing the $\delta$ value, determining the value of the general and optimum criteria, for checking the simple hypothesis $H_0$:($\theta_1^*$, $\theta_2^*$, $\theta_3^0$) versus the alternatives $H_1$:($\theta_1^*$, $\theta_2^*$, $\theta_3'$) with breakdown into 10 equiprobable (from the $H_1$ point of view) intervals

$$\delta = 0.04\,(\theta_3' - \theta_3^0)^2\,\theta_2^{*2}, \qquad (10)$$

making it possible to compute the value of the tests with a relative error not greater than 10-15%. Formulas (6) and (10) indicate that the $\delta$ value is several times greater than the true measure of discrepancy between the alternative and the hypothesis $\delta_0$.

In [2] the statistical tests method was used in investigating the value of the approximate general $\chi^2$ test for checking the hypothesis $H_0$:$C_s/C_v = \theta_3^0 = 1, 3, 4$ versus the alternatives $H_1$: $\theta_1 = 1$; $\theta_2 = 0.5$; $\theta_3 = 2$. With n = 100 and breakdown into k = 20 equiprobable intervals the values of the statistical evaluations $\mu^*(\alpha)$ of the value for different $\alpha$ are given in Table 1. In this same table, as a comparison, we give the theoretical $\tilde{\mu}_T(\alpha)$ values of the approximate general $\chi^2$ test obtained using formula (3) with k = 20. The data cited in Table 1 confirm the applicability of the general asymptotic $\chi^2$ test in hydrological computations.

Table 2 gives theoretical evaluations of the value of the general approximate and precise general and optimum tests with n = 100 and $\theta_3^0 = 4$, confirming the point that there is a substantial exaggeration of the value of the approximate test and the advantages of the optimum test over the general test when the class of alternatives is limited by a three-parameter gamma distribution.

Assume that we have m series of observations $x_{i\,1},\ldots,x_{in_i}$, each of which conforms to a three-parameter gamma distribution with the parameters $x_0 = \theta_{1\,i}$; $C_v = \theta_{2\,i}$; $C_s/C_v = \theta_{3\,i}$; $i = 1,\ldots, m$. It is necessary to check the $H_0$ hypothesis on the general type of gamma distribution corresponding to the value $C_s/C_v = \theta_3^0$. When using the optimum $\chi^2$ test for each of m samples we compute the $t_{0\,i}$ value using formula (4) and the $H_0$ hypothesis is refuted in the case of high values of $t_0$ statistics,

$$t_0 = \sum_{i=1}^{m} t_{0\,i}, \tag{11}$$

If all m series are independent of one another, the statistics have the central distribution $\chi^2_m$ in a case when the $H_0$ hypothesis is true and $\theta_{3\,i} = \theta_3^0$, and the noncentral distribution $\chi^2_{m,\,\lambda_0}$ in the opposite case:

$$\lambda_0 = \sum_{i=1}^{m} n_i \delta_{0\,i}, \tag{12}$$

where the $\delta_{0\,i}$ values can be determined using formula (6).

The value $\mu_0(\alpha)$ of the optimum criterion (test) can be determined quite precisely:

$$\mu_0(\alpha) = P\{\xi > \xi(\alpha) - \varepsilon\} = \frac{1}{\sqrt{2\pi}} \int_{\xi(\alpha)-\varepsilon}^{\infty} e^{-\frac{x^2}{2}}\, dx; \tag{13}$$

$$\varepsilon = \frac{\lambda_0}{\sqrt{2m}}. \tag{14}$$

Here $\xi$ is a canonical normal random value with the parameters (0, 1); $\xi(\alpha)$ is the corresponding probability quantile $1 - \alpha$.

Similarly, the approximate optimum $\chi^2$ test refutes the $H_0$ hypothesis in the case of high values of the $\tilde{t}_0$ statistics:

$$\tilde{t}_0 = \sum_{i=1}^{m} \tilde{t}_{0\,i}. \tag{15}$$

In the case of nondependence of the series of observations the $\tilde{t}_0$ statistics have the distribution $\chi^2_{m,\lambda}$, where

$$\lambda = \sum_{i=1}^{m} n_i \delta_i. \tag{16}$$

The value $\tilde{\mu}_0(\alpha)$ of the approximate optimum test when using m independent series can also be determined using formulas (13) and (14) with the replacement of $\lambda_0$ by $\lambda$.

In a case when the generalized series are correlated, the $t_0$ statistics behave asymptotically as the sum of the squares of m correlated normal values relative to which joint normality is assumed. It follows from the asymptotic theory of the $\chi^2$ test that the correlation coefficient between $t_{0\,i}$ and $t_{0\,j}$ is approximately equal to the correlation coefficient between the corresponding evaluations $(C_s/C_v)$ [3]. Using the nomograms cited in [1] it can be computed that this coefficient is approximately equal to the correlation coefficient between the values of the initial hydrological series $x_{is}$, $x_{js}$.

Thus, if we use $\rho$ to denote the mean value of the correlation coefficient between m initial series of hydrometric observations, the $\mu_0(\alpha)$ value of the optimum $\chi^2$ test for checking the hypothesis of a common value of the $C_s/C_v$ parameter for all series can be determined with a sufficient accuracy using the formula

$$\mu_0(\alpha) = P\left\{ \xi > \xi(\alpha) - \frac{\sum_{i=1}^{m} 10^{-3} n_i \sqrt{k_i - 3}\,(\theta_3^0 - \theta_{3i})^2 \,[0,70 - 0,25\,\theta_{2i}\,(6 - \theta_{3i})]}{\sqrt{2m}\,\sqrt{1 + \rho^2 (m-1)}} \right\} \quad (17)$$

The relative error in determining the value using formula (17) does not exceed 15%.

Similarly, the value of the approximate optimum $\chi^2$ test can be evaluated using the formula:

$$\tilde{\mu}_0(\alpha) = P\left\{ \xi > \xi(\alpha) - \frac{\sum_{i=1}^{m} 0,04\, n_i\, \theta_{2i}^2\, (\theta_{3i} - \theta_3^0)^2}{\sqrt{2m}\,\sqrt{1 + \rho^2 (m-1)}} \right\}. \quad (18)$$

It is possible to determine the critical value $\varepsilon_0$ in formula (13) with which the probability $\mu(\alpha)$ of refuting the $H_0$ hypothesis when it is not true is assumed to be inadequately large in comparison with the probability $\alpha$ of refuting the $H_0$ hypothesis when it is true. For example, with $\varepsilon \leqslant 1$ in formula (13) $\mu(10\%) \leqslant 40\%$, that is, the probability of adopting an untrue $H_0$ hypothesis is 60% and is only 1 1/2 times less than the probability of adopting a true $H_0$ hypothesis.

This makes it possible to find the mean probable deviations of the true $C_s/C_v$ value from the hypothetical value for each specific drainage basin, still not checked using the Pearson test. For example, when using the approximate optimum $\chi^2$ test with a stipulated critical $\varepsilon_0$ the mean maximum deviation $\tilde{\Delta}^2 = (\theta_{3i} - \theta_3^0)^2$ for the i-th drainage basin, which must be expected in the case of adoption of the hypothesis $H_0$: $C_s/C_v = \theta_3^0$, is determined as

$$\tilde{\Delta}^2 = \frac{\varepsilon_0}{m} \frac{\sqrt{2m}\,\sqrt{1 + \rho^2 (m-1)}}{0,04\, n_i\, \theta_{2i}^2}. \quad (19)$$

Similarly, the maximum deviations $\Delta^2$, not checked by the optimum $\chi^2$ test, are determined:

$$\Delta^2 = \frac{\varepsilon_0}{m} \frac{\sqrt{2m}\,\sqrt{1 + \rho^2 (m-1)}}{10^{-3} n_i \sqrt{k_i - 3}\,[0,70 + 0,25\,\theta_{2i}\,(6 - \theta_{3i})]}. \quad (20)$$

Formula (20) determines considerably greater values of the maximum deviations of the hypothetical $C_s/C_v$ value from the true values and these deviations correspond to the real possibilities of statistical checking of the correctness of the choice of the type of gamma distribution, taking into account, in contrast to formula (19), the influence of the errors in determining the norm and variation coefficient.

As an illustration we will examine the problem of checking the hypothesis of a common $C_s/C_v$ value for the probability curves for minimum 30-day discharges of the rivers of Transbaykalia, adopted on the basis of data for 89 drainage basins.

Table 1

Statistical $\mu^*(\alpha)$ and Theoretical $\tilde{\mu}_T(\alpha)$ Evaluations of the Value of the General Approximate $\chi^2$ Test in Percent

| $\alpha$ % | $\theta_3^0 = 1$ | | $\theta_3^0 = 3$ | | $\theta_3^0 = 4$ | |
|---|---|---|---|---|---|---|
| | $\tilde{\mu}_T(\alpha)$ | $\mu^*(\alpha)$ | $\tilde{\mu}_T(\alpha)$ | $\mu^*(\alpha)$ | $\tilde{\mu}_T(\alpha)$ | $\mu^*(\alpha)$ |
| 1 | 5 | 5 | 4 | 3 | 18 | 17 |
| 5 | 16 | 21 | 14 | 14 | 40 | 40 |
| 10 | 25 | 30 | 22 | 24 | 52 | 50 |
| 25 | 47 | 50 | 45 | 40 | 73 | 70 |
| 50 | 70 | 74 | 68 | 64 | 89 | 83 |

Table 2

Value of Approximate General $\tilde{\mu}(\alpha)$, Precise General $\mu(\alpha)$ and Optimum $\mu_0(\alpha)$ $\chi^2$ Tests With $\theta_3^0 = 4$; $n = 100$

| $\alpha$ % | $\tilde{\mu}(\alpha)$ | $\mu(\alpha)$ | $\mu_0(\alpha)$ |
|---|---|---|---|
| 1 | 18 | 2 | 10 |
| 5 | 40 | 9 | 22 |
| 10 | 52 | 17 | 34 |
| 25 | 73 | 35 | 50 |
| 50 | 89 | 62 | 75 |

Table 3

$\tilde{\Delta}$ and $\Delta$ Values for Minimum 30-Day River Discharges in Transbaykalia

| River | Station | n | $C_V^*$ | $(C_S/C_V)^*$ | $\tilde{\Delta}$ $\rho = 0$ | $\tilde{\Delta}$ $\rho = 0.5$ | $\tilde{\Delta}$ $\rho = 1.0$ | $\Delta$ $\rho = 0$ | $\Delta$ $\rho = 0.5$ | $\Delta$ $\rho = 1.0$ |
|---|---|---|---|---|---|---|---|---|---|---|
| Olov | Soktuy | 12 | 1.13 | 4 | 0.3 | 0.7 | 0.9 | 1.5 | 3.3 | 4.6 |
| Aga | Aginskoye | 21 | 0.95 | 3 | 0.4 | 1.9 | 1.2 | 1.4 | 3.0 | 4.3 |
| Chitinka | Chita | 38 | 0.63 | 2 | 0.5 | 1.01 | 1.5 | 1.1 | 2.4 | 3.4 |
| Mogocha | Mogocha | 23 | 0.68 | 4 | 0.6 | 1.3 | 1.8 | 1.6 | 3.5 | 4.9 |
| Ingoda | Deshulan | 25 | 0.36 | 1 | 1.0 | 2.2 | 3.1 | 1.6 | 3.5 | 4.9 |
| Nercha | Kyker | 19 | 0.38 | 2 | 1.2 | 2.6 | 3.7 | 1.8 | 3.9 | 5.5 |

For each of the 89 points we computed the mean maximum uncontrollable deviations $(\theta_{3_i} - \theta_3^0)$ of the true values $\theta_{3_i}$ of $C_s/C_v$ from the regional hypothetical value $\theta_3^0$, corresponding to the approximate optimum Pearson test $(\tilde{\Delta})$ and the optimum Pearson test with a breakdown of each of the samples in 10 equiprobable intervals $(\Delta)$ for $\varepsilon_0 = 1$. The $\tilde{\Delta}$ and $\Delta$ values were computed for different values of the mean correlation coefficient $\rho$ between the minimum 30-day discharges of the rivers of Transbaykalia. The case $\rho = 1$ corresponds to checking of the $H_0$ hypothesis: $C_s/C_v = \theta_3^0$ for each individual series.

Table 3, listing six drainage basins, gives the durations of the series of observations n, evaluations of the variation coefficient $C_v^*$ and the ratio $(C_s/C_v)^*_\sim$ and for $\rho = 0$; 0.5; 1 gives the maximum statistical uncontrollable deviations $\tilde{\Delta}$ and $\Delta$ from the adopted hypothesis for the approximate and precise optimum Pearson tests.

The data cited in Table 3 show that if one does not take into account the influence of the errors in determining $X_0$ and $C_v$, the approximate optimum Pearson test is not capable of checking even insignificant deviations of the true distribution from the hypothetical distribution, even when using an individual series $(\rho = 1)$. The correlation of the series considerably lowers the value of the statistical tests, and accordingly, the effectiveness of regional generalizations.

## BIBLIOGRAPHY


1. Blokhinov, Ye. G., RASPREDELENIYE VEROYATNOSTEY VELICHIN RECHNOGO STOKA (Distribution of the Probabilities of River Runoff Values), Moscow, Nauka, 1974.

2. Zhuk, V. A., Yevstigneyev, V. M., Chutkina, L. P., "Characteristics of Use of Matching Tests in Checking Hypotheses Concerning the Laws of Distribution of Characteristic Runoff Values," PROBLEMY GIDROLOGII (Problems in Hydrology), Moscow, Nauka, 1978.

3. Kendall, M. Dzh., St'yuart, A., STATISTICHESKIYE VYVODY I SVYAZI (Statistical Conclusions and Correlations), Moscow, Nauka, 1973.

4. Kritskiy, S. N., Menkel', M. R., "On Evaluating the Probabilities of Frequency of Recurrence of Rarely Observed Hydrological Phenomena," PROBLEMY REGULIROVANIYA RECHNOGO STOKA (Problems in Regulation of River Runoff), No 6, Moscow, Izd-vo AN SSSR, 1956.

5. Rozhdestvenskiy, A. V., OTSENKA TOCHNOSTI KRIVYKH RASPREDELENIYA GIDROLOGICHESKIKH KHARAKTERISTIK (Evaluation of the Accuracy of the Distribution Curves of Hydrological Characteristics), Leningrad, Gidrometeoizdat, 1977.

6. Leman, E., PROVERKA STATISTICHESKIKH GIPOTEZ (Checking of Statistical Hypotheses), Moscow, Nauka, 1964.

7. UKAZANIYA PO OPREDELENIYU RASCHETNYKH GIDROLOGICHESKIKH KHARAKTERISTIK. SN 435-72 (Instructions on Determining Computed Hydrological Characteristics. SN [Construction Norms] 435-72), Leningrad, Gidrometeoizdat, 1972.

8. Khristoforov, A. V., "Checking Statistical Hypotheses in Computations of the Maximum Water Discharges With a Low Guaranteed Probability," METEOROLOGIYA I GIDROLOGIYA (Meteorology and Hydrology), No 9, 1977.

UDC 627.51(470.23)

HYDROLOGICAL BASIS OF A PLAN FOR PROTECTING LENINGRAD FROM FLOODS

Moscow METEOROLOGIYA I GIDROLOGIYA in Russian No 11, Nov 80 pp 87-91

[Article by V. A. Znamenskiy, State Hydrological Institute, manuscript submitted 2 Jun 80]

[Text]

Abstract: The article gives formulation of the problem, method and range of hydrological, hydrochemical and hydrobiological investigations of the water system Lake Ladoga-Neva River-Neva Inlet and also a method for making predictions of changes of the regime of this system as a basis for protecting Leningrad from floods.

In order to protect Leningrad against floods, prior to 1990 plans call for creating a complex of structures which at the time of floods will block the path of waters from the Gulf of Finland into the Neva Inlet and the Neva delta. In the protective complex situated along the line Lomonosov-Kotlin Island-Gorskaya village and having an extent of 24.5 km there will be stone-earth dikes, two structures through which ships can pass and six structures through which water can pass. The construction of protective structures will fully solve the problem of protection of the city against floods and is clear evidence of the concern of the Party and government for the city of Lenin and its four-million people.

At the same time, during 1980-1985 plans call for the carrying out of complex natural and model hydrological and ecological investigations of the water system including Lake Ladoga, the Neva River and Neva Inlet. These investigations become the scientific basis of measures for protecting Leningrad against floods and for preservation and sanitizing Lake Ladoga, the Neva River and the Neva Inlet.

The formulated scientific problem is extremely complex due to the need for taking into account the complex regime of individual elements of the hydrographic system and the influence of economic activity on it.

The upper link in this water system is Lake Ladoga, the largest lake in Europe, whose regime, despite extensive investigations carried out in the past, has still been inadequately studied.

During recent years the water quality in the lake has been influenced to a considerable degree by economic activity, in particular, the development of industry and the implementation of agricultural and meliorative measures on its shores and in the territory of the basin.

All the mentioned factors act on the ecosystem of this large fresh-water body.

The waters of Lake Ladoga, entering the Neva River and then into the Gulf of Finland, for a distance of 32 km in the lower course flow through the territory of Leningrad. The hydrological regime of the Neva, as one of the segments of the water system, differs sharply from the regime of a lake. In its upper part the water quality, level regime, current velocity, ice-thermal conditions, etc. are determined by the regime of Lake Ladoga. The lower part is under the influence of the Gulf of Finland. In addition, the conditions for the forming of water quality and the ecosystem of the Neva River is influenced to a great degree by the cities and industry on its shores, including the economic activity of Leningrad. The plan for the development of Leningrad provides for a complex system of measures for the sanitizing of water bodies within the city. It includes the clearing of rivers and channels, prevention of the dumping of waste water and ground, and much else. This has already brought substantial results and during the last decade the quality of the water in the Neva River and in the arms of its delta has substantially improved.

The delta part of the Neva River is in the backwater of the Neva Inlet of the Gulf of Finland, whose influence is reflected not only during the period of floods, but also in the day-to-day regime. Each day the Neva Inlet experiences the influence of the Gulf of Finland, whose waters periodically enter it under the influence of atmospheric processes during the passage of cyclones over the Baltic Sea. As a result of penetration of long waves and the wind effect surges develop in the Neva Inlet which together with the runoff of the Neva are the basic distinguishing characteristics of its hydrological regime. These regime characteristics are manifested most clearly during periods of floods. The combination of these factors determines the physical background against which the elements of the ecosystem of the natural regime of this water body are formed.

In addition, the regime of the Neva Inlet is presently influenced to a great degree (and will be so influenced in the future) by the economic activity: the existing and proposed discharge of waste water of the Leningrad sewer system, the construction of structures for the protection of the city from floods and the proposed shifting of part of the runoff from the Lake Ladoga basin. An evaluation of its influence on the ecosystem of water bodies is the objective of the planned investigations.

Thus, the object of the investigation is a complex water system with different characteristics of the water, chemical and biological regimes and diverse types of the effect exerted on it by elements of man's economic activity. In order to evaluate its changes it is necessary to take into account the conditions of interaction among individual parts of the system and the interrelationship of the elements of the hydrological, hydrochemical and hydrobiological regimes. In developing the programs for complex investigations it is evidently necessary to

take into account the following principal problems:
-- study of the principal laws of vital functioning of the ecosystem Lake Ladoga-Neva River-Neva Inlet and establishing interrelationships among its abiotic and biotic parts;
-- development of the methodological principles for the mathematical modeling of multicomponent ecological systems;
-- development of a mathematical model of the ecosystem Lake Ladoga-Neva River-Neva Inlet;
-- preparation of a forecast of the ecosystem Lake Ladoga-Neva River-Neva Inlet under the influence of economic activity;
-- evaluation of the possibility of automated monitoring and optimum control of the ecosystem of Neva Inlet with respect to the conditions for the formation of water quality.

The research methods must provide for the carrying out of an in-situ study of water bodies for all elements of the regime and the carrying out of physical, physicobiological and mathematical modeling.

The program developed by the State Hydrological Institute includes:
1. A complex in-situ study of the conditions of the present-day status of hydrological, hydrochemical and hydrobiological regimes of the water system for obtaining initial data for predicting changes in the regime under the influence of economic activity. The in situ investigations must give information on the present status of the ecosystem of water bodies and the river and serve as a basis for a comparative evaluation of different elements of the regime in individual parts of the system. On their basis it will be possible to develop the methodological aspects of prediction of the change in the regime under the influence of planned economic measures. These investigations will also be used in developing mathematical models of individual regime elements for different parts of the water system and also in a study of the regime in places where economic measures are being directly implemented (protective structures and waste water outlets).

In situ investigations must be carried out for the entire complex of the investigated regime simultaneously at prestipulated times and under a unified program. Only in this case will there be assurance of the necessary comparability of results for all parts of the water system. The program of in situ investigations takes into account the need for materials necessary for developing models and forecasting.

2. Development of a method of physicochemical principles for prediction, specifically prediction of changes in the hydrological, hydrodynamic and hydrochemical regimes of the water system. On the basis of in situ investigations there should be refinement of the principal patterns of behavior of the hydrological, hydrodynamic and hydrochemical regimes of the water system, including determination of the balance of chemical substances for all parts of the water system.

The basis for prediction should be a mathematical model reproducing the hydrological, hydrodynamic and hydrochemical regimes of both individual parts and the entire water system. Such a model will take into account the processes of transport, dilution and chemical transformation of matter. It is checked using materials from field investigations and will serve as the mathematical basis for predicting the quality of water with further allowance for changes in the volumes of river runoff, systems of currents under the influence of protective structures and volumes of centralized discharge of waste water.

The results of the hydrological and hydrochemical forecasts will serve as a basis for evaluating the influence of economic measures on the ecosystem and determination of zones and sectors dangerous with respect to eutrophication and also for obtaining recommendations on the sanitizing of water bodies.

3. The development of forecasts of change in the ecosystem of water bodies under the influence of planned economic measures, which is the main objective of the formulated problem. Its implementation is based on a preceding field study of the energy characteristics and functioning of the ecosystems of water bodies in their present state in combination with study of abiotic factors and the hydrochemical regime, and also on the results of proposed investigations using physical-hydrobiological models having the purpose of evaluating the influence of discharge of waste water on the ecosystem of Neva Inlet. For this purpose on the basis of purification structures it is necessary to create apparatus reproducing the physical conditions of water exchange in combination with the entry of waste water and the influence of the principal climatic factors, which will make it possible to model the biological processes at the sites of discharge of urban waste waters in the Neva Inlet.

Probably one of the important aspects of the investigation will be a study of the interaction of the water and bottom ecosystems in Neva Inlet and evaluation of its possible change under the influence of economic activity. As a result, information should be obtained on exchange processes in water bodies and the stability of their ecosystems, modeled functions and parameters will be selected and expressions will be derived which will formalize the cause-and-effect relationships in the ecosystem for their further application in the form of a mathematical model. On the basis of such a model it will be possible to develop a quantitative forecast taking into account the possible changes in the ecosystem as a result of the planned economic measures and proposals on the sanitizing of the water system.

4. The use of results of field and laboratory investigations and prediction of changes in the hydrological, hydrodynamic, hydrochemical and hydrobiological regimes for the scientific validation of measures for preserving and sanitizing of the Lake Ladoga-Neva River-Neva Inlet water system.

For this purpose, in addition to the studies provided for in points 1-3, plans call for the carrying out of investigations using a large-scale hydraulic model of Neva Inlet, in which studies should be made of the processes of water exchange between Neva Inlet and the Gulf of Finland under existing conditions and after the construction of protective structures and an evaluation should be made of the change in the structure of flows in a confined water body. Particular attention must be given to an investigation of the mechanism of surge phenomena and their influence on the structure of currents, taking into account the influence of protective structures. The siting and size of water flow-through structures must ensure the creation of an optimum flow system in Neva Inlet for dilution and transport of waste water from existing and planned outlets of purification structures serving the city and its suburbs. On the basis of an investigation of water exchange processes and the processes of dilution of waste water a study will be made of the possibility of control of the regime of flows and the processes of dilution of waste water, measures will be developed for the organization of optimum structure of flows in Neva Inlet, stagnant and eddy zones will be detected and requirements will be established on the norms for discharged waste water.

All the mentioned investigations must take into account the conditions related to the possible extraction of part of the runoff from the basin of Lake Ladoga.

As a result of comparison of information on the existing and predicted hydrochemical and hydrobiological regimes with materials from investigations on a hydraulic model it should be possible to develop a scientific basis of measures for the sanitizing of Neva Inlet, including the problem of contending with eutrophication, contamination of bottom sediments and secondary contamination of the water mass.

The system of measures for the sanitizing of Neva Inlet developed on this basis should include:
-- recommendations on the degree of purification and prepurification of waste waters;
-- recommendations on the siting of planned outlets of purification structures;
-- proposals on the creation of optimum regimes in Neva Inlet in different seasons of the year;
-- recommendations on control of the system of currents (by construction of permanent and temporary flow-controlling structures in delta distributaries and in the ocean and also by maneuvering the gates of water flow openings in protective structures);
-- proposals for creating an automated system for control and monitoring of the regime of Neva Inlet.

The results of investigations carried out in Lake Ladoga and Neva River will be used in developing a system of measures for sanitizing these water bodies.

For this purpose a scientific basis must be obtained for measures in the basin, on the shores and over the area of Lake Ladoga, directed, in particular, to contending with eutrophication and contamination of both individual regions and the entire lake. Similar recommendations on the sanitizing of the Neva River must also be prepared for measures on its shores and in its drainage basin.

As important results of the investigations recommendations must be developed on the creation of an automated system for monitoring the quality of water and control of protective and purification structures in Neva Inlet, taking into account measures for the preservation and sanitizing of the water system. Provision must be made for the automation of control of the technological process of purification of waste water in sewage purification structures (including the formulation of algorithms and control models) and the gates of openings in protective structures for the passage of water in dependence on the information obtained by an automated system for monitoring water quality in different parts of the water system.

In the investigations of 1980-1985 provision is made for the participation of institutes of the USSR Academy of Sciences and agencies of the ministries of electric power, melioration and water management, fishing, geology, health, higher and intermediate special education. The functions of the key department are assigned to the USSR State Committee on Hydrometeorology and Monitoring of the Environment, and the functions of the key agency are assigned to the State Hydrological Institute.

UDC 556.531.4

METHOD FOR EVALUATING THE ADMISSIBLE CONTAMINATION OF WATER BY SMALL SHIPS WITH ENGINES

Moscow METEOROLOGIYA I GIDROLOGIYA in Russian No 11, Nov 80 pp 92-99

[Article by V. K. Plotnikov, candidate of physical and mathematical sciences, and S. K. Revina, candidate of chemical sciences, Institute of Theoretical and Experimental Physics and Institute of Applied Geophysics, manuscript submitted 13 May 80]

[Text]

Abstract: An attempt was made to ascertain the maximum admissible discharge of contaminating substances into water bodies and watercourses from a nonstationary source of contamination -- ships with small engines. Formulas are derived for estimating the admissible number of ships with small engines for a particular water body.

Small ships with engines must be regarded as a source of water contamination on a par with other water users, which makes it possible to raise the question of the maximum admissible discharge of contaminating substances by these ships for each specific water body -- rivers, lakes, reservoirs. The specific characteristics of small ships with engines as a source of contamination are the following: their number in each water body is great, their tracks of movement quite uniformly cover the surface of the water body (since the draft of such ships is small, they also move outside the channel), and the concentration of contaminating substances in the wake of a moving ship does not differ greatly from the mean for the water body (the latter will be demonstrated below). Everything said makes it possible to assume that ships with small engines are continuously distributed over the surface of a water body and a constantly operative source of contamination. In principle the chemical composition of the contamination, the mean quantity of each of the substances entering into the water in a unit time from one ship and the mean time of operation of one ship are known, that is, the mean discharge of each substance by one ship during a definite time, for example, during the navigation season, is known. Accordingly, the concept of the maximum admissible discharge applicable to small ships must be replaced by the concept of the maximum admissible number of ships for each water body. The mathematical formulation of the problem in this case is as follows: assume that $M_i$ is the admissible discharge of the i-th substance into the water of a particular water body during the time T, and $\overline{q}_i$ is the mean discharge of the i-th substance during this same time by one ship. Then the number of ships for which the discharge of the i-th substance will be less than the maximum admissible is

$$N \leq N_i = \frac{M_i}{q_i}, \tag{1}$$

and the maximum admissible [ma] number of ships $N_{ma}$ for a particular water body is equal to the minimum of the $N_i$ values, that is, $N_{ma} = N_{i_{min}}$.

In order to determine the maximum admissible discharge (MAD) of any substance it is necessary to determine the correlation between the MAD and the maximum admissible concentration (MAC) of this substance. We will take into account the process of self-purification of water and we will assume that the source of contamination is distributed over the surface of the water body; the length of the sector of change in the source distribution density is everywhere much greater than the distance over which the contaminating substance diffuses in the water during the characteristic time of the self-purification process. Then, taking into account the exponental nature of the self-purification process [6], we will write an equation for the mass of the contaminating substance per unit area of the water body at the time T:

$$\frac{dm}{dS} = \int_0^T \frac{d\mu(t)}{dS} e^{-\frac{T-t}{\tau}} dt + \frac{dm_0}{dS} e^{-\frac{T}{\tau}}; \tag{2}$$

where $\mu(t) = dM/dt$ is the rate of discharge of the contaminating substance into the water, $dm_0/dS$ is the mass of the contaminating substance per unit area at the initial moment in time, $\tau$ is the self-purification time constant.

The discharge of matter in a unit area in the time T is

$$\frac{dM}{dS} = \int_0^T \frac{d\mu(t)}{dS} dt. \tag{3}$$

If the discharge is distributed uniformly over the area of the water body and the rate of the discharge is constant and equal to

$$\mu = \frac{m_0}{\tau}, \tag{4}$$

then the mass of contaminating substance in the water at any moment in time is equal to $m_0$ and the mass of the effluent is proportional to time and at the time T is

$$M = m_0 \frac{T}{\tau}. \tag{5}$$

The concentration of contaminating substance in the water in this case is

$$c = \frac{m_0}{V}, \tag{6}$$

where V is the part of the water volume in the water body in which the contaminating substance is mixed.

In accordance with the assumptions made above the contamination occurs uniformly over the surface of the water body S. Therefore

$$V = Sh, \tag{7}$$

where h is the thickness of the water layer mixed with the substance. Wave action is evidently the most effective process ensuring mixing. The amplitude of the water fluctuations in a water body with a depth much greater than the wave length decreases with an increase in the distance from the water surface exponentially with the exponent $-2\pi/\lambda$ z (here $\lambda$ is the wave length and z is the distance from the surface). The distribution of the contaminating substance in the water upon the ending of mixing will also be exponential with the same exponent. With an identical concentration of substance at the surface equal quantities of matter are contained in the entire water volume with an exponential density distribution and in a layer with a thickness $\lambda/2\pi$ with a uniform density distribution. Accordingly, the thickness of the layer of mixed water can be assumed equal to

$$h = \frac{\lambda}{2\pi}. \tag{8}$$

We note that this assumption exaggerates the mean concentration of contamination. Waves can be caused either by the ships themselves or by the wind. Since the first factor constantly accompanies the process of contamination of water by effluent from ships, in estimating the thickness h of the layer it is necessary to take into account the length of the ship's wave specifically. The mixing of the impurity discharged by one ship is produced by all the ships passing along this path after it. The length of the ship's wave is determined by the ship's speed $v_{ship}$:

[c = ship]

$$\lambda = \frac{2\pi}{g} v_c^2. \tag{9}$$

Here g is the acceleration of free falling.

With a wind velocity greater than the ship's speed the length of the wind wave, and accordingly, the thickness of the mixing layer will be greater than that caused by the movement of the ship. However, in order to simplify the computations (with some understatement of the volume of mixed water) we will assume that the thickness of the layer is determined from the ship's wave:

$$h = \frac{\overline{v}_c^2}{g}. \tag{10}$$

In this expression $\overline{v}_{ship}$ is the mean speed of ship movement. As a result, the water volume into which contaminating substances enter from ships with engines is

$$V = \frac{S\overline{v}_c^2}{g}, \tag{11}$$

if the mean depth of the water body is $H > h$. If $H < h$, in (6) it is necessary to substitute the water volume in a particular water body.

Substituting $m_0$ from (6) into (5), we will represent the discharge in the form

$$M = \frac{cVT}{\tau}. \tag{12}$$

Assuming, with allowance for other water users in addition to the small ships, that the concentration c is equal to a definite fraction of the MAC ($c = \varkappa c_{ma}$), from (12) we obtain the sought-for correlation between the MAD and the MAC:

$$M_{ma} = \varkappa c_{ma} VT/\tau . \quad (13)$$

As a simplification, this expression is written here for a non-flowthrough water body, but it is easy to show that it is also correct for flowthrough water bodies. Since the water discharge Q and the current velocity v are usually known for rivers, expression (13) for a river is conveniently represented in the form

$$M_{ma} = \varkappa c_{ma} QLT/v\tau , \quad (14)$$

where L is the length of the considered river reach (in this reach the water discharge must be constant). The following expression was used in the derivation of (14)

$$V = \frac{QL}{v}. \quad (15)$$

We note that in a river the mixing occurs quite rapidly in the entire depth of the flow as a result of the turbulence of water movement. In order to estimate the rate of mixing it is possible to use an empirical formula for computing the distance of total mixing of contamination from a point source [7]. Using this formula for a river with the width 500 m and the depth 10 m the distance of mixing is found to be 2,500 m and the mixing time with a current velocity of 2.5 km/hour is 1 hour. We note that the mixing of contamination from a source distributed over the surface transpires far more rapidly. Substituting (13) and (14) into (1), we obtain expressions for determining the admissible number of ships:

$$N_{ma} = \begin{cases} \varkappa c_{ma} VT/\bar{q}\tau & \text{for lakes and reservoirs,} \\ \varkappa c_{ma} QLT/\bar{q}v\tau & \text{for rivers and flowthrough canals.} \end{cases} \quad (16)$$

It is obvious that this expression was written for matter giving a minimum N value, that is, for matter having a minimum value of the parameter

$$\varepsilon = \varkappa c_{ma}/\bar{q}\tau . \quad (17)$$

Expressions (16), solved relative to $\varkappa c_{ma} = c$, can be used in estimating the contribution and concentration of contaminating substances in the water of a particular water body if the real number of ships based in the water body is substituted in them in place of $N_{ma}$.

The literature contains no data on the composition of the exhaust of Soviet-produced boat engines. However, some estimates can nevertheless be made. Source [3] presents data from the United States Environmental Protection Agency on the total discharge of contaminating substances by outboard motors in the United States during 1971 when there were about 7.3 million such motors in use in the United States (see

Table 1). The exhaust of outboard motors occurs in the water. Carbon dioxide and monoxide and nitrous oxide are not dissolved and escape into the air, but hydrocarbons, sulfur oxides and the higher oxides of nitrogen remain in the water. Since carbon dioxide is formed from carbon monoxide more easily than nitrogen dioxide is formed from nitrous oxide, it can reasonably be assumed that the ratio of masses of nitrogen and carbon dioxides and oxides is identical and the mass of the higher oxides of nitrogen is equal to 5% of the total mass of nitrogen oxides.

Table 1

| Substance | Total discharge by engines and motors in USA per year, thousand tons | Mean discharge per motor or engine per year, kg | Mean discharge per motor or engine into water per year, kg |
|---|---|---|---|
| Hydrocarbons | 184.0 | 25 | 25 |
| Carbon monoxide | 47.5 | 6.5 | -- |
| Carbon dioxide | 966.0 | 133 | -- |
| Nitrogen oxides | 0.39 | 0.53 | 0.025 |
| Sulfur oxides | 0.058 | 0.08 | 0.08 |
| Total substances | 1198.0 | 165 | 25 |

The composition of the effluent into the water estimated in this way per one ship or boat per year (navigation season) for American motors is also given in this table. It should be noted that source [2] also gives data on the lead content in the exhaust of outboard motors in the United States. The total discharge of lead was about 300 tons per ~ 100 000 tons of hydrocarbons, that is, about $3 \cdot 10^{-3}$ of the total mass of the effluent. However, A-72 gasoline, on which operate all Soviet outboard motors without exception, does not contain a lead additive (tetraethyl lead). Automobile engines mounted on launches use gasoline containing tetraethyl lead, but in this case the exhaust is usually discharged into the air. Thus, tetraethyl lead is not among the contaminating substances entering the water during the operation of small ships.

Source [4] gives data on the mean time of operation of different types of small boats in the United States in 1974. It follows from [4] that the average operating time is ~130 hours annually. It is reported in [5] that the average operating time for one outboard motor in the Swiss canton of Zug is 45 hours per year. In our country, the average operating time is also about 40-45 hours, and the substantially greater operating time in the United States is attributable to the fact that in contrast to the USSR and Switzerland, where the navigation season for small boats is 4 months, in the United States in many regions the navigation season for small boats is year-round. Thus, the effluent for one Russian boat must be reduced by a factor of approximately 3 in comparison with American boats, but taking into account that in the fuel mixture of Soviet motors and engines there is lubricating oil which gives a substantial contribution to the hydrocarbon component and which is 1/20th of the mixture, whereas in foreign countries it is 1/50th, and we will assume that the quantitative composition of exhaust into the water per boat coincides with that cited in the last column of the table.

It should be noted that the average power of an outboard motor in the United States in 1971, to which the data cited in the table apply, was 30-40 HP, and the maximum was 125 HP, whereas the maximum power of Soviet motors is 25 HP and the average is evidently 15-20 HP. Therefore, the use of the data in the table in the evaluation of water contamination by Soviet outboard motors would result in an exaggeration of the mass of effluent.

Hydrocarbons constitute most of the effluent. We will first assume that they all constitute petroleum products, for which, in accordance with the "List of Maximum Admissible Concentrations of Harmful Substances in the Water of Water Bodies Used for Fishing Purposes," $c_{ma}$ = 0.05 mg/liter. The time constant of self-purification can be determined using the data in [1], which gives the concentrations of petroleum products at different points in the Moskva River above Moscow; in three reaches there are no sources of contamination by petroleum products nor are there tributaries ensuring the entry of pure water. According to data for these reaches $\tau = 27 \pm 1$ hour. As a result, for petroleum products we have $\varepsilon/\chi = 0.74 \cdot 10^{-4}$ mg/(kg·liter·hour) = $0.74 \cdot 10^{-10}$ (liter·hour)$^{-1}$. This value will be minimum if for the remaining components of water contamination, that is, for sulfur oxides and the higher oxides of nitrogen, $c_{ma}/\tau$ is not less than $5.9 \cdot 10^{-6}$ and $1.9 \cdot 10^{-6}$ mg/(liter·hour) respectively.

Since the self-purification constants for these contamination components are unknown, we will assume them to be equal to the navigation season, that is, $\sim$3000 hours $\simeq$ 4 months. This can be done, since once a year, regardless of the length of the navigation season, it is known that the water is renewed at the time of high water. Then $c_{ma}$ for sulfur and nitrogen oxides must not be less than 0.017 and 0.006 mg/liter. In the list of maximum admissible concentrations there is not one substance which can contain sulfur and nitrogen oxides or the products of their reactions, that is, substances not satisfying this condition. Thus, the exhaust components containing sulfur and nitrogen do not limit the admissible number of boats to a greater degree than petroleum products and therefore may be dropped from further consideration.

It can be assumed that with respect to mass all 100% of the hydrocarbon component is attributable to petroleum products, but it also includes a small quantity ($\sim 10^{-5} \pm 10^{-6}$ in mass) of polycyclic aromatic hydrocarbons having carcinogenic properties. Benzapyrene (BP) can be adopted as an indicator of this group of hydrocarbons, since this substance has strong carcinogenic properties and is most stable in the presence of different influences. Source [2] gives the results of measurement of the quantity of BP present in the exhaust of different Soviet outboard motors, and it is shown that depending on the operating regime the mass of discharge of BP is from 0.2 to 0.6 mg per motor per hour. Assuming that the average operating time is 45 hours per year, we obtain a mass of discharge of BP during the navigation season of $q_{BP} \simeq 27$ mg. The self-purification constant $\tau_{BP}$ was determined using the data from [1], similarly to the constant for petroleum products and was equal to $\sim$80 hours. The maximum admissible concentration for BP is $5 \cdot 10^{-6}$ mg/liter. Hence we obtain the value of the $\varepsilon/\chi$ parameter for BP -- $(\varepsilon/\chi)_{BP} = 2.1 \cdot 10^{-9}$ (liter·hour)$^{-1}$, which is approximately 30 times greater than for petroleum products. This means that the admissible number of boats is limited by the discharge of petroleum products and the BP concentration, with a number of boats equal to the admissible number (and equal to the $\chi$ values for BP and petroleum products), will be approximately 30 times less than $c_{ma} \cdot \varkappa$.

Assuming that the Moskva River, with respect to self-purification conditions, is quite typical for the central zone of the European USSR, and also taking into account that the self-purification constants were determined using data for measurements made in September, when the water is colder than the average for the navigation season, and the self-purification process transpires more slowly, we obtain the following formulas, somewhat understating the result, for estimating the admissible number of ships:

$$N_{ma} = \begin{cases} 0.7 \cdot 10^{-7} \varkappa VT \text{ for reservoirs and lakes,} \\ 0.7 \cdot 10^{-7} \chi QLT/v \text{ for rivers and canals.} \end{cases} \quad (18)$$

Here [T] = hours, [Q] = $m^3$/sec, [v] = m/sec, [V] = $m^3$. It should be recalled that with a great depth of the water body (H > h) the V value is determined from expression (11). With a boat speed of 7 m/sec (that is, 25 km/hour) the thickness of the mixed layer is h = 5 m.

It should be noted that in the derivation of the formulas (18) and in determining the parameters entering into them a number of simplifying assumptions were made, leading to definite errors. There are several (4-6) factors, each of which can give an error in $N_{ma}$ by a factor of 1.5-2 in any direction. These errors are independent and therefore their squares should be summed, that is, the total error is equal to (1.5-2) $\sqrt{(4-6)} \simeq 4$ and the admissible number of boats can be greater or less than that estimated using the formulas (18) by several (up to four) times.

We will also estimate the local concentration of petroleum products in the wake of a moving boat, that is, directly at the time of their discharge into the water. It is obvious that the local concentration is

[KC = wake]

$$c_{local} = \frac{dq}{dt} \Big/ \frac{dV_{KC}}{dt}, \quad (19)$$

where dq/dt is the rate of discharge, $dV_{wake}/dt$ is the rate of increase in the volume of the wake.

We will assume that

$$\frac{dq}{dt} \simeq \frac{\overline{q}}{T_Э},$$

[Э = op]

where $T_{op}$ is the time a boat is operated during the navigation season, $\overline{q}$ is the discharge of petroleum products during this same time

$$dV_{wake}/dt = v_{boat}s,$$

where $v_{boat}$ is the ship's speed, s is the area of the flow entrained by a boat in motion in which, as a result of flow turbulence, there is mixing of water and effluent. Then

$$c_{local} = \overline{q}/T_{op}v_{boat}s. \quad (20)$$

Assuming $\bar{q} = 25 \cdot 10^6$ mg, $T_{op} = 50$ hours, $v_{boat} = 25$ km/hour, $s = 1$ m$^2$, we obtain $c_{local} = 0.02$ mg/liter, that is, 2.5 times lower than the maximum admissible concentration and only four times greater than the mean concentration with a number of ships equal to the admissible number, and $\varkappa = 0.1$. The latter circumstance and allowance for the rather rapid widening of the wake behind the boat's stern make it possible to assume that the assumption of a uniformity of the distribution of the effluent over the surface of the water body is entirely legitimate.

It is also necessary to examine the problem of contamination of water by small boats with motors and engines at anchor. As a limiting case we will examine an anchorage with a closed water body, for example, anchorage in a specially dug canal. Usually at such an anchorage the volume of water $V_1$ per ship is about 40 m$^3$ (width 2 m, length of anchorage 10 m and depth of canal 2 m). It is obvious that in this case it is necessary to estimate what quantity of petroleum products can be discharged into the water by one ship during the navigation season, that is, ascertain the admissible discharge per ship $q_{ma1}$. This can be done by using equation (16), assuming there that N = 1. Then

$$\bar{q}_{ma1} = \varkappa c_{ma} V_1 T/\tau . \qquad (21)$$

Usually there are no other sources of contamination in the anchorage, other than small boats. Accordingly, it can be assumed that $\varkappa = 1$. Substituting in (21) $c_{ma} = 0.05$ mg/liter, $V_1 = 40$ m$^3$, $T = 3000$ hours, $\tau = 27$ hours, we obtain $\bar{q}_{ma1} = 0.22$ kg. The mean discharge during operation of the motor or engine per unit time $d\bar{q}/dt \simeq \bar{q}/T_{op}$ is $\simeq 0.5$ kg/hour. At the anchorage the rate of discharge is 2-3 times less, since the motors and engines there usually operate with few rpm. For the anchorage we assume $d\bar{q}/dt = 0.22$ kg/hour. Then the admissible time of operation of the motor or engine in the waters of the anchorage during the navigation season is about an hour. If during the navigation season the boat leaves its anchorage 30 times, in each entry and return event it is possible to allow only one minute of motor or engine operation, assuming in this case that there are no other fuel losses. It follows from the cited estimates that at anchorages, that is, the places of high concentration of ships, it is necessary to virtually exclude the operation of motors and engines both during movement and especially during their regulation. Evidently, at anchorages it is possible to permit the use of engines only by large boats which cannot move under sail. It is also necessary to preclude the entry of fuel into the water during fueling, the raising of the screws of outboard motors from the water and in other cases.

As an example we will estimate the admissible number of ships in a water body with a volume of the layer of mixed water equal to $10^9$ m$^3$, assuming that the fraction of contamination introduced by small boats with motors can constitute 10% of the total contamination with petroleum products (that is, with $\varkappa = 0.1$) and the navigation time is 3000 hours (about 4 months).

Then the admissible number of ships is 2000. As a comparison we note [8] that the volume of water in Kuybyshevskoye Reservoir (the largest on the Volga) is $34.6 \cdot 10^9$ m$^3$ with a mean depth of 5.4 m, whereas in Ivan'kovskoye Reservoir it is $0.97 \cdot 10^9$ m$^3$ with a mean depth of 3 m. These data show that for the Volga reservoirs the volume of the mixed water virtually coincides with the water volume in the water body.

The considerations and computations presented above make it possible to draw the following conclusions:

1. The concept of the number of small boats with motors and engines which is admissible from the point of view of water contamination must be introduced for each water body (river, lake, reservoir).

2. The admissible number of small boats is determined from the admissible contamination of water in the water body by petroleum products entering from boats.

3. The local contamination of water (in the wake) by a moving boat does not differ greatly from the mean with a number of ships in the water body equal to the admissible number.

4. The admissible discharge of petroleum products during the navigation season per one boat during operation of a motor or engine at anchorage is two orders of magnitude less than the total discharge during the same time, making it necessary, on a practical basis, to preclude the operation of motors and engines of small boats with exhaust into the water at anchorages.

BIBLIOGRAPHY

1. Gvil'dis, V. Yu., "Investigation of Self-Purification Processes in the Moskva River from Contamination by Organic Substances," OKHRANA VODNOY SREDY (Preservation of the Water Medium), Moscow, Moskovskiy Rabochiy, 1978.

2. Klubkov, V. G., "Role of the Small Boat Fleet in the Contamination of Water Bodies by Carcinogenic Hydrocarbons," OKHRANA VODNOY SREDY, Moscow, Moskovskiy Rabochiy, 1978.

3. Libefort, G. B., SUDOVYYE DVIGATELI I OKRUZHAYUSHCHAYA SREDA (Ship Engines and Motors and the Environment), Leningrad, Sudostroyeniye, 1979.

4. Nachinskiy, V. M., Shvarts, E. S., Recreational Fleet in the United States," KATERA I YAKHTY (Launch and Yacht), No 63, 1976.

5. "Rest in the Water and its Surroundings," KATERA I YAKHTY, No 63, 1976.

6. Pentl, R., METODY SISTEMNOGO ANALIZA OKRUZHAYUSHCHEY SREDY (Methods of Systemic Analysis of the Environment), Moscow, Mir, 1979.

7. Rufel', M. A., GIGIYENA I SANITARIYA (Hygiene and Sanitation), No 4, 1960.

8. Tonyayev, V. I., GEOGRAFIYA VNUTRENNIKH VODNYKH PUTEY SSSR (Geography of Internal Water Ways of the USSR), Moscow, Transport, 1977.

UDC 551.579

EVALUATION OF ACCURACY IN COMPUTING MEAN SOIL MOISTURE RESERVES IN RAINY PERIODS

Moscow METEOROLOGIYA I GIDROLOGIYA in Russian No 11, Nov 80 pp 100-107

[Article by A. R. Konstantinov, professor, and V. Ya. Lakhovskaya, Leningrad Hydrometeorological Institute, manuscript submitted 17 Apr 80]

[Text]

Abstract: Different models of the variation of soil moisture reserves are considered for some time interval in dependence on the initial and final moisture reserves, the quantity of precipitation, times of its falling and intensity of evaporation. A number of expressions are derived which make it possible to compute the mean soil moisture reserves. Using an electronic computer the authors evaluated the accuracy in computing the mean moisture reserves using different formulas. As a result, recommendations are given for computing the mean soil moisture reserves during rainy periods.

In making different hydrological, meliorative and agrometeorological computations the need arises for computing the mean moisture reserves of the soil during some time intervals. As a rule, the minimum duration of these intervals is 10 days because large-scale regular observations of soil moisture content in agricultural fields and drainage basins are made each 10 days. An expression in the form

$$W_{mean} = \frac{W_{beg} + W_{end}}{2} \quad \text{is used,} \qquad (1)$$

where $W_{beg}$ and $W_{end}$ are the moisture reserves at the beginning and end of the computation period.

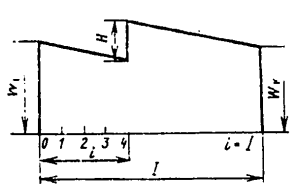

Fig. 1. Very simple diagram used in taking precipitation into account. $W_{beg}$ and $W_{end}$ are the moisture reserves at the beginning and end of the period I; H is the quantity of precipitation; i is the number of days elapsing from the onset of the period I to the moment of falling of precipitation.

Formula (1) assumes a linear change in the moisture reserves and the time of falling of precipitation during the computation period is not taken into account. This problem was examined in [1], where a computation method was proposed which makes it possible, in computing the mean water reserves, to take into account the times of falling of precipitation and its quantity.

1. Simplified Model for Computing the Mean Moisture Reserves With Allowance for the Quantity of Precipitation and the Time of Its Falling

The diagram shown as Fig. 1 was used in the derivation of the simplified computation formula in [1]. In this diagram the assumption is made that the intensity of the decrease in soil moisture reserves remains constant during the entire computation period (that is, is identical before and after the falling of precipitation). Such an assumption is far from reproachless, but it makes it possible to derive formulas which in the first approximation can be used in computing the mean moisture reserves during periods with precipitation and thereby give results more precise than those which are obtained using formula (1). Determining the mean moisture reserves as the mean weighted value during the periods i and I - i (where I is the duration of the computation period, i is the number of days from the beginning of the period to the falling of the first precipitation), the following expressions were derived in [1]:

[Here and below cp = mean; H = beg; K = end]

$$W_{cp} = \frac{W_H + W_K}{2} + \left(\frac{1}{2} - \frac{i}{I}\right) H. \qquad (2)$$

If during the considered period precipitation falls n times, the formula has the form

$$W_{cp} = \frac{W_H + W_K}{2} + \Sigma \left(\frac{1}{2} - \frac{i_n}{I}\right) H_n. \qquad (3)$$

Using formulas (2) or (3), we will show the influence of the time of falling of precipitation on the quantity of the mean moisture reserves.

1) With i = 0, that is, if precipitation falls directly after determining the initial moisture reserves (on this same day), formulas (2) and (3) assume the form

$$W_{cp} = \frac{W_H + W_K + H}{2}. \qquad (4)$$

2) With i = I, that is, if precipitation falls directly before determination of the final moisture reserves,

$$W_{cp} = \frac{W_H + W_K - H}{2}. \qquad (5)$$

3) With i = 1/2 I, that is, when the precipitation falls in the middle of the interval,

$$W_{cp} = \frac{W_H + W_K}{2}. \qquad (6)$$

4) With H = 0, that is, if precipitation did not fall,

$$W_{cp} = \frac{W_н + W_к}{2}. \qquad (7)$$

Expressions (4)-(7) confirm the necessity for taking precipitation into account, especially during its falling at the beginning or end of the selected time interval. In computing the mean moisture reserves the precipitation falling at the beginning of the interval should be added to the sum of initial and final moisture reserves (4) and that falling at the end of the interval should be subtracted from it. The precipitation falling in the middle of the interval exerts no influence on computation of the mean moisture reserves (6). In the absence of precipitation (7) formula (2) is transformed into the initial formula (1), where precipitation is not taken into account.

Formulas (2) and (3) are simple for practical application, but the assumption of a constancy of the diurnal sum of evaporation, before and after the falling of precipitation serving as the basis for their derivation makes them inadequately rigorous.

We will evaluate the influence exerted on mean moisture reserves simultaneously by two factors: precipitation and the variability of the intensity of evaporation with time. Since in nature there can be a countless number of combinations of quantities of precipitation and the times of its falling, and there also can be the most diverse changes in evaporation (caused by weather factors), for greater clarity in solving the formulated problem it is possible to consider the examined process in schematic form.

We will construct several models of the variation in moisture reserves, assuming that the initial and final moisture reserves, the quantities of precipitation and the times of its falling, as well as the intensity of evaporation are stipulated. For these models we derive formulas which can be used to compute the mean moisture reserves and then, stipulating different values of the initial parameters, we use an electronic computer to carry out a numerical experiment and we will show what the difference is when computing the mean moisture reserves using different formulas.

In constructing the models we make the following assumptions:
a) the falling precipitation evaporates with the evaporability intensity $E_0$ (accordingly, the number of days m during which the falling precipitation evaporates is equal to $m = H/E_0$);
b) prior to the falling of precipitation and after its evaporation the decrease in moisture reserves occurs with the identical intensity E, less than the evaporability.

2. Model of Change in Moisture Reserves in Soil During the Falling of One Rain

2.1. The falling precipitation is completely evaporated within the interval between the times of measurement of moisture reserves ($i + m \leqslant I$). In deriving the formula we use the graphic construction shown in Fig. 2a. The mean moisture reserves during the period I are determined as the mean weighted value during the intervals i, m, I - m - i, that is

$$W'_{cp} = \frac{1}{I} \cdot \left[ W_{cp,\,i}\, i + W_{cp,\,m}\, m + W_{cp,\,I-m-i}\,(I - m - i) \right]. \tag{8}$$

Expressing the mean moisture reserves during the intervals i, m, I - m - i through the initial parameters and carrying out simple transforms, we obtain

$$W'_{cp} = \frac{W_н + W_к}{2} + \frac{m}{2I}\left[H + \frac{(W_к - W_н)(m + 2i - I)}{I - m}\right]. \tag{9}$$

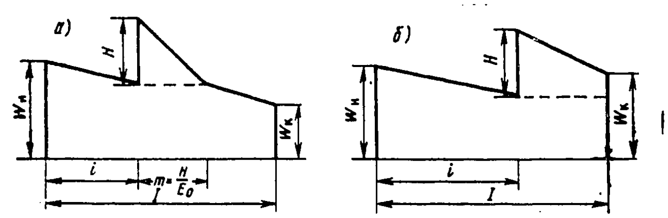

Fig. 2. Diagram of variation of soil moisture reserves as function of time of falling of precipitation, its quantity and evaporability during the falling of one rain. a) diagram for model 2.1; b) diagram for model 2.2.

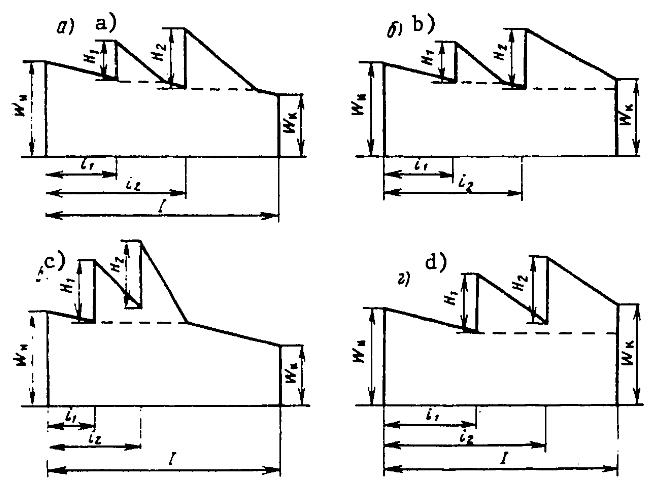

Fig. 3. Diagram of variation of soil moisture reserves as function of time of falling of precipitation, its quantity and evaporability during the falling of two rains. a) for model 3.1; b) 3.2; c) 3.3; d) 3.4.

2.2. The falling precipitation only partially evaporates within the interval between the times of measurement of moisture reserves ($i + m \geqslant I$). Reasoning as in the derivation of the preceding formula, we obtain the following expressions for computing the mean moisture reserves during the interval I (Fig. 2b):

$$W_{cp} = \frac{W_H + W_K}{2} + \frac{1}{2I} [(W_K - W_H + E_0 I)(I - i) - Hi]. \quad (10)$$

3. Model of Change in Soil Moisture Reserves in the Case of Falling of Two Rains During Computation Period

3.1. A second rain falls after total evaporation of the first and evaporates during the computation interval I ($i_2 + m_2 \leqslant I$, $i_1 + m_1 \leqslant i_2$). In the considered case, using the scheme shown in Fig. 3a, we obtain the following formula for computing the mean moisture reserves:

$$W_{cp} = \frac{W_H + W_K}{2} + \frac{W_K - W_H}{2I(i_2 - m_1)(I - m_1 - m_2)} \{(I - m_1 - m_2) \times$$
$$\times (Ii_2 - Im_1 + m_1^2 - i_2^2 + 2m_1 i_1) - (I - i_2 - m_2) \times$$
$$\times [(i_2 - m_1)^2 + 2m_1 i_1] - [(I - i_2)^2 - m_2^2](i_2 - m_1)\} + \frac{H_1 m_1 + H_2 m_2}{2I}, \quad (11)$$

[Here and below cp = mean; H = beg; K = end]

where the subscripts 1 and 2 correspond to the first and second rains.

3.2. The second rain falls after the total evaporation of the first and is partially evaporated during the computation interval I ($i_1 + m_1 \leqslant i_2$, $i_2 + m_2 \geqslant I$). The model of variation of the moisture reserves is represented in Fig. 3b. The computation formula for this case has the form

$$W_{cp} = \frac{W_H + W_K}{2} + \frac{(W_K - W_H)[m_1^2 - i_2^2 + 2m_1 i_1 + I(i_2 - m_1)]}{2I(i_2 - m_1)} - \quad (12)$$
$$- \frac{[H_2 - E_{0,2}(I - i_2)][(i_2 - m_1)^2 + 2m_1 i_1]}{2I(i_2 - m_1)} + \frac{E_{0,2}(I - i_2)^2 + H_1 m_1}{2I}.$$

3.3. The second rain falls after partial evaporation of the first and all the rain evaporates completely in the interval I ($i_1 + m_1 > i_2$, $i_2 + m' \leqslant I$) (Fig. 3c). The computation formula assumes the following form:

$$W_{cp} = \frac{W_H + W_K}{2} + \frac{(W_K - W_H)[(i_2 + m')^2 - i_1^2 - I(m' + i_2 - i_1)]}{2I(I - i_2 + i_1 - m')} + \quad (13)$$
$$+ \frac{(i_2 - i_1)(H_1 + c) + m'(H_2 - c)}{2I},$$

where

$$m' = \frac{H_1 + H_2 - E_{0.1}(i_2 - i_1)}{E_{0,2}}; \quad (14)$$

$$c = H_1 - E_{0,1}(i_2 - i_1). \quad (15)$$

3.4. The second rain falls after partial evaporation of the first and total evaporation of precipitation ends beyond the limits of the interval I ($i_1 + m_1 \geqslant i_2$, $i_2 + m_2 \geqslant I$) (Fig. 3d). The computation formula for determining the mean moisture reserves has the form

Table 2

Corrections to Mean Moisture Reserves as Function of Time of Falling of Precipitation i, Its Quantity H and Evaporability $E_0$ During the Falling of Two Rains in a 10-Day Period

| $\Delta W = W_{end} - W_{beg}$ | $H_1/H_2$ | $E_1/E_2$ | $i_1/i_2$: 1/3 | 1/5 | 1/7 | 1/9 | 3/5 | 3/7 | 3/9 | 5/7 | 5/9 | 7/9 |
|---|---|---|---|---|---|---|---|---|---|---|---|---|
| −20 | 5/5 | 3/3 | 3(3)* | 2(2) | 1(1) | 0(0) | 1(1) | 0(0) | −1(−1) | −1(−1) | −2(−2) | −3(−3) |
| | 5/25 | 6/3 | — | — | — | −9(−8) | — | — | −10(−9) | −8(−5) | −11(−10) | −12(−11) |
| | 5/25 | 9/3 | — | — | −6(−3) | −10(−8) | — | −7(−4) | −10(−9) | −8(−5) | −11(−10) | −11(−11) |
| | 30/30 | 9/9 | 17(18) | 11(12) | 7(6) | 0(0) | 3(6) | −6(0) | −5(−6) | −3(−6) | −10(−12) | −16(−11) |
| | 30/20 | 9/6 | 10(8) | 6(12) | 2(8) | — | 4(6) | 2(2) | −2(−2) | −4(−4) | −6(−8) | −13(−18) |
| 0 | 15/5 | 3/3 | — | — | — | 3(4) | — | — | 3(1) | 1(1) | 0(0) | −4(−5) |
| | 10/10 | 3/3 | — | — | — | −1(0) | — | — | −1(−2) | 0(−2) | −2(−4) | −5(−6) |
| | 10/10 | 6/3 | — | — | — | −2(0) | — | — | −2(−2) | — | −2(−4) | −3(−6) |
| | 30/20 | 9/6 | — | 7(12) | 3(8) | — | 2(6) | −1(2) | −3(−2) | −5(−4) | −5(−8) | −13(−14) |
| | 30/30 | 6/6 | 18(18) | 12(12) | 6(6) | — | 6(6) | — | −6(−6) | −6(−6) | −12(−12) | −18(−18) |
| 30 | 25/25 | 3/3 | — | — | — | — | — | — | — | −3(−5) | −8(−10) | −14(−15) |
| | 30/25 | 3/3 | — | — | — | — | 8(6) | 3(1) | −2(−4) | −4(−5) | −8(−10) | −15(−16) |
| | 30/30 | 3/3 | 18(18) | 12(12) | 6(6) | 0(0) | 6(6) | 0(0) | −6(−6) | −6(−6) | −12(−12) | −18(−18) |

* The corrections computed using a simplified method are indicated in parentheses.

$$W_{cp} = \frac{W_н + W_к}{2} + \frac{1}{2l}\left[(W_к - W_н)(l - i_1) + E_{0.1}\, i_2 (i_2 - i_1) + \right.$$
$$\left. + E_{0.2}(l - i_2)(i_2 - i_1 + l) + H_2 (i_1 - 2 i_2) - H_1 i_1\right]. \qquad (16)$$

In formulas (9)-(13) the first term is in fact formula (1). The remaining terms can be considered as corrections to formula (1) to take into account the precipitation falling during the period between measurements of the moisture reserves. The absolute value of the correction is dependent on the difference between the initial (beginning) and final moisture reserves. Accordingly, the following initial parameters were stipulated for the results of checking computations of the mean moisture reserves using different formulas: the difference in moisture reserves, time of falling of precipitation and its quantity, and also evaporability. For the purpose of carrying out a numerical experiment the following values were assigned to these parameters.

The selected parameters were:

-- the difference between the final and initial moisture reserves in the case of the falling of one rain was assumed to be -20, -10, 0, 10 mm, and in the case of the falling of two rains -- -20, 0, 30 mm;
-- the duration of the computation period was 10 days;
-- the precipitation falling during one rain was 5, 10, 15, 20, 25 and 30 mm;
-- the number of days elapsing from the onset of the period to the time of falling of the first precipitation in the case of one rain was 1, 3, 5, 7, 9 days, and in the case of two rains -- 1, 3, 5, 7 days;
-- the number of days elapsing from the beginning of the period to the time of falling of the second rain was 3, 5, 7, 9 days;
-- evaporability was 3, 6, 9 mm/day.

The program for making computations on an electronic computer was prepared in such a way that from the set of different combinations of initial parameters the computer selected and read out only those combinations which do not contradict the conditions of the problem and which are probable under natural conditions (for example, the time of falling of the second rain cannot be less than the time of falling of the first, the increase in moisture reserves by the end of the computation period cannot be greater than the sum of the falling precipitation, etc.). Using the results of analysis of the groups of initial data the computer selected one of the formulas (9), (10), (11), (12), (13), (16) applicable for these conditions and carried out computations of the correction to formula (1). Corrections using formula (3) were made for the corresponding conditions. The results of the computations are summarized in Tables 1-3.

It follows from the contents of the table that:
1. The absolute values of the corrections, computed using the new formulas and using formula (3), in most cases either completely coincide or are extremely close.
2. The corrections attain a maximum value (16-18 mm) during the falling of precipitation at the beginning or end of the computation period.
3. The corrections attain values of tens of millimeters or more during a single rain exceeding 20 mm.

Some conclusions can be drawn on the basis of the described materials. Formulas of the type (9)-(13) and (16), although they take into account a whole series of factors (precipitation, evaporation and moisture reserves), are more unwieldy, inconvenient for use in large-scale practical computations and in addition do not give substantial advantages in the accuracy of determination of the mean moisture reserves in comparison with formula (3). If an attempt is made to make these factors more detailed the formulas will become more complex. Source [2] gives a formula for computing the mean moisture reserves in the case of their change in conformity to an exponential law. Comparative computations using this formula and formula (3) give close results (discrepancy up to 5%), which fall in the limits of accuracy in measuring precipitation and soil moisture reserves).

Table 1

Corrections to Mean Moisture Reserves in Dependence on Time of Falling of Rainfall i, Its Values H and Evaporability $E_0$ for Given Changes in Moisture Reserves With the Falling of One Rain in 10-Day Period

| $\Delta W = W_K - W_H$ | $i$ | $E_0$ | H: 5 | 10 | 15 | 20 | 25 | 30 |
|---|---|---|---|---|---|---|---|---|
| −20 | 5 | 6 | — | — | 0(0) | 0(0) | 1(0) | 2(0) |
| | 7 | 6 | 0(−1)* | 0(−2) | 0(−3) | −1(−4) | −3(−5) | −4(−6) |
| −10 | 1 | 3 | 1(2) | 3(4) | 5(6) | 8(8) | — | — |
| | 7 | 6 | 0(−1) | 0(−2) | 1(−3) | 0(−4) | −1(−5) | −3(−6) |
| 0 | 1 | 3 | — | — | — | — | — | 12(−12) |
| | 9 | 3 | — | −3(−4) | −5(−6) | −8(−8) | −10(−10) | −12(−12) |
| +10 | 9 | 3 | — | — | — | −7(−8) | −9(−10) | −11(−12) |
| | 7 | 6 | — | — | — | — | −3(−5) | −5(−6) |

K = end
N = beg

* The corrections computed using the simplified method (3) are indicated in parentheses.

Table 3

Corrections to Mean Moisture Reserves Taking Into Account the Time of Falling of Precipitation and its Quantity H

| H | i: 1 | 2 | 3 | 4 | 5 | 6 | 7 | 8 | 9 | 10 |
|---|---|---|---|---|---|---|---|---|---|---|
| 2 | 1 | 1 | 0 | 0 | 0 | 0 | 0 | −1 | −1 | −1 |
| 5 | 2 | 2 | 1 | 0 | 0 | 0 | −1 | −2 | −2 | −2 |
| 10 | 4 | 3 | 2 | 1 | 0 | 1 | −2 | −3 | −4 | −5 |
| 15 | 6 | 4 | 3 | 1 | 0 | 1 | −3 | −4 | −6 | −7 |
| 20 | 8 | 6 | 4 | 2 | 0 | 2 | −4 | −6 | −8 | −10 |
| 25 | 10 | 8 | 5 | 2 | 0 | 2 | −5 | −8 | −10 | −12 |
| 30 | 12 | 9 | 6 | 3 | 0 | 3 | −6 | −9 | −12 | −15 |

Expression (3), proposed in [1], despite its inherent limitations, nevertheless makes possible computation of the mean moisture reserves during the rainy period more precisely in comparison with formula (1). In the range of moisture reserves from 250 to 80 mm in the meter soil layer the use of formula (1) can introduce an error from 5 to 15% into computation of the mean moisture reserves (for the conditions of falling of precipitation investigated in the study). An identical quantity of precipitation, in the case of greater moisture reserves, naturally gives a lesser relative error. As a result, for a zone of excess moistening, where the moisture reserves are great, in making the computations it is desirable to use formula (3) in those cases when the precipitation sum during the 10-day period exceeds 20 mm. In the zone of unstable and inadequate moistening formula (3) makes it possible to increase the accuracy of the computations beginning with precipitation exceeding 10 mm. For convenience in computations of the mean moisture reserves formula (3) was used in compiling a table of corrections to expression (1) in the case of falling of a single rain during the considered period: with the falling of several rains the corrections are summed.

BIBLIOGRAPHY

1. Konstantinov, A. R., ISPARENIYE V PRIRODE (Evaporation in Nature), Leningrad, Gidrometeoizdat, 1968.

2. Konstantinov, A. R., Astakhova, N. I., Levenko, A. A., METODY RASCHETA ISPARENIYA S SEL'SKOKHOZYAYSTVENNYKH POLEY (Methods for Computing Evaporation from Agricultural Fields), Leningrad, Gidrometeoizdat, 1971.

STOCHASTIC DYNAMIC PROGRAMMING METHOD FOR COMPUTING THE MOST ADVANTAGEOUS SHIP NAVIGATION ROUTES

Moscow METEOROLOGIYA I GIDROLOGIYA in Russian No 11, Nov 80 pp 108-110

[Article by S. I. Khalilov, "Geofizika" Scientific Center Azerbaydzhan Academy of Sciences, manuscript submitted 27 Mar 80]

[Text] Abstract: The author proposes a new approach to computation of the optimum ship navigation routes by means of taking into account the errors in prognostic hydrometeorological information, that is, the introduction into the computation formulas for the duration of navigation of the numerical values of the guaranteed probability of forecasts of hydrometeorological information.

In computing the most advantageous navigation routes specialists at the USSR State Committee on Hydrometeorology and Environmental Monitoring now use the isochronal method first proposed by R. James for the servicing of ships. It is characterized by simplicity of the computations and graphic constructions [1, 3, 6].

However, the isochronal method has a considerable shortcoming -- the lack of proof of its optimality. For example, when the interval of discreteness of laying out of courses tends to zero the method for guiding a ship is reduced to the continuous informing of the ship on the direction of development of hydrometeorological conditions, for example, the direction of propagation of waves, which in most cases is not optimum.

There are also other methods [3]:
1) the method developed by the Computation Center USSR Academy of Sciences;
2) the variational calculus method;
3) a method based on the Fermat principle;
4) a method based on the eikonal equation.

The first two methods, similar to the isochronal method, have no optimality proof. The latter two, although having proofs, are very complex in practical application.

There is also the dynamic programming (DP) or dynamic planning method, a specific characteristic of which is that the finding of optimum control is accomplished by breaking the planned operation down into a number of successive "intervals" or "stages," that is, the seeking of the maximum of the function of many variables is replaced by the multiple seeking of the maximum of the function of a small number of variables [2, 4, 5].

The DP method was developed by R. Bellman [2] and is based on the optimality principle. Applicable to the problem of guiding ships, the latter means that, all other conditions being equal, the most advantageous routes, computed by other methods, cannot give better results than the DP method. This circumstance can be used in checking the optimality of some guidance method: if it gives the same results as the DP method, it is one of its modifications. However, if the method gives other results they are invariably poorer, that is, the method is not optimum.

The described classical DP method, like other methods for computing the most advantageous navigational routes for ships, are determined, that is, they are used only when precisely known initial data are available. This fundamental shortcoming does not make it possible to use them with the maximum effectiveness when guiding ships along the most advantageous routes. Indeed, in guiding ships in the seas and oceans use is made of prognostic hydrometeorological information, and forecasts, as is well known, are filled with errors, sometimes rather significant.

Accordingly, it is necessary to find such a method for computing the most advantageous route as would make it possible to find the optimum routes, taking into account the errors in forecasts of hydrometeorological conditions.

The method of stochastic dynamic programming which we have proposed is directed to the use of probabilistic-statistical characteristics of the arguments of the optimality criterion, in this case, the duration of navigation. Such an approach is possible due to the use of the numerical values of the parameters of guaranteed success in forecasts of hydrometeorological elements, in particular, forecasts of waves and weather.

The essence of the method can be explained in a simplified scheme for computing the most advantageous route by the DP method (see Fig. 1).

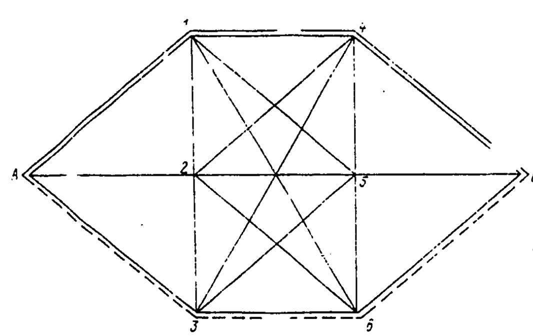

Fig. 1. Scheme for computing most advantageous route for ship by DP method.

For simplicity in reasoning and ease in exposition, the hydrometeorological conditions are represented in two gradations: favorable (F) and unfavorable (U). Stipulating the durations of coverage of all segments of the route by a definite ship, by the DP method we calculated the most advantageous routes, using as a point of departure the conditions F and U, A-1-4-B and A-3-6-B respectively. In navigational practice these computations will serve as the basis for our recommendations to navigators: when "B" arrives (the quotation marks denote a forecast) it is necessary to move along the route A-1-4-B, and when "U" arrives -- along the route A-3-6-B.

The durations, computed on the basis of forecasts of conditions F and U, will differ substantially from the real durations of passage along the corresponding routes due to failure to take into account the degree of probable success of the mentioned forecasts.

In this article we propose a method for taking into account the probability of realization of forecasts of hydrometeorological conditions when computing the most advantageous routes.

Obviously, depending on the probable success of the forecasts "F" and "U," the durations of movements of ships along the routes A-1-4-B and A-3-6-B will be different.

The degree of guaranteed success of these forecasts can be taken into account through numerical indices. In the first approximation it is necessary to find the mathematical expectation of the durations of navigation corresponding to cases of justification and nonjustification of "F" and "U". For example, for the i-th segment of the route we can write

$$\overline{T}_i^F = T_i^{F/F} P_i^{SF} + T_i^{U/F} (1 - P_i^{SF})$$
$$\overline{T}_i^U = T_i^{U/U} P_i^{SU} + T_i^{F/U} (1 - P_i^{SU}), \quad (1)$$

where $T_i^{F/F}$ and $T_i^{U/U}$ are the durations of navigation under the condition that the forecasts "F" and "U" are justified (respectively);

$T_i^{U/F}$ and $T_i^{F/U}$ are the durations of navigation under the condition that the forecasts "F" and "U" are not justified; $P_i^{SF}$ and $P_i^{SU}$ is the guaranteed success of "F" and "U" respectively $(1 - P_i^{SF})$ and $(1 - P_i^{SU})$ are the corresponding numerical values of the probability of nonjustification of forecasts of the conditions F and U.

We point out that the probability of the realization of forecasts of hydrometeorological conditions is not taken into account at the present time.

The transformation (1) makes it possible to compute the refined durations of navigation on the basis of existing forecasts.

The total time of movement along the routes A-1-4-B and A-3-6-B is expressed accordingly by formulas of the type

$$\overline{T}^F = \sum_{i=1}^{n} \overline{T}_i^F = \sum_{i=1}^{n} [T_i^{F/F} P_i^{SF} + T_i^{U/F} (1 - P_i^{SF})].$$

$$\overline{T}^U = \sum_{i=1}^{n} \overline{T}_i^U = \sum_{i=1}^{n} [T_i^{U/U} P_i^{SU} + T_i^{F/U} (1 - P_i^{SU})]. \quad (2)$$

It goes without saying that the navigation routes, computed on the basis of $\overline{T}^F$ and $\overline{T}^U$, will be the best.

The transformations (1) and (2) are correct not only for the case of application of the DP method, but also for any method for computing the most advantageous route. It must be noted that the use of the stochastic DP method is a qualitatively new step in the servicing of navigation with the most advantageous routes, as is noted by K. P. Vasil'yev [3]. The DP method, in comparison with the isochronal method, is characterized by the rigor of the mathematical approach and gives the optimum ship navigation routes.

However, the application of the stochastic DP method in the servicing of navigation requires the availability not of intervals of gradations of hydrometeorological elements, but their definite values and the corresponding probabilities of realization of $P_i^{SF}$ and $P_i^{SU}$. This requirement is not satisfied today, but its realization is a real possibility. For this it is necessary to collect statistical data on forecasts (naturally, in gradations) and accordingly, the observed values of the hydrometeorological elements. Computing the mathematical expectations of these specific values, it is possible to determine the numerical equivalent of the undetermined text of the forecast. Then it is easy to find the values $P_i^{SF}$ and $P_i^{SU}$ corresponding to these mathematical expectations.

In these reasonings and computations it is assumed that there is one forecast for the entire movement from A to B. In actual practice, depending on the route, it is possible to use a number of such forecasts for the entire movement route. In this case it is necessary to take the DP method, developed by R. Bellman [2], with a feedback.

Finally, if not all the $P_i^{SF}$ and $P_i^{SU}$ values corresponding to each gradation of hydrometeorological conditions are known, it is possible to use the DP method with adaptation [2].

Thus, the use of the stochastic DP method unquestionably will increase the effectiveness of hydrometeorological servicing of the merchant marine with recommended optimum courses, which rightfully can be considered an achievement of the USSR State Committee on Hydrometeorology [8].

BIBLIOGRAPHY

1. Abuzyarov, Z. K., Sirotov K. M., REKOMENDOVANNYYE KURSY PLAVANIYA V OKEANAKH (Recommended Navigation Courses in the Oceans), Leningrad, Gidrometeoizdat, 1976.

2. Bellman, R., Kaloba, R., DINAMICHESKOYE PROGRAMMIROVANIYE I SOVREMENNAYA TEORIYA UPRAVLENIYA (Dynamic Programming and Modern Control Theory), Moscow, Fizmatgiz, 1969.

3. Vasil'yev, K. P., "Most Advantageous Navigation Routes for Ships Under Stipulated Hydrometeorological Conditions in the Seas and Oceans," TRUDY GIDROMETTSENTRA SSSR (Transactions of the USSR Hydrometeorological Center), No 97, 1972.

4. Venttsel', Ye. S., ELEMENTY DINAMICHESKOGO PROGRAMMIROVANIYA (Elements of Dynamic Programming), Moscow, Nauka, 1964.

5. Venttsel', Ye. S., ISSLEDOVANIY OPERATSIY (Investigation of Operations), Moscow, Znaniye, 1976.

6. Dremlyug, V. V., Shifrin, L. S., NAVIGATSIONNAYA GIDROMETEOROLOGIYA (Navigational Hydrometeorology), Moscow, Transport, 1978.

7. Kudryavaya, K. I., et al., MORSKIYE GIDROLOGICHESKIYE PROGNOZY (Sea Hydrological Forecasts), Leningrad, Gidrometeoizdat, 1974.

8. RUKOVODSTVO PO RASCHETU NAIVYGODNEYSHIKH PUTEY PLAVANIYA SUDOV V MORYAKH I OKEANAKH (Manual on Computing the Most Advantageous Navigation Routes for Ships in the Seas and Oceans), Leningrad, Gidrometeoizdat, 1976.

UDC 556.342

MORE ON EVALUATING THE ACCURACY IN MEASURING WATER DISCHARGES

Moscow METEOROLOGIYA I GIDROLOGIYA in Russian No 11, Nov 80 pp 110-113

[Article by I. F. Karasev, doctor of technical sciences, State Hydrological Institute, manuscript submitted 8 Jan 80]

[Text]

Abstract: The author demonstrates the inapplicability of the limiting errors method and some dependences of a special type for evaluating the accuracy in measuring the discharges of channel flows.

The water discharge determined by the "velocity-area" method is the result of indirect multiposition measurements. An evaluation of their accuracy is one of the complex problems in mathematical statistics, not having a rigorous solution.

On the basis of the hypothesis of absence of correlation of particular errors of elementary discharges $q_i$ in their totality N, in [6], jointly with A. N. Chizhov, we derived a formula for the mean square error in measuring water discharge

$$\tilde{\sigma}_Q = \left[\frac{3}{2N}(\tilde{\sigma}_h^2 + \tilde{\sigma}_v^2)\right]^{1/2}. \quad (I^*)$$

[Note: We will use Roman numerals in numbering the formulas in order not to confuse it with the numbering of formulas employed by G. V. Zheleznyakov and B. B. Danilevich, reference to which is given in the text which follows.]

Here $\tilde{\sigma}_h$ and $\tilde{\sigma}_v$ denote the relative errors in measuring depths and mean velocities at the verticals. In contrast to other known dependences, formula (I) includes the parameter

$$\beta = N \sum_{s=1}^{s=N} q_s^2/Q^2, \quad (II)$$

where $q_s$ are partial discharges; with allowance for the incompleteness of shore "sections," their number N is assumed equal to the number of velocity verticals.

The $\beta$ parameter is introduced so that, first of all, despite concepts concerning the "accumulation" of errors of discrete measurements it is possible in explicit form to take into account the decrease in the relative error in measuring discharge with an increase in the number of velocity verticals, and second, so as to reflect the influence of the different distribution of elementary discharges in the width of the flow on the accuracy of the measurement results.

In the process of further development of methodological principles of optimization and evaluation of the accuracy of measurements formula (I) was generalized and represented in the form [5]

$$\tilde{\sigma}_Q = \left[ \frac{\beta}{N} \left( \tilde{\sigma}^2_{\omega_s} + \tilde{\sigma}^2_{v_s} \right) \right]^{1/2}. \qquad \text{(III)}$$

The errors $\tilde{\sigma}\omega_S$ and $\tilde{\sigma}_{vS}$ entering into this formula relate to the characteristics of the set N of partial discharges — to the area of the section $\omega_S$ and the mean velocity in the sections between the velocity verticals $v_S$. The $\tilde{\sigma}\omega_S$ and $\tilde{\sigma}_{vS}$ values, in addition to instrumental values, include a series of other components caused by the method of discretization of the elements of water discharge, channel morphology and kinematic structure of the flow. The computed evaluations $\tilde{\sigma}\omega_S$ and $\tilde{\sigma}_{vS}$ are dependent on the models used and the methods for measuring the water discharges. Source [5] gives formulas for $\tilde{\sigma}_Q$ relating to existing and improved measurements of water discharge by the "velocity-area" method. Emphasis is on the metrological desirability of the $\beta$ parameter as a quality index for the organization of observations. With $\beta \approx 1$, which corresponds to an equality of the partial discharges $q_S$, the greatest statistical smoothing of the errors $\tilde{\sigma}\omega_S$ and $\tilde{\sigma}_{vS}$ is ensured.

Article [5] drew objections from G. V. Zheleznyakov and B. B. Danilevich [4], who in contradiction to our formulas cite dependences which they derived and make a number of comments concerning some general premises for evaluating the accuracy of measuring water discharge.

The authors of [4] cite a formula for the limiting error in measuring water discharge $\Delta Q$ in which the weighting factors for $\Delta v$, $\Delta h$ and $\Delta b$ are determined on the basis of geometric expressions. Already in 1969, in collaboration with A. N. Chizhov [7], we indicated the fundamental inapplicability of the method of limiting errors for evaluating the accuracy of such multiposition indirect observations as measurement of water discharge (according to the calculations of N. K. Sibiryakova, the values of the errors are exaggerated in comparison with the statistical evaluations by a factor of 3-8). With an increase in the number of velocity verticals the formula for the limiting error does not reflect the increase in measurement accuracy occurring in this case and even leads to a directly opposite tendency, which is already incompatible with the data from practical experience in hydrometry.

Later G. V. Zheleznyakov and B. B. Danilevich proposed another dependence in the form of an expression for the mean square error $\sigma_Q$ [3]. The derivation of the formula is based on the different degree of discretization of the elements of water discharge: for the errors $\sigma_h$ and $\sigma_B$ we used the sections between the measurement verticals, and for $\sigma_v$ the sections between the velocity verticals. This led to a sharp distortion of the weighting factors and the contributions of the partial errors to the composite error in measuring water discharge. This can be confirmed in simple numerical examples. N. K. Sibiryakova [10], applicable to a number of hydrological posts on characteristic rivers, indicated that the weight of the errors $\sigma_v$ by many times (by 4-6 orders of magnitude) exceeds the values of the weighting factors for other errors. In other words, the accuracy in determining the discharges, despite the representations of the authors of [3], was for all practical purposes dependent only on the errors in measuring flow velocity.

In [4] the authors eliminate the mentioned incongruity and cite dependence (8), which follows from the discharge model (3) which they adopted, assuming correction of its recurrent part, adding the terms $0.5\ h_n\ U_n\ b_n$. In their calculations G. V. Zheleznyakov and B. B. Danilevich use the same procedure as we for the discretization of water discharge elements and the representation of partial derivatives ensuring conversion to the relative values of the errors. It is easy to see that the structure of formula (8), if one discards the mutually compensating errors in determination of the width of the sections, coincides in form with dependence I with the substitution into it of the $\beta$ parameter from expression II. The presence of the coefficient 0.5 in our formula reflects the fact that it was derived for the standard analytical method for computing the water discharge, whereas the basis for the formula derived by G. V. Zheleznyakov and B. B. Danilevich was a determination of the partial discharges as the half-sums of the elementary $q_i$. Such a model is considerably rougher and therefore is not used in practical work. Equally imperfect is the model on which the Hershey formula [9] is based, applicable only in the case of a great number of velocity verticals (over 20). Under ordinary conditions there can be considerable errors and it is not accidental that Hershey, although without adequate tie-in to the analytical structure of the discharge model, introduces the additional error of determination of the mean velocity of the entire flow.

The structure of our formula (I), in contrast to (8), corresponds to the premise of an equal accuracy in measuring the principal elements of water discharge, that is, an approximate equality of the relative errors $\tilde{\sigma}_h$ and $\tilde{\sigma}_{v_b}$. This premise is more realistic than the assumption of an equality of the absolute $\sigma_h$ and $\sigma_v$ values, on which the authors of [4] insist. In actuality, if the genesis of these errors is considered in the entire completeness of its factors [10], it appears that with an increase in depth and velocity there is an increase in the absolute errors in their measurement, which reflects the influence primarily of the so-called methodological components caused by the uncertainty of the contact of the instrument with the bottom, the ridged structure of the bottom and the displacement of the verticals from the hydrometric line by velocity fluctuations and uncertainty in their vertical distribution. An equal accuracy in measuring depths is also ensured by the use of different instruments: sounding leads for great h and a reading rod for small h. The idea of equal accuracy is still more legitimate for the generalized dependence III, in which $\tilde{\sigma}\omega_s$ and $\tilde{\sigma}v_s$ characterize the random errors in measuring the $\omega_s$ and $v_s$ values relating to the sections between the velocity verticals. We also find such an assumption in the international standard [9].

With a sufficiently complete coverage of the influencing factors the expressions for evaluating the accuracy in the change of water discharge naturally become more complex. This relates especially to the error $\tilde{\sigma}v_s$, which must be determined taking into account the correlation of its structural components in the width of the segment $b_s$. Formulas making specific dependence III on the basis of more than

250 variants of the processing of discharges with different numbers of velocity verticals, using measurement data for the Neva, Volkhov, Neman, Syrdar'ya, Varzob and Vakhsh Rivers, for the Bol'shoy Stavrapol'skiy Canal and the Columbia River (United States), are given in [5]. In their derivation the assumption was made that there is no cross-correlation of errors in determining the partial discharges $q_S$, and not $q_S$ themselves, as asserted by G. V. Zheleznyakov and B. B. Danilevich. With a fixed total discharge Q the $q_S$ values represent the results of individual measurements. Accordingly, the correlation between them is entirely determined by the correlation of errors $\tilde{\sigma}\omega_S$ and $\tilde{\sigma}_{vS}$, and the latter can be neglected for two reasons. First, because the additional terms of the total error include the paired products of the corresponding partial errors and the correlation coefficients for all the sections together, not only adjacent sections. Second, the actual values of the errors in determining $\omega_S$ and $v_S$ are attributable not only to errors in measuring $h_i$ and $v_i$ at the velocity verticals, but also primarily to the uncorrelated morphometric and structural components, mentioned above. The comments of the authors of [4] are all the more inadmissible in that they proceed from the same premises as we. In actuality, according to expression (2) cited in [4], the water discharge is represented as the sum of mutually independent terms -- partial discharges, although they include the elementary discharges $q_i$ common for adjacent verticals, and this means, the velocities $v_i$ and the depths $h_i$.

Thus, the authors of [4] derived a formula for the error $\tilde{\sigma}_Q$ applicable to one of the special methods for processing the measured water discharges and it must not be compared with the dependence which we derived in a more general form III. The latter is distinguished by the fact that the computed evaluations of the partial errors are not included in advance and therefore it is suitable not only for existing, but also newly developed methods for accelerated measurements of water discharges with the use of echo sounders and integrators of current velocity in the depth and width of the flow, but also with a considerable reduction in the number of velocity verticals. The fundamental characteristic of dependence III is that the computational expressions for evaluating the pertinent partial errors $\tilde{\sigma}_S$ and $\tilde{\sigma}_{vS}$ entering into it, like the total error $\tilde{\sigma}_Q$ itself, follow from the analytical basis of the used models for water discharge and therefore can assume different form. The $\beta$ parameter in the structure of formula III reflects the general character of discretization of the water discharge elements and at the same time serves as one of the criteria for optimizing measurements. All this gives basis for assuming that the dependence III is more rational than others, including the formulas of the international standard [9].

BIBLIOGRAPHY

1. Zheleznyakov, G. V., TEORIYA GIDROMETRII (Theory of Hydrometry), Leningrad, Gidrometeoizdat, 1976.

2. Zheleznyakov, G. V., Danilevich, B. B., TOCHNOST' GIDROLOGICHESKIKH IZMERENIY I RASCHETOV (Accuracy of Hydrological Measurements and Computations), Leningrad, Gidrometeoizdat, 1966.

3. Zheleznyakov, G. V., Danilevich, B. B., "Computation of Accuracy in Determining Water Discharges in Open Channels," METEOROLOGIYA I GIDROLOGIYA (Meteorology and Hydrology), No 9, 1971.

4. Zheleznyakov, G. V., Danilevich, B. B., "Evaluation of the Accuracy in Determining Water Discharges of River Flows," METEOROLOGIYA I GIDROLOGIYA, No 11, 1979.

5. Karasev, I. F., "Improvement in a Model of Water Discharge and Evaluation of the Accuracy of its Measurement by the 'Velocity-Area' Method," METEOROLOGIYA I GIDROLOGIYA, No 12, 1978.

6. Karasev, I. F., Chizhov, A. N., "Analysis of Accuracy and Rationalization of a Method for Measuring Water Discharges," TRUDY GGI (Transactions of the State Hydrological Institute), No 264, 1968.

7. Karasev, I. F., Chizhov, A. N., "Accuracy in Determining Runoff Using Hydrometeorological Data," METEOROLOGIYA I GIDROLOGIYA, No 2, 1969.

8. Kramer, G., MATEMATICHESKIYE METODY STATISTIKI (Mathematical Methods in Statistics), Moscow, Mir, 1975.

9. MEZHDUNARODNYY STANDART 748. IZMERENIYE ZHIDKOGO STOKA V RUSLAKH. OPREDELENIYE RASKHODA METODAMI ISSLEDOVANIYA POLYA SKOROSTEY (International Standard 748. Measurement of Liquid Runoff in Channels. Determination of Discharge by Methods for Investigating the Velocity Field), Moscow, Izd-vo Standartov, 1977.

10. Sibiryakova, N. K., "Methods for Evaluating the Accuracy of Measured Water Discharges," TRUDY GGI, No 202, 1973.

UDC 532.517.4

INVESTIGATION OF THE STRUCTURE OF A FLUID FLOW IN A CHANNEL USING AN OPTICAL DOPPLER HYDROMETER

Moscow METEOROLOGIYA I GIDROLOGIYA in Russian No 11, Nov 80 pp 114-117

[Article by A. M. Gusev, professor, N. K. Shelkovnikov, candidate of physical and mathematical sciences, V. V. Rozvanov and M. V. Solntsev, Moscow State University, manuscript submitted 16 May 80]

[Text]

Abstract: The article describes the use of a laser Doppler velocity instrument (LDVI) for studying the kinetic structure of a fluid flow in a rectangular open channel. The authors describe the operating principle of this instrument and the advantages of its use in comparison with methods employed earlier. The vertical profiles of the velocity distribution were obtained for different Reynolds numbers and it is shown that the maximum current velocity value is not at the upper free boundary, but below it. An interpretation of the results is given.

An extensive arsenal of instrumentation is used in investigating the kinematics and dynamics of turbulent flows. The most commonly used among these are contact methods. Among the principal shortcomings of these methods are the perturbing effect exerted on the flow and spatial averaging. The latter is especially important in an investigation of the flow region near the wall, whose dimensions as a rule are commensurable with the dimensions of the sensors usually employed.

In an investigation of turbulent flows it is common to use the method of a motion picture survey, making it possible to obtain both qualitative and quantitative data on flow structure. However, in addition to a number of merits of this method it also has its shortcomings. For example, prior to the measurements it is necessary to carry out a careful choice of the size and density of indicators in the form of neutral buoyancy spherules. The motion picture survey process is rather complex and the processing of the collected data is an extremely time-consuming operation which for the time being cannot be automated.

However, during recent years the possibility has appeared of using the optical Doppler method in aerohydrodynamics. It involves the use of diffuse scattering of monochromatic light by moving inhomogeneities of the investigated medium and makes possible overcoming the above-mentioned shortcomings of other methods.

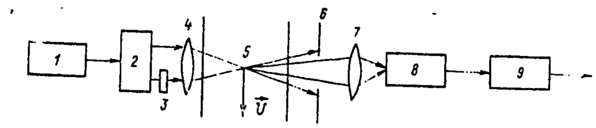


Fig. 1. Block diagram of experimental apparatus. $\vec{U}$ is the velocity vector of the fluid at the measurement point.

The optical Doppler method for measuring the velocity of flows is virtually inertialess, it makes it possible to obtain a good spatial ($10^{-11}$ $cm^3$) and temporal resolution, does not require calibration, makes it possible to carry out measurements in a great velocity range ($10^{-5}$–$10^{6}$ m/sec), and makes it possible to study non-Newtonian fluids, active media and boundary layers. In addition, this method is contactless and accordingly during the measurements no additional perturbations are introduced into the investigated medium. It makes it possible to automate data processing.

Among the shortcomings of this method is the complexity in its implementation, need for precise adjustment, and for the time being, its high cost. It can be seen from a comparison of these two methods that they complement each other well and in specific experiments preference can be given to one or another.

In this article we give data on the vertical distribution of velocity of fluid flow in an open rectangular channel with a free boundary, obtained using a laser Doppler velocity instrument (LDVI) for both laminar and turbulent regimes.

In creating the experimental apparatus we selected a differential scheme for the LDVI as satisfying the formulated problem most completely. In differential schemes there is visualization of the measurement point (working volume), the choice of the observation direction is not critical and the adjustment process is simpler since it does not require special matching of the light wave fronts.

A block diagram of the experimental apparatus is shown in Fig. 1. The radiation source used was a He-Ne laser 1 (continuous action LG-52-1 type) with a power of 15 mW with a wavelength $\lambda = 0.63 \mu$m. The laser ray is split by an optical cell 2, consisting of a translucent mirror and a rotating prism. By means of the rotating polaroid 3 the rays are evened out in intensity and then by the lens 4 are focused at the investigated point of the flow 5. After passage through the fluid flow the reference rays are cut off by the diaphragm 6. The radiations scattered by fluid microinhomogeneities passing through the point of intersection of the rays are collected by the lens 7 on a photocathode of the photomultiplier 8. The photocurrent at the photomultiplier output has a component at the Doppler frequency $f_D$ which is registered by the spectrum analyzer 9.

The value of the registered Doppler frequency is linearly related to the flow velocity at the point of intersection of the beams:

$$f_D = 2U\frac{\sin\frac{\theta_0}{2}}{\lambda_0} = kU,$$

where U is the projection of the flow velocity vector onto the perpendicular to the direction of propagation of the rays lying in the plane formed by intersecting rays, $\theta_0$ is the angle between the rays in a vacuum, $\lambda_0$ is the wavelength of the laser radiation in a vacuum [5].

As can be seen from the cited expression, the value of the k coefficient is not dependent on the properties of the investigated medium, but is determined only by the geometry of the apparatus and for each LDVI scheme is a constant value. In our case k = 3.6 KHz·sec/cm.

One of the important characteristics of the LDVI is the size of the working volume, determined as [5]

$$b_x = \frac{d_f}{2\cos\frac{\theta}{2}};\quad b_y = \frac{d_f}{2\sin\frac{\theta}{2}};\quad b_z = \frac{d_f}{2},$$

where $b_x$, $b_y$, $b_z$ are the halves of the main axes of the ellipsoid of scattering (the scattering volume is an ellipsoid whose center is situated on the optical axis of the system in the focal plane of the lens), $d_j$ is the diameter of the beam at the level of intensity distribution 1/e, $\theta$ is the angle between the rays in the investigated medium. With a given geometry the working volume measures 40 x 470 x 40 $\mu$m.

Using the described laser Doppler velocity instrument measurements were made of the vertical distribution of current velocity of a fluid in an open rectangular channel with a slope 0.003. The channel was fabricated from plastic with a thickness of 3 mm measuring 56 x 60 x 400 mm. At the channel input there was a grid for extinguishing macroscale perturbations. In the investigation use was made of water without artificially introduced inhomogeneities. The depth of the flow was H = 6 mm with Re = 490 and H = 9.7 mm with Re = 2720.

The channel was mounted on a bench with a micrometer screw mechanism, which made it possible to move it in a vertical direction with an interval 0.25 mm. The measurements were made in the axial part of the channel in the region of relative depths $0.007 \leqslant \eta \leqslant 0.993$.

The vertical distribution of current velocity was measured for the purpose of refining the kinematic structure of the steady fluid flow in the open channel.

Until recently the opinion prevailed that in open flows the maximum current velocity is at the upper free boundary. Its distribution in this region is such that either dU/dz = 0 or dU/dz > 0 [3, 5-8]. Another point of view has existed — [1] -- that the maximum velocity is lower than the free boundary at a relative distance from the bottom $\eta = z/H \simeq 0.8$. Measurements of the vertical profiles of current velocity U(z), published in [1], were made by a contact method with spatial averaging on the vertical of about 1 cm. This did not make it possible to carry out measurements in the immediate neighborhood of the free surface.

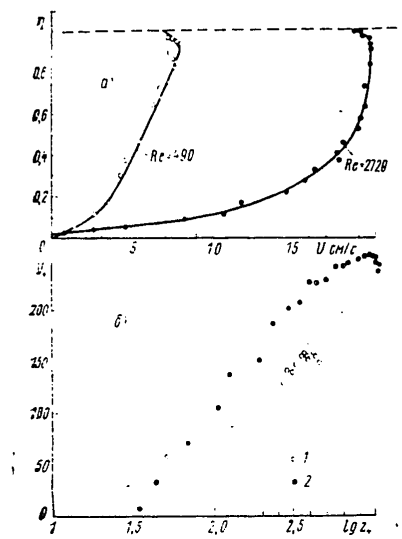


Fig. 2. Profiles of vertical distribution of current velocities in ordinary (a) and generalized (b) coordinates. 1) Re = 380, 2) Re = 1360; $\eta$ is the relative distance from the bottom; U is mean current velocity; $U_+$ is generalized velocity, $z_+$ is the generalized coordinate.

In connection with the contradictory character of the collected data it was important to make U(z) measurements near the free boundary, to determine the presence and value of the velocity gradient, and also the position of the U(z) extremum in the surface part of the flow. For this purpose measurements were made of the vertical profiles U(z) using the LDVI for both laminar (Re = 490) and turbulent (Re = 2720) regimes.

Figure 2 shows curves of the vertical distribution of current velocities in ordinary (a) and generalized (b) coordinates. The dynamic velocity $U_* + \sqrt{\tau_0/\rho}$ was determined from the friction value on the wall

$$\tau_0 = \mu \frac{dU}{dz} .$$

The dU/dz value was determined graphically from the experimental profile of current velocity in the bottom region and was 37 $sec^{-1}$ with Re = 490 and 95 $sec^{-1}$ with Re = 2720.

Figure 2b shows that the experimental points in the central part of the flow are described entirely satisfactorily by a logarithmic law of the velocity profile [4]

$$U_+ = A \lg z_+ + B,$$

where A and B are some constants,

$$U_+ = \frac{U}{U_*}, \quad z_+ = \frac{zU_*}{\nu}.$$

A deviation from the logarithmic law is manifested only in the near-surface boundary layer.

The collected data confirm the results in [1] and their comparison with [1] shows that the sector with a negative value of the current velocity gradient near the upper boundary of the open flow is in a broad range of Reynolds numbers, at least from Re = 490 to Re = $10^4$.

The nature of the current velocity distribution in the subsurface region is of fundamental importance for a proper understanding of the kinematics and dynamics of open flows. For example, the idea that at the upper boundary turbulent friction has a negative value gave basis for assuming that (with $dU/dz > 0$) the coefficient of turbulent viscosity is negative. However, taking into account data on the change of sign on turbulent friction with $\eta = 0.9$ [8] and taking into account the results in [1] and our measurements it can be concluded that in the region $\eta > 0.9$ the coefficient of turbulent friction is a positive value.

The collected data also make possible a somewhat broader representation of the kinematic structure of the flow. According to [2], the entire channel of turbulent flow is filled with rotating eddies, the largest of which are commensurable with the flow as a whole. Such a scheme reflects the real processes transpiring in a turbulent flow in the presence of one solid boundary. However, in those cases when the frictional forces on the upper interface can no longer be neglected (that is, when the current velocity in the near-surface layer decreases), it is necessary to introduce some changes into the scheme of the kinematic flow structure, to wit: it is proposed that the existing scheme be supplemented by the presence of a chain of rotating eddies in the near-surface layer as well.

BIBLIOGRAPHY


1. Bukina, L. A., Shelkovnikov, N. K., "On the Velocity Distribution in a Fluid Flow With a Free Surface," VESTNIK MGU, FIZIKA, ASTRONOMIYA (Herald of Moscow State University: Physics, Astronomy), No 6, 1975.

2. Grinval'd, D. I., TURBULENTNOST' RUSLOVYKH POTOKOV (Turbulence of Channel Flows), Leningrad, Gidrometeoizdat, 1974.

3. Levich, V. G., FIZIKO-KHIMICHESKAYA GIDRODINAMIKA (Physicochemical Hydrodynamics), Moscow, Fizmatgiz, 1959.

4. Loytsyanskiy, L. G., MEKHANIKA ZHIDKOSTI I GAZA (Mechanics of Fluid and Gas), Moscow, Nauka, 1973.

5. Mass, Ye. I., Teplitskiy, E. Sh., Kakichashvili, Sh. D., OPTICHESKIYE METODY V PRIKLADNOY GIDRODINAMIKE (Optical Methods in Applied Hydrodynamics), Tbilisi, Vol 2, 1974.

6. Minskiy, Ye. M., "Principal Characteristics of Flow Turbulence in Long Channels," TRUDY TsAGI (Transactions of the Central Aero-Hydrodynamics Institute), No 625, 1947.

7. Monin, A. S., Yaglom, A. Ya., STATISTICHESKAYA GIDROMEKHANIKA (Statistical Hydromechanics), Moscow, Nauka, Part 1, 1965.

8. Nikitin, I. K., "Characteristics of the Structure of Turbulent Flow at its Free Surface," GIDROTEKHNIKA I GIDROMEKHANIKA (Hydroengineering and Hydromechanics), Kiev, 1964.

FORMING AND DEVELOPMENT OF THE THEORETICAL INVESTIGATIONS OF THE ATMOSPHERE IN THE STUDIES OF V. A. KHANEVSKIY (ON THE HUNDREDTH ANNIVERSARY OF HIS BIRTH)

Moscow METEOROLOGIYA I GIDROLOGIYA in Russian No 11, Nov 80 pp 118-121

[Article by N. Z. Pinus, professor, and I. V. Khanevskaya, Central Aerological Observatory, manuscript submitted 12 Jun 80]

[Text]

Abstract: This is a review of the work of Professor V. A. Khanevskiy, who early in the 20th century laid and developed the basis of the theoretical direction in aerological and meteorological investigations of the atmosphere, examining it as a whole and combining experimental and analytical research methods.

Fig. 1. V. A. Khanevskiy (second row, fourth from the right) and his students -- aerosynoptic specialists of the first planned graduation from the Moscow Hydrometeorological Institute, 1934. In the second row: V. A. Belinskiy (second from the right), A. T. Bergun (third from the left); in the fourth row: O. G. Krichak (first from the right), I. A. Klemin (fourth from the right).

The science of the atmosphere began to develop rapidly late in the 19th and early in the 20th centuries with the organization of more or less regular soundings of the atmosphere with balloons, kites and pilot balloons. At that time in Russia, at Petrograd, at the Main Physical Observatory, and at Moscow, at the university, two major schools of professional geophysicists were formed. They played a major role in establishing and developing the science of the earth. These schools, over the course of many years, determined and headed the principal directions in research in the field of geophysics.

Vladimir Andreyevich Khanevskiy (1880-1943) belonged to the Moscow school of geophysicists. He was one of the founders of theoretical investigations in the field of aerology and meteorology, a leading scientist and teacher, training many Soviet meteorologists who later distinguished themselves in their scientific, scientific-teaching and practical work.

V. A. Khanevskiy was born on 14 November 1880 in Putyaty village in Mstislavskiy District of Mogilevskaya Province in a family of servants. In 1906 he graduated from the Mathematics Division of the Physics-Mathematics Faculty of Moscow University and remained at the university for training to professorial rank and was assigned as an assistant in the Geophysics Department, then called the Department of Physical Geography and Meteorology. At the same time he worked at Moscow Observatory at the university (this interesting period of the activity of Moscow geophysicists was described in an article by A. Kh. Khrgian). [See A. Kh. Khrgian: "Life and Activity of Vladimir Andreyevich Khanevskiy (1880-1943)," VESTNIK MOSKOVSKOGO UNIVERSITETA, No 1, pp 85-88, 1961.] From this time and to 1930 Moscow University was the principal place of work of V. A. Khanevskiy. In 1914 he was certified as Private Reader, and in 1918 as Professor in the Geophysics Department.

During the early period of activity of V. A. Khanevskiy the development of aerology proceeded primarily in the direction of accumulation of observational data and improvement in observation methods. V. A. Khanevskiy was one of the first to recognize the need for a changeover from the practice of accumulating data to their theoretical analysis with subsequent synthesis of the investigated phenomena and processes. Along these lines he wrote a great number of studies, including several textbooks and monographs.

From the first days of Soviet rule V. A. Khanevskiy was among the young Moscow geophysicists who actively participated in work on the organization and reorganization of Soviet scientific and academic institutions. Jointly with a group of scientists he participated in the creation of the Institute of Space Physics near Moscow (Kuchino) on the basis of the small Aerodynamics Institute.

At this institute, solving a complex of geophysical problems, V. A. Khanevskiy successively organized meteorological, aerological and theoretical divisions and headed them. Later the institute was reorganized, moved to Moscow and renamed the State Scientific Research Geophysical Institute (SSRGI).

In 1930, after separation of the Geophysics Department from Moscow State University and the organization of the Moscow Hydrometeorological Institute (MHMI) on its basis, the SSRGI became the principal center of V. A. Khanevskiy's work. At the same time (up to 1934) he worked as a hydrometeorologist in the administration of the Kazan' Railroad, where, in addition to the operational servicing of transport, he organized three specialized scientific research stations.

Early in 1934 V. A. Khanevskiy again returned to teaching activity. At the MHMI he presented lectures on dynamic meteorology and aerology, organized the Aerology Department and headed it. In 1937 V. A. Khanevskiy moved to constant work at Khar'kov, to the newly organized Khar'kov Hydrometeorological Institute (KHMI). At the KhHMI he headed the Meteorology Department, was dean of the Meteorology Faculty and Director of the Meteorology Observatory up to the German-Fascist occupation of Khar'kov during the Great Fatherland War.

Being together with most of the professorial-teaching staff and students in the occupation, V. A. Khanevskiy endured all its severity. He moved to Poltava, where prior to the liberation of the city by the Soviet Army he was bestially tortured by the German-Fascist invaders for his refusal to cooperate with them and betray the Motherland.

Already during his first studies (1906-1914) V. A. Khanevskiy made extensive use of the methods of mathematical statistics applicable to meteorological observations at Moscow Observatory, work in which he participated. During this period a number of his publications appeared with generalized annual data, as well as a climatic description of one of the physiographic regions of Russia. His work STROYENIYE ZEMNOY ATMOSFERY (Structure of the Earth's Atmosphere) (1914) was an extremely deep and many-sided investigation laying the basis for theoretical generalizations in the field of aerology and bringing V. A. Khanevskiy into the ranks of well-known Russian scientists. In this book V. A. Khanevskiy, using materials from all types of observations and the results of indirect investigations of the atmosphere, made a global study of the structure of the earth's atmosphere to great altitudes, about 70-80 km. For the first time he established and demonstrated that the "stratification of the atmosphere should be regarded as a constant phenomenon, one of its principal properties," that the presence of a stratosphere, which extends over the entire earth, is an integral property of the atmosphere. Above the stratospheric layer in the atmosphere there is also stratification with an alternation of layers of decrease and considerable increase in temperature. In this work V. A. Khanevskiy for the first time approached the problem of a multilayer tropopause and called this phenomenon "lamination."

An example of a thorough theoretical analysis of a physical phenomenon in the atmosphere was a study by V. A. Khanevskiy entitled "Blue Color of the Sky," reported in 1914 and published in 1921.

V. A. Khanevskiy made his most weighty scientific contribution to study of the physics of the atmosphere during the Soviet period. In addition to scientific-organizational and pedagogic activity, in 1918 he undertook investigations in the field of dynamic meteorology. Among the first studies in this cycle was investigation of the diurnal variation of the wind in the lower troposphere (1918-1920). Then V. A. Khanevskiy developed this direction, representing the system of air currents in the lower half of the troposphere (1919-1925). The final part was investigations of general circulation of the atmosphere (1923-1925).

Another article by V. A. Khanevskiy (1919) which belongs to this same cycle of studies is one in which he described the phenomenon of a change in tropospheric westerly transfer to a stable easterly transfer in the stratosphere above 20 km which he noted in the example of a high ascent of a pilot balloon which took place in the summer of 1919. He dealt with this phenomenon in greater detail in articles devoted to general circulation of the atmosphere.

In studies of the diurnal variation of the wind on the basis of materials from systematic aerological observations (four scheduled observations daily) V. A. Khanevskiy finally demonstrated the presence of a reverse daily variation of wind velocity in the atmospheric layer to 3,000 m and made an attempt at a physical explanation.

An investigation of air currents in the troposphere to altitudes of 3,000 m was undertaken by V. A. Khanevskiy for ensuring flights in controlled vehicles. He established that a distinguishing characteristic of air currents in the temperate latitudes is a predominance of strong winds in directions with a westerly component (maximum winds with a height to 500 m have a westerly direction) and vice versa, weak winds have an easterly component. An important characteristic extremely unfavorable for flights is a rapid increase in wind velocity with altitude in directions with a westerly component, especially significant in the layer from the earth's surface to an altitude of 500 m. Winds of easterly directions are characterized by a considerable increase only in the layer between the ground and 500 m, whereas above there are small changes in velocity with a tendency to some decrease with altitude. In the temperate latitudes with increasing distance from the ground the wind rotates to the right, especially sharply in the layer from the ground to 500 m.

The most significant contribution to science was in the final studies in this cycle which dealt with general circulation problems. Prior to these there were only speculative schemes with the classical Trades and Anti-Trades.

V. A. Khanevskiy was the first to systematize and mathematically process extensive material from observations in the world aerological network of stations and all expeditions for the period 1905-1912. He physically profoundly analyzed it and prepared schemes of general circulation of the atmosphere to altitudes of about 20 km.

The schemes of general circulation are represented by typical distributions of the wind for enlarged latitude zones. It was established that the wind regime in the temperate latitudes (70-35°N) is characterized by a predominance of westerly flow. "The wind velocity exhibits an increase to 10-12 km (to the lower boundary of the stratosphere) and then a decrease to an altitude of 20 km." With the mean wind velocities at the lower boundary of the stratosphere cited in the studies and the proper emphasis of their change above this layer it must be assumed that V. A. Khanevskiy came close to the discovery of the subtropical jet stream. Later he returned to this problem, noting that the "most significant maximum wind velocities were measured at altitudes 8-11 km, to be specific, 65 m/sec. But without question, in these layers there may sometimes be still greater wind velocities and there are already measured velocities greater than 100 m/sec."

The fact of a summer predominance of easterly transfer in the temperate latitude stratosphere, demonstrated by V. A. Khanevskiy, was a discovery made in this period. Proceeding to the wind regime of the subtropical latitudes, V. A. Khanevskiy indicated that there above a thin layer with the Northeast Trades (1-2 km) there is a westerly flow of great thickness. On this basis he drew the proper conclusion, bold for that time: "Such wind conditions persist in a region to an altitude of 16 km, that is, to the maximum altitude for which observations are available. Accordingly, there can be no talk of the Anti-Trades here."

The tropical wind regime, characterized by easterly winds, is established in the zone 20-15°N, immediately over the Northeast Trades. V. A. Khanevskiy notes that "in the Sudan, beginning with an altitude of 10 km, the wind velocities are almost twice as great as over the Atlantic Ocean. They average 21-29 m/sec." Thus, here also attention is brought to the now well-known fact of the presence of a climatic easterly jet stream with its center over the Indian Ocean and Africa. To the south of 10°N and in the equatorial zone to 5°S a tropical wind regime already dominates from the ground itself to definite altitudes. Winds with a westerly component are discovered only during a period of monsoonal rains in the troposphere. Westerly winds were also observed by V. A. Khanevskiy in the equatorial zone in the stratosphere as a phenomenon which does occur, although rarely.

The distribution of temperature in the system of general circulation of the atmosphere was represented by V. A. Khanevskiy in the form of the mean meridional section between 70°N and the equator. Such a section was constructed for the first time on the basis of factual material. Its most important characteristics and the typical nature of the distribution of isotherms are repeated in later sections constructed by many scientists on the basis of modern observational data. Using the mean temperature for air columns of different thickness V. A. Khanevskiy computed the mean altitudes of the isobaric surfaces (not standard) in the layer from the ground to 16-17 km. In the vertical section of the atmosphere between 7°N and 5°S it is easy to see a characteristic pattern of isobars. A comparison of the empirical and theoretical (geostrophic) wind velocities enabled V. A. Khanevskiy to draw the conclusion that the pattern of change in the slope of the isobaric surfaces with altitude at different latitudes in general agrees with the vertical change in wind velocity.

Thus, the studies of V. A. Khanevskiy, devoted to general circulation of the atmosphere, constitute a classical theoretical-experimental investigation essentially outpacing the scientific concepts of that time. On the basis of an analysis of the wind field, the first vertical sections of the thermal and pressure fields between the pole and equator, there was detailed development of the idea of a close relationship between the temperature and wind fields in the free atmosphere. As is well known, this idea was later one of the fundamental scientific principles in the pressure pattern method. Over a period of many years the results of the investigation by V. A. Khanevskiy remained unsurpassed. Such investigations of general circulation were repeated and substantially developed only during the post-war years by a number of Soviet and foreign scientists.

He devoted an investigation extremely significant in its scientific results to an investigation of the influence of macroscale turbulence on heat transfer in the atmosphere. By means of computations he was able to demonstrate the decisive role which is played by macroturbulence of extratropical atmospheric circulation in the redistribution of heat between the equator and the pole (1921). Climatic data were used in determining the mean transfer of heat from the equator to the pole -- about 1.1 gcal/cm$^2$sec, which according to calculations as a long-term average creates a mean temperature increase of 5°C in the temperate latitudes, up to 13°C at the north polar circle and up to 10°C near the pole.

In 1937 V. A. Khanevskiy carried out an extremely interesting scientific investigation of cold waves useful for the practical weatherman. On the basis of a 20-year series of weather reviews he studied the cold waves propagating over the European USSR. He discriminated five types of synoptic situations during which there was a marked temperature decrease attaining 35°C per day and sometimes even 10°C per hour and detected the characteristic changes of the main meteorological elements. For the first time it was demonstrated that cold waves are a result of advection of cold masses. These masses have a great thickness and over them there is warm air moving in the other direction. The cold waves are propagated at velocities considerably exceeding the wind velocity and accordingly the advection of cold is accompanied by descending movements in the entire thickness of cold air. Thus, during the initial period of development of synoptic meteorology V. A. Khanevskiy studied the most important properties of a cold front, demonstrated the role of advection and represented typical synoptic situations.

In the early 1930's the problem arose of studying the stratosphere. A commission of the Hydrometeorological Committee was formed for this purpose and it formulated a number of problems which had to be studied first. V. A. Khanevskiy took an active part in the work of this commission and was one of the principal speakers at the First All-Union Conference on Study of the Stratosphere, called by the USSR Academy of Sciences in 1934 in Leningrad. A number of articles by V. A. Khanevskiy were specially devoted to the characteristics of the stratosphere (1933, 1934, 1938).

An original investigation was that of the spatial structure of high anticyclones. In two articles (1929, 1932), on the basis of a detailed examination of the development of a high anticyclone on 30 September-1 October 1908, V. A. Khanevskiy clarified, using the high-level charts which he constructed (for the first time in our country), that a high anticyclone consists of two air flows: cold northeasterly and warm southwesterly of a great thickness (more than 16 km). These flows are separated by a clear transition zone whose average slope is about 1:450 with the absence or very weak exchange of masses between the flows. A temperature decrease was associated with the intrusion of this cold flow. It was especially significant in the upper troposphere (5-7° at altitudes 6-8 km) and in the stratosphere (12-15° at 11-13 km). Thus, in this study it was demonstrated for the first time that high anticyclones, the same as cyclones, have a frontal structure. Later this fact was confirmed and found further development in the studies of Soviet scientists.

A logical result of the 35 years of teaching and scientific activity of V. A. Khanevskiy was writing of textbooks and study aids. He was the coauthor of our nation's first (1923) course in geophysics. A second supplemented and enlarged edition of this textbook appeared in 1938.

On the basis of courses of lectures presented by V. A. Khanevskiy at Moscow University on atmospheric optics and meteorology he published his famous book SVETOVYYE YAVLENIYA V ATMOSFERE (Light Phenomena in the Atmosphere) (1930), as well as two academic aids on meteorology written in collaboration with A. P. Loidis. During the last years of his life V. A. Khanevskiy worked on a textbook in the field of aerology, but he did not succeed in finishing it.

V. A. Khanevskiy endeavored to transmit his rich scientific experience to the younger generation. His students, many of whom became leading scientists, brought to science the capabilities of their teacher to employ the physicomathematical method, the striving to ascertain the quantitative relationships between atmospheric phenomena, the endeavor to develop physical concepts concerning the processes transpiring in the entire thickness of the atmosphere, combining experimental and theoretical methods.

REVIEW OF MONOGRAPH BY A. I. LAZAREV, A. G. NIKOLAYEV AND YE. V. KHRUNOV: 'OPTICAL INVESTIGATIONS IN SPACE' ('OPTICHESKIYE ISSLEDOVANIYA V KOSMOSE'), LENINGRAD, GIDROMETEOIZDAT, 1979, 256 PAGES

Moscow METEOROLOGIYA I GIDROLOGIYA in Russian No 11, Nov 80 pp 122-123

[Review by V. A. Dzhanibekov, USSR flier-cosmonaut]

[Text] Beginning with the first space flight of Yuriy Alekseyevich Gagarin optical investigations from space have been used extensively in a study of the earth's natural resources, physical properties of the atmosphere, interplanetary and cosmic space. During the years of space conquest many highly important results have been obtained from investigations of the atmosphere and atmospheric-optical phenmena. Each space flight has brought new data on the optical characteristics of the environment observed from space.

The authors of the book, two of whom are USSR flier-cosmonauts, and the third being a well-known scientist in the field of optical investigations in space, have carried out much work in the systematic arrangement, analysis and generalization of the optical investigations carried out for the most part from Soviet manned spaceships.

The book opens with a chapter devoted to optical investigations from Soviet manned spaceships during 1961-1978. It describes in adequate detail the principal stages in the development of these investigations from the first flight of Yu. A. Gagarin to the flight of the second expedition of the "Salyut-6" orbital station.

The authors successively analyze the programs and results of visual observations and instrumental investigations of Soviet cosmonauts. In special detail they examine the materials obtained during the flights of the "Vostok" and "Vostok-3," "Voskhod" and "Voskhod-2," "Soyuz-5" and "Soyuz-9", and also during the time of the manned flights of the orbital stations "Salyut-4" and "Salyut-6."

The reliability of the visual observations of cosmonauts is dependent to a considerable degree on the influence of spaceflight conditions on the principal functions of the visual system. Accordingly, it is entirely natural that the next chapter is devoted to an investigation of vision in space. It is shown convincingly that in space the visual system remains as reliable an information channel as under ordinary terrestrial conditions, and that the results of visual observations of cosmonauts can be used extensively in the study of the environment from space. On the basis of my own spaceflight experience I fully concur with this conclusion.

The possibility of observing extended radiation sources in space (the same as under ordinary conditions) is determined by the relationship of the frequency contrast characteristics of the visual system of the cosmonauts, the observed objects, the earth's atmosphere and the windows in spaceships. In this connection the book gives fundamental information on the frequency-contrast characteristics of the visual system, the atmosphere and windows. These concepts are supplemented by an analysis of the possibilities of observing point and linear sources against a radiating background.

A considerable place in the book is devoted to an investigation of the earth's atmosphere and atmospheric-optical phenomena. On the basis of materials from space experiments and data from rocket sounding the authors present a schematic model of radiation of the earth's upper atmosphere when making observations from space. The greatest detail is given in descriptions of some phenomena for the first time observed from space on the earth's nighttime side and in the twilight zone. These include the spatial structure of radiation of the nighttime atmosphere in the visible region of the spectrum, scintillation of stars and the planets at the earth's nighttime horizon and the phenomenon which has been called the earth's "blue zone." On the basis of the materials of the observations made by two of the authors, and on the basis of the results of observations of other cosmonauts, the book gives a picture of development of the twilight glow in dependence on the angle of solar depression. For the first time the book gives an analysis of the phenomenon of hanging of the twilight radiation of the upper atmosphere above the earth's horizon, having the name "whiskers effect," observed by the crew of the "Soyuz-9" spaceship, which included one of the authors of the book. Thereafter this phenomenon was observed by many cosmonauts, including the crews of the orbital stations "Salyut-4" and "Salyut-6."

In connection with the observations from the "Voskhod-2" spaceship a study was made of the possibility of investigating the solar corona and zodiacal light at the earth's twilight horizon prior to sunrise and afterward, in the second case -- with allowance for the attenuation of direct solar radiation in the dense layers of the atmosphere. A further development of these observations was the "artificial solar eclipse" experiment carried out during the joint Soviet-American flight under the "Soyuz"-"Apollo" program.

On the daytime side of the earth the authors examine the characteristics of the spatial structure of emissions of the upper atmosphere. In this connection there is a detailed exposition of the results of observations from the spaceships "Soyuz-3" and "Soyuz-9," serving as a basis for clarifying the vertically rayed structure (horizontal inhomogeneity) of the daytime emission of the earth's upper atmosphere in the twilight zone. The authors also give the results of similar observations from the "Salyut-4" orbital station. The book presents hypotheses concerning the interrelationship between the horizontal nonuniformity of daytime emission of the upper atmosphere and acoustic-gravitational waves, as well as one of the reasons for the appearance of gravitational waves. This hypothesis is evidently not completely indisputable. Methods for investigating the spatial nonuniformity of daytime emission of the upper atmosphere from rockets and satellites are also examined and described in detail.

The section devoted to auroras briefly describes the spatial and optical characteristics and also gives the results of visual observations of auroras from space.

The last chapter in the book gives observational data and develops the concept of Fresnel reflection of radiation from the atmospheres of planets and comets as a new experimental method in astronomy and astrophysics. This phenomenon was for the first time observed from space by the crew of the "Voskhod-2" spaceship in March 1965. Later it was photographed by one of the authors of the book from the "Soyuz-5" spaceship and other Soviet and American cosmonauts and astronauts. The authors examined the possibility of observing and using this phenomenon for remote investigation of the physical properties of the atmospheres of the planets and comets. In particular, from this point of view there is an analysis of one of the phenomena observed by M. V. Lomonosov during the transit of Venus across the solar disk on 26 May 1761.

The authors of the book were able to achieve their objective of systematizing, analyzing and generalizing the results of optical investigations from space. The book is written in good literary language, is easily read and will be extremely useful to many specialists in the fields of astronomy, astrophysics, geophysics and space optics. It will be a good aid in the training of cosmonauts for new flights.

EIGHTIETH BIRTHDAY OF NIKOLAY FEDOROVICH GEL'MGOL'TS

Moscow METEOROLOGIYA I GIDROLOGIYA in Russian No 11, Nov 80 p 124

[Article by V. M. Mikhel', N. S. Shishkin and N. I. Novozhilov]

[Text] Candidate of Geographical Sciences Nikolay Fedorovich Gel'mgol'ts, one of the oldest Soviet aerologists, marked his 80th birthday on 28 October 1980.

The many years of scientific activity of N. F. Gel'mgol'ts before the Great Fatherland War transpired for the most part at the Borispol'skaya Aerological Observatory near Kiev, but in part was also associated with the aerological observatory at Pavlovsk, near Leningrad, but after the war it was at the Kazakh Scientific Research Institute, where he worked as head of the aerology section.

The first scientific investigations of Nikolay Fedorovich (1925-1927) were in the field of improvement of nephoscopic observations, at that time, with the still inadequately developed network of pilot balloon stations, playing a major role in determining wind aloft. Later N. F. Gel'mgol'ts invested much work and creative initiative in the development of the pilot balloon method and its applications and the organization of pilot balloon observations. Here he did work on the aeroclimatic characterization of the wind in the free atmosphere (both on the basis of direct measurements of the wind by the pilot balloon method and indirectly, on the basis of computation of wind velocity and direction aloft on the basis of data on the distribution of surface isobars and isotherms) and proposals on improvement of the system of pilot balloon observations and publication of observational data.

An important scientific-methodological and organizational role for the development of the network of pilot balloon stations was played by the RUKOVODSTVO PO BESTEODOLITNYM PILOTNYM NABLYUDENIYAM (Manual on Observations of Pilot Balloons Without Use of Theodolites) (Kiev, 1937) and other methodological studies.

Being a major specialist on clouds, Nikolay Fedorovich did much for the development of observations of clouds in the network of aerological and meteorological stations, for the methods for their climatological processing and for characterizing the natural probability of different cloud genera. His investigations of the climatology of clouds belong to this same cycle of studies.

The monograph by N. F. Gel'mgol'ts entitled GORNO-DOLINNAYA TSIRKULYATSIYA SEVERNYKH SKLONOV TYAN-SHANYA (Mountain-Valley Circulation of the Northern Slopes of the Tien Shan) (1963) is of special importance; it is characterized by breadth of coverage of the investigated atmospheric phenomena, original approach and practical applicability. The author completes his deep and many-sided investigation with an excellent review of the results he obtained and the conclusions which he drew on mountain-valley circulation and its dependence on geographical conditions, on its regime in the foothill zone, the atmospheric and physical phenomena associated with it and the peculiarities of the diurnal variation of meteorological elements (alternate migration of atmospheric moisture and dust at nighttime from the mountains, and during the daytime -- into the mountains), on the moving force of circulation, on the vertical structure of circulation in a mountain valley and in the foothills, etc.

During this same period of work at the Kazakh Scientific Research Hydrometeorological Institute Nikolay Fedorovich, continuing and developing his aerological and aeroclimatic investigations of cloud cover over an extensive area of Kazakhstan, worked successfully on timely problems related to the physics of clouds and precipitation. He actively participated in interesting and important experiments conducted jointly with the Section on the Physics of Clouds and Artificial Modification of the Main Geophysical Observatory for inducing summer and winter precipitation in Tselinnyy Kray. Then, in collaboration with V. I. Rogozin, he thoroughly investigated the structure, liquid-water content and radar reflectivity in the Zailiyskiy Alatau.

We could mention a number of other interesting and valuable aerological and meteorological studies of N. F. Gel'mgol'ts, but we will limit ourselves in conclusion to only one other, relating to a problem of much timely importance: monitoring pollution of the air medium. We have in mind an investigation of Nikolay Fedorovich in which he emphasizes the special significance of the singular climatic conditions in Alma-Ata, during some atmospheric processes favoring a considerable contamination of the air basin in this region. A number of important characteristics of mountain-valley circulation, associated with contamination of the urban atmosphere in Alma-Ata, were set forth earlier in the above-mentioned monograph by N. F. Gel'mgol'ts.

Nikolay Fedorovich did much productive work in the field of preparation of professional meteorologists and aerologists. As a man he is characterized by sincerity, responsiveness, great erudition and breadth of interests.

We sincerely congratulate Nikolay Fedorovich Gel'mgol'ts on his noteworthy birthday and with all our hearts we wish him new creative successes, good health and well-merited rest.

## SEVENTIETH BIRTHDAY OF ANATOLIY IVANOVICH KARAKASH

Moscow METEOROLOGIYA I GIDROLOGIYA in Russian No 11, Nov 80 pp 125-126

[Article by workers of the USSR Hydrometeorological Scientific Research Center]

[Text] Anatoliy Ivanovich Karakash, senior scientific specialist in the Marine Hydrological Forecasts Section of the USSR Hydrometeorological Center, one of the leading specialists in the field of marine forecasts, marked his 70th birthday on 11 September 1980.

All the scientific activity of Anatoliy Ivanovich, extending over 30 years, was associated with the USSR Hydrometeorological Center, where he arrived in 1947. However, his first scientific studies on forecasts of the level and appearance of ice in the southern seas of the USSR were published as early as 1939 when after graduating from Moscow Hydrometeorological Institute he worked first at the Baku and then at the Sevastopol' Administrations of the Hydrometeorological Service.

The Great Fatherland War interrupted the scientific activity of Anatoliy Ivanovich. He was delegated an important assignment: rendering assistance to the partisan detachments of Yugoslavia in the organization of a meteorological service. He manifested personal valor and courage, for which he was awarded the Yugoslav order of the Partisan Star Second Degree. His participation in the war earned him the Order of the Fatherland War Second Degree and medals.

During the first post-war years A. I. Karakash worked at the headquarters of the Main Administration of the Hydrometeorological Service in the main inspectorate. While in this post he did much for strengthening the hydrometeorological service in the country.

In 1947 A. I. Karakash arrived at the Central Institute of Forecasts (USSR Hydrometeorological Center) and completely devoted himself to scientific work.

Under his direction and with his direct participation he carried out scientific investigations for the purpose of developing methods for predicting sea level, water temperature and ice phenomena in nonarctic seas, etc.

In the course of all his activity he has devoted great attention to introducing research results into practice. This was reflected in the routine compilation of marine hydrological forecasts on the basis of his methods, the writing of methodological instructions, etc. A. I. Karakash was one of the initiators and organizers of the creation of a service in our country for supplying recommended courses to navigators. He devoted a number of investigations to this problem. A. I. Karakash dealt with an extremely broad range of problems, but the main place in his scientific interest was occupied by investigations in the field of development of methods for the long-range forecasting of ice conditions in the seas of the USSR. A. I. Karakash has been the author of more than 40 published studies in the field of marine hydrological forecasts.

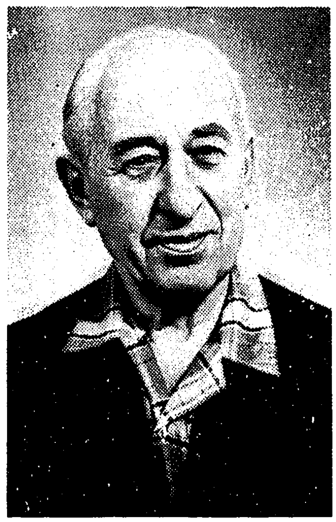

During the period 1964-1979 A. I. Karakash worked as head of the Sea Forecasts Section. His rich experience in operational and scientific work has been meticulously handed down to the young specialists in the section and to graduate students.

In noting the scientific services of Karakash on his birthday, it is impossible to pass over his great social and political work. A member of the CPSU since 1942, A. I. Karakash has repeatedly been elected Secretary of the Party organization. He was a propagandist for many years. A thorough-going Communist, a specialist loving his work: that is how Anatoliy Ivanovich is known among his associates. He has been awarded the Honorary Diploma of the USSR Supreme Soviet. His name has been added to the Honor Roll of the USSR Hydrometeorological Center.

Anatoliy Ivanovich meets his 70th birthday with full strength and creative thought. We wish him good health, creative successes and long years of productive activity.

CONFERENCES, MEETINGS, SEMINARS

Moscow METEOROLOGIYA I GIDROLOGIYA in Russian No 11, Nov 80 pp 126-127

[Article by D. A. Tarasenko]

[Text] The 23d COSPAR Session (Committee on Space Research) was held in Budapest during the period 2-14 June. Within the framework of this session there were seven symposia, two working groups and specialized sessions.

Specialists of many countries in the world participated in the work of COSPAR. The meteorological aspects of the upper atmosphere were examined in the symposium "Operation of Systems and First Results of Observations Under the Global Atmospheric Research Program" and at a session of the Interdisciplinary Scientific Commission (ISC) on the subject: "Study of the Upper Atmosphere of the Earth and Planets from Space, Including Models of the Atmosphere." There were four subcommissions in this commission: 1. "Methods for the Representation of Energy Sources in the Earth's Upper Atmosphere and Ionosphere." 2. "Upper Atmospheres and Ionospheres of the Planets." 3. "Models of the Earth's Mesosphere and Thermosphere" and 4. "Observations of the Planets Using Circumterrestrial Space Vehicles."

Problems associated with the meteorology of the upper atmosphere were discussed in a number of reports examined in subcommission 3. We will briefly discuss some of them.

The first paper presented at subcommission 3 was from the Soviet Union. The report entitled "Models of the High-Latitude Stratosphere and Mesosphere" (G. A. Kokin, D. A. Tarasenko, L. A. Ryazanova) was requested. It examined problems relating to the accuracy of rocket sounding and comparability of instruments. Methods were proposed for taking into account longitude, latitude, interhemisphere and interannual (for the winter season) differences in the thermodynamic parameters and wind in the stratosphere and mesosphere. A study was made of the influence of solar activity in the 11-year cycle on the temperature regime of different layers of the atmosphere in winter in the polar region.

The second report was devoted to the global distribution of temperature in the mesosphere, obtained from a satellite. Its authors K. Labitzke (West Berlin) and G. Barnett (Great Britain) for all months in the year constructed maps of the distribution of temperature in the mesosphere on the basis of the intensity of outgoing radiation and analyzed the influence of stratospheric dynamics on the temperature regime of the upper mesosphere. The intensity of outgoing atmospheric radiation was determined by a group headed by Professor G. Houghton from Oxford with a pressure-modulated radiometer (PMR). The radiometer was carried by the "Nimbus-6" satellite. It had a number of channels with peaks of the weighting functions in different layers of the atmosphere. The authors of the report used the 3000 channel. The data obtained using this channel are for the time being unique and very valuable satellite materials on the upper mesosphere (about 90 km).

P. Chakabarthi and D. Chakabarthi (India) presented a report entitled "Variations of Temperature and Density in the Course of a Solar Eclipse and Their Influence on the Positive Concentration of Mesospheric Ions."

In a report entitled "Variations of Mesospheric Ozone Determined from the 'Intercosmos' Satellite" W. Lippert, R. Knut and others (GDR) examined the ozone profiles in the range of altitudes 55-95 km and their variability with a clear minimum at the mesopause. The data were obtained using photometers carried on satellites.

A report by D. Offerman (West Germany) and others, entitled "Mesospheric Structure and Anomalies in the D Region," outlined a definite scheme attributing the phenomena of the winter anomaly of the D layer to the combined effect of variations in temperature, vertical mixing and horizontal wind velocity. A region of increased NO concentration and increased ionization is formed due to increased vertical transport from above. A temperature change increases the effect. An increasing horizontal wind drifts the NO cloud and this explains the great temporal and spatial anomaly of the D region. An increase in NO at the expense of the lower-lying layers is excluded by the authors.

The session of subcommission was devoted to the thermosphere and exosphere. Eight reports were presented there, of which four were Soviet: two from the Institute of Applied Geophysics, one from the Institute of Applied Mathematics and one from the Central Aerological Observatory One report was from the United States and three from West Germany.

Now we will discuss a report by K. Champion (United States) entitled "Properties of the Mesosphere and the Lower Thermosphere." It contains a section devoted to turbulent diffusion in the mesosphere and thermosphere. In addition, its author determined the diurnal variations of the altitude of the turbopause for summer and winter in the temperate, polar and equatorial latitudes. Also examined is the relationship between the variability of the equatorial turbopause, temperature at an altitude of 120 km and the geomagnetic index $A_p$. It is shown that the turbulent transfer of heat is the dominating mechanism controlling the energy flux.

A report by specialists of the Central Aerological Observatory, S. S. Gaygerov, D. A. Tarasenko, and others was devoted for the most part to wind models. An attempt was made to ascertain the longitude differences. For this purpose charts of the topography of the isobaric surfaces were used in computing the geostrophic wind. A map of the topography of the isobaric surface 0.001 mb (above 90 km), presented in the report, was of the greatest interest.

A report by L. Jacchia (United States), entitled "Empirical Models of the Thermosphere and Requirements on Their Improvement," was presented in subcommission 1.2. It enumerated the factors which must be considered in the modeling of atmospheric parameters. It is indicated that the use of different solar indices is incorrect. It is necessary to use data on ultraviolet and x- radiations obtained from a satellite.

We will briefly discuss two reports presented at the symposium.

A report by D. Pick and G. Brownscomb (Great Britain) was entitled "First Results Obtained From Stratospheric Channels of the TOVS Operational Satellite of the 'TIROS-H' Series." The TOVS ("TIROS," Operational, Vertical Sounding) includes HIRS-2 radiometers (high-altitude infrared sounding model 2), MSU (microwave sounding instrument) and SSU (stratospheric sounding instrument). The report describes the stratospheric fields of geopotential altitudes obtained for the most part using the SSU. The authors gave the diurnal changes of stratospheric temperature, examined zonal temperatures, presented a comparison of satellite data with data from rockets and radiosondes, and also compared data obtained simultaneously by the two satellites "TIROS-H" and "NOAA-6." It was shown that it is possible to use satellite information in an investigation of stratospheric warmings, and also in the solution of problems related to theoretical modeling of dynamic processes.

The contents of a report entitled "Evaluation of Stratospheric Meteorological Analysis Made Using Satellites and Rockets" were of great interest. The authors feel that a reduction of the rocket network would have a bad effect on the quality of high-altitude charts. The differences between the results of computations of eddy heat flows and the transfer of moment of momentum according to measurements made on a satellite and satellite data, corrected on the basis of rocket measurements, indicate the importance of rocket information.

The reports presented at the 23d COSPAR Session made it possible to examine the directions of work in the field of space meteorology on which research is being carried out in different countries. Abroad studies are being further developed for the measurement of parameters on satellites, both standard parameters and atmospheric composition.

The investigations carried out in the United States and Great Britain indicated the importance of rocket information for correcting satellite materials. Rocket data are necessary for a proper determination of geopotential and temperature in the fields of their maximum and minimum values.

The next COSPAR session will be held in 1982 in Canada.

NOTES FROM ABROAD

Moscow METEOROLOGIYA I GIDROLOGIYA in Russian No 11, Nov 80 pp 127-128

[Article by B. I. Silkin]

[Text] About 65 million years ago numerous species of sea and land animals died out during an extremely short time span (on a geological scale). All the hypotheses, especially those associated with cosmic factors, could not give an exhaustive explanation of this catastrophe.

As reported in GEOLOGY, Vol 6, No 12, and in SCIENCE NEWS, Vol 116, No 21, 1979, the geologist S. Gartner and the meteorologist G. McGurk, specialists at the University of Texas, speaking at a conference of the American Geological Society, held in San Diego, California, in December 1979, advanced their hypothesis based on paleoclimatological and geological data.

Earlier S. Gartner, in collaboration with G. Kinney, a scientific specialist with the Phillips Petroleum oil company, made an analysis of cores of abyssal sedimentary rocks taken from the floor of the North Sea. In layers deposited 65 million years ago they discovered a sudden and complete disappearance of plankton and animal organisms characteristic for the Cretaceous period (136-65 million years ago). They were replaced by species characteristic for the Tertiary (68-1.8 million years ago). This was not unexpected for the researchers. However, in that part of the core which related to the Tertiary the organisms characteristic for the Cretaceous suddenly appeared again. These fossil organisms were encountered over some time, after which they again disappeared, this time being finally replaced by Tertiary plankton.

It therefore followed that the catastrophe had a selective character and at least in the North Sea occurred twice. It is probable that in the Late Cretaceous (about 80 million years ago) the Labrador Sea, Baffin Bay and Bering Strait still did not exist and as a result the Arctic Ocean was an isolated, closed basin. Fresh waters entering from the rivers of Eurasia and North America greatly reduced its salinity. But 65 million years ago, according to data from geology and geophysics, a temporary strait developed between Greenland and the Scandinavian Peninsula through which fresh water began to enter into the North Sea. This event coincides with the abundance of animal and plant species of a Tertiary character in the sediments which were capable of tolerating the reduced salinity of the medium.

However, when the strait connecting the Arctic Ocean with other parts of the world ocean became permanent, all the arctic waters with a reduced content of salts entered the Atlantic and then the Pacific Ocean and finally covered all these basins with slightly saline waters. This led to the death of a great many marine organisms, associated with three factors: 1) their nontolerance of a low content of salts; 2) a decrease in the quantity of oxygen dissolved in the water; 3) a breaking of the ecological food chain.

Joining in which these arguments, the meteorologist G. P. McGurk applied this hypothesis to the inhabitants of the land. He pointed out that the Arctic Ocean, isolated from the remaining oceans, during the Cretaceous was approximately 15°C colder than the other oceans. On the basis of a model of global circulation of the atmosphere in the Cretaceous it can be asserted that with sudden outpouring of cooled waters of the Arctic Ocean into the other basins there should be a cooling of the latter by approximately 10°C. The cooling of the sea, and after it, the atmosphere, caused a decrease of precipitation which could attain 57%.

This should cause a severe drought, cooling and increase in the seasonal variations of weather. A considerable part of the rich tropical vegetation, extending up to that time into the high latitudes, disappeared. The animals depending on it directly or indirectly perished if they did not succeed in adapting.

*****

In SCIENCE NEWS, Vol 116, No 25/26, 1979, it is reported that a group of geological engineers, headed by M. Robinet (University of Idaho, United States), developed a method for detecting the degree of contamination of ground water using electrodes. In this method the uncontaminated water is a poor conductor of current and as the content of dissolved solid substances increases in it this property increases. Thus, the dissolved substances can serve as an indicator of the degree of water contamination. The method does not completely preclude the necessity for drilling in order to confirm facts, but to a considerable degree reduces the errors and expenditures associated with this.

In this method two steel rods are driven into the ground to a depth of about 30 cm as a current receiver and two are used as a transmitter. The decrease in current strength on the path between the "receiver" and the "transmitter" is dependent on the local geology and on the quality of the ground water. Such a terrain survey can be made by a change in the positioning of the network or an increase in the distance between the rods, which forces the current to flow at a greater depth.

Field tests of the M. Robinet method gave positive results. The United States Nuclear Energy Commission has signed a contract for testing this method for the purpose of detecting ground water uranium contamination forming in atomic industry sumps. The Environmental Protection Agency in the United States is working out a national program for using this method for the monitoring of contamination in ground water dangerous for health.


[4-1864]

- END -

5303
CSO: 1864